Tidal inlet channel stability in long term process based modelling

Roy Teske BSc. 3345939
MSc. Traineeship report
March-July 2013
Host organisation: Deltares, Delft
Supervisor Deltares: dr.ir.E.Elias
Utrecht University supervisor: dr.M.G.Kleinhans
Version 2

Abstract

The Dutch Waddenzee is characterised by a large number of tidal inlets between sandy barrier islands. The general morphodynamics and hydrodynamics of tidal inlets are relatively well understood, but the detailed interactions remain a prominent research interest. Recent studies have used process-based computer models as a tool to investigate the long term mechanisms, interactions and morphologic development. One of the major problems identified in these models is an unrealistic development of tidal channels. The exact reasons for this inconsistency are not yet know. The aim of this report is to improve the model performance by using more natural "morphological" boundary conditions instead of currently used schematizations. An idealized representation of the Ameland inlet was used to evaluate different modelling strategies. It was found that the incorporation of the TRANSPOR 2004 sediment transport predictor and a space and time dependent bedform roughness led to a reduced incision and more stable channels over a 40 year period, without additional tuning parameters. Further potential improvement in channel stability was found with a more complex transverse bedslope predictor. The outcome of the modelling contributes the development of tidal inlet models that are able to produce more valid long term morphologic simulation in order to study the inlet sensitivity to future sea level rise and determine sound nourishment strategies.

Preface

This internship report was written as a finalization of the Master Study Earth, surface and water with the River and coastal morphodynamics specialization at Utrecht University. The 5 month internship period is research oriented and provides student with the opportunity to familiarize themselves with a company or governmental organization. The contents of this report focus on the development of process-based model of the Ameland inlet. It was written at Deltares, Delft as a part of the KPP-B&O kust (Beheer en Onderhoud) collaboration between Rijkswaterstaat and Deltares.

Acknowledgements

I would like to thank my traineeship supervisor Edwin Elias for his enthusiasm and support during my time at Deltares. Furthermore the support from Giorgio Santinelli, Mick van de Wegen and Pieter-Koen Tonnon is greatly appreciated. Finally Maarten Kleinhans for his interest and ideas to improve the model.

Table of content

List of figures

List of tables

1.1 Introduction

Tidal inlets are found along many of the world's coastal areas and include both estuaries and barrier island inlets. These inlet systems serve an important role in coastal ecosystems and local biodiversity. The focus of this report is on the sandy coast barrier island inlet of Ameland in the Dutch Waddenzee. Dutch Waddenzee inlets formed during the Holocene transgression that sparked the formation of the barrier islands.

Tidal inlets are dynamic systems that are shaped by the local interactions of waves, currents and tides (De Swart and Zimmerman, 2009). Although the basic morphodynamics and hydrodynamics of tidal inlet systems are relatively well understood the detailed physical processes and interactions remain unclear. Various attempts have been made to solve parts of this uncertainty by developing models of tidal inlet systems. These models include conceptual equilibrium relations (Cheung et al,. 2007), process-based computer models (Lesser 2009, Elias, 2006, Van de Vegt et al. 2006, Van der Wegen, 2010, Dastgheib, 2012, Dissanayake, 2012) and physical scale experiments (Stefanon, 2009, Kleinhans et al., 2012).

In long term process-based models the inlet development is characterised by an unrealistic incision of the main tidal channel. This led to the development of several non-natural schematizations to reduce the channel incision (Dastgheib, 2012, Dissanayake, 2012). The main aim of this report is to determine realistic morphologic boundaries in order to create a long term (50-100 year) process-based model of the Ameland tidal inlet system, with stable main channels. This is done by combining and evaluating different processes-based computer modelling studies and strategies for Waddenzee inlets.

With more stable models it should be possible to, investigate the stability of the barrier islands and determine the response of the system under external forcing's, such as sea level rise and sediment nourishments.

1.2 Outline of the report

This internship report consists of a summary of literature (chapter 2) that is relevant for understanding tidal inlets and especially the Ameland environment. This is followed by a description of the state-of-the-art Delft3D modelling software, which is specified in terms of the components used in the modelling section of this report. The various long term process-based modelling studies of the Ameland area are presented together with the tidal channel stability problems and solutions. Next a brief synthesis of the literature is given that summarizes the common tidal inlet modelling practices and the corresponding issues (chapter 3). The modelling strategy, model setup and evaluation methods are presented (chapter 4). This is followed by a description of the natural system development and the modelling results (chapter 5). Finally the results are discussed (chapter 6) and the main conclusions (chapter 7) are given.

2. Literature

In this section a brief explanation is given of the study area (chapter 2.1) and the main components and morphodynamics of Waddenzee barrier inlets (chapter 2.2). This is followed by a description of the process based Delft3D software is presented (chapter 2.4) and various modelling studies and approaches regarding Dutch Waddenzee tidal inlets (chapter 2.5).

2.1 Study reference area

2.1.1 Ameland inlet

The Waddenzee is located in the south of the North-Sea and spans the coastal area from the western coast of Denmark to the Netherlands. In total 33 tidal inlets are present separated by barrier islands (Ehlers, 1988). The Dutch barrier islands formed during the Holocene transgression over the gently sloping Pleistocene deposits (De Swart and Zimmerman, 2009). Wave and tidal influences reworked the sands and formed migrating barrier ridges separated by tidal inlets. Through these tidal inlets water is transported towards the basin during flood and seaward during ebb. The tidal inlets are characterised by narrow and deep channels with ebb-tidal delta shoals on the seaward side. On the basin side the channels branch out in to smaller channels that flow into tidal flats and salt marshes (Dastgheib, 2012).

The tidal inlet, which serves as the frame of reference for the modelling in this report, is the Ameland inlet in the Dutch Waddenzee (figure 2.1a). The Ameland inlet consists of a main inlet channel, the Borndiep, which becomes narrower in the basin direction, where it is called the Dantziggat. A second smaller inlet channel is present in the west near Terschelling, the Boschgat. The main shoal of the ebb-delta is called the Bornrif (figure 2.1b).

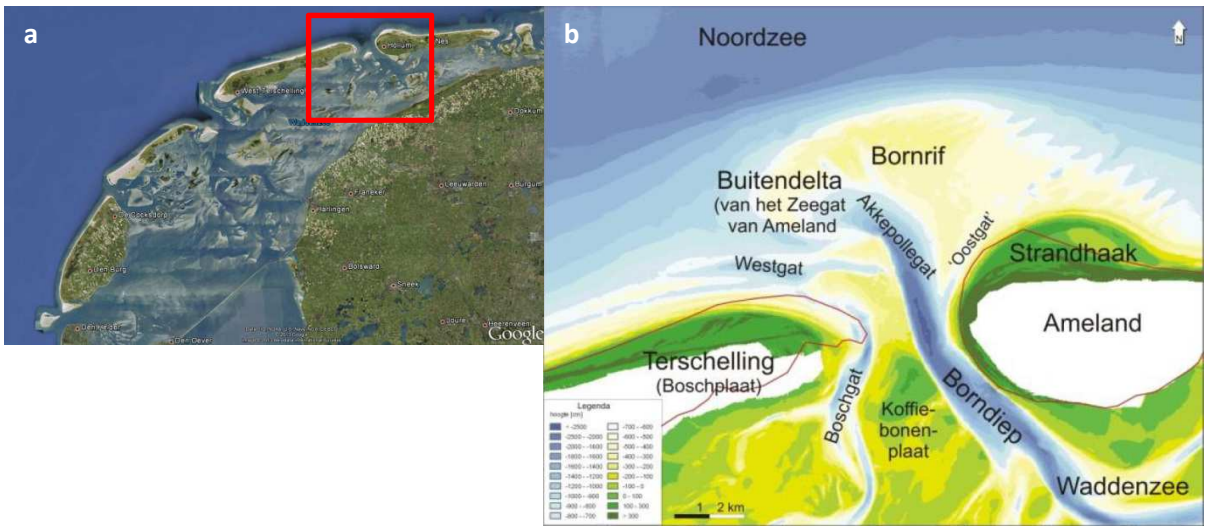

Figure 2.1. (a) The Waddenzee with the different tidal inlet systems. The Ameland system is given in the red highlighted area. (b) The Ameland inlet with the names of the channels and shoals (Elias and Bruens, 2012).

Sedimentary deposits in the Ameland basin

The sedimentary basis of the Ameland inlet is formed by Pleistocene deposits filling the former Boorne drainage valley. The top of the Pleistocene surface is found at -5 m NAP on the Frisian landward margin. It dips in the north-western direction, to -30 m NAP below Ameland. It is largely unaffected by channel reworking. This means an undisturbed succession of sediments is present (Van der Spek, 1994).

In figure 2.2 it can be seen that the deposits on the Frisian landward margin of the basin consist of Saalian glacial tills at the base that are covered by Weichselian windblown sands. Towards the Ameland inlet the tills and sands disappear and Eemian interglacial marine sands and clays are found on top of older Elsterian Potclay. The Potclay forms the top of the Pleistocene layer in the Bordiep gorge at depths of –30 m NAP (figure 2.2). The Pleistocene surface in the basin is covered by younger

Holocene deposits. The oldest Holocene deposits in the basin (10ka) consist of a basal peat layer and humic clays that formed during the Holocene transgression. The peat and humic clay layers are covered by bioturbated sand and clay deposits that fill the basin up to the current level.

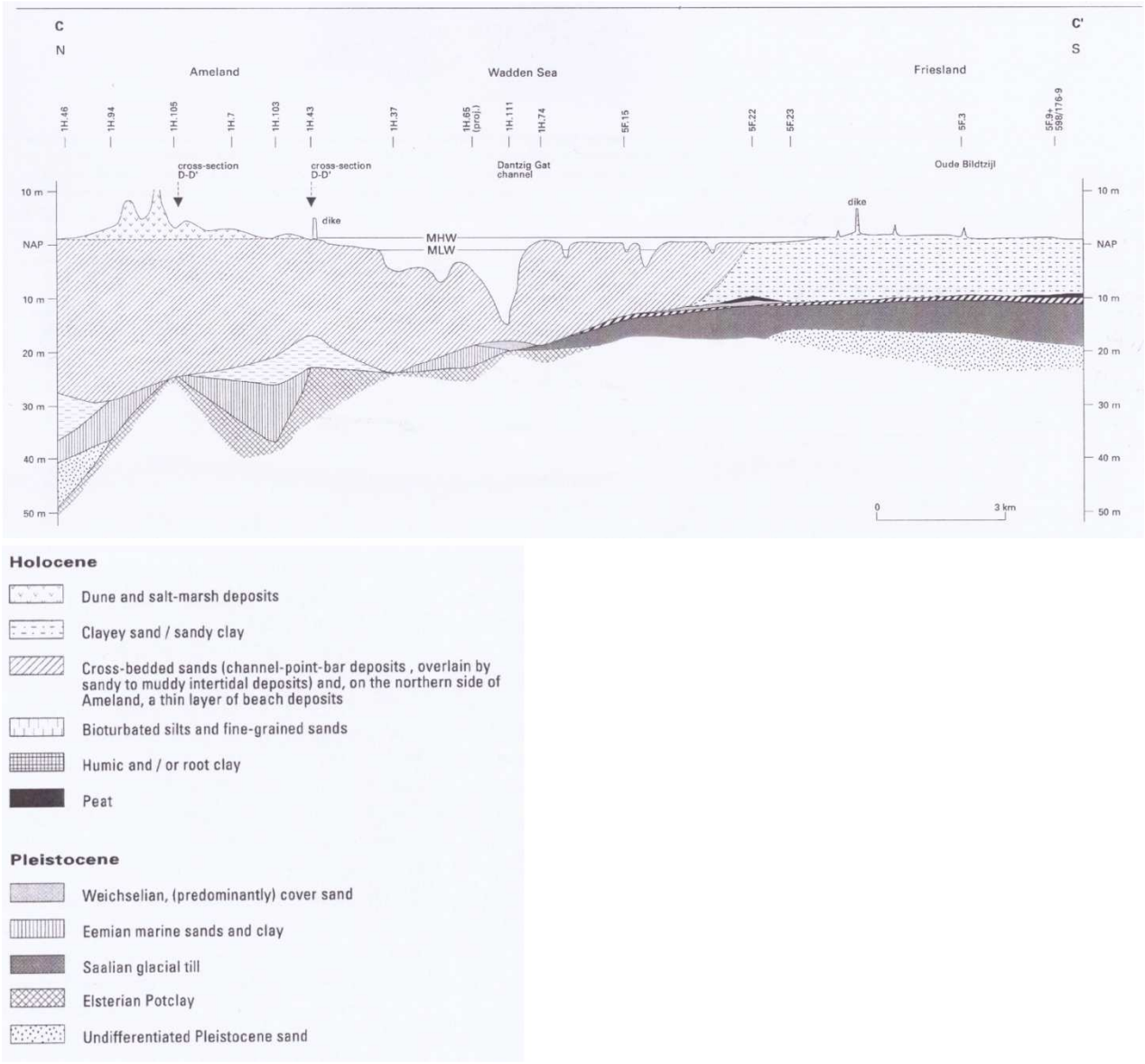

Figure 2.2. Pleistocene and Holocene sedimentary deposits in the Ameland basin (Van der Spek, 1994).

2.1.2 Disturbances in the Waddenzee

Human disturbance

The Dutch Waddenzee has been subjected to human interventions since the early 12th century (Van der Spek, 1996). The early human influence consist of the progressive reduction of the basin by polders along the landwards margin. The neighbouring inlets of Texel, the Zoutkamperlaag and the Zeegat van Terschelling were subject to more recent large scale human interference in the back barrier. These changes are the closure of the Zuiderzee (1932) and Lauwerszee (1969). The effect of the partial basin closure differed for both inlets.

The tidal prism of the Texel inlet increased after the closure of the Zuiderzee. The tidal wave changed from propagating to standing due to the reduced basin length. This resulted in an increase in amplitude and tidal prism. The larger tidal prism increased the need for sediment in the back-barrier and led to a reduction of the ebb-delta sediment volume (Elias, 2006). In the Zoutkamperlaag the closure of the Lauwerzee led to a 30% reduction of the tidal prism. This reduction caused a decrease in the ebb-delta volume (Oost, 1995).

The Ameland inlet has not been subject to large changes in the back barrier area, apart from land reclamation along the Friesland coast and the closure of the Middelzee (13th century) (Van der Spek, 1996). The absence of recent (<150 year) human interventions makes the inlet suitable for the long-term stability modelling aim of this report.

Future disturbance

Tidal inlets remain susceptible to changes in the local environment. The main change in the near future is sea level rise. Relative sea level rise (RSLR) is defined as the eustatic (global) rise in sea level and the subsidence of the ground. Both components are severely affected by human interference due to anthropogenic global warming and the mining of natural gas in the Waddenzee (De Fockert, 2008). Current estimates of RSLR are a 0.35-0.85 m increase during the 21st century, with 2-4 m by 2200.

The effect of future sea level rise is an increased water level and thus of the wet volume (area below high water). The larger wet volume is an indicator of an increased sand demand of the basin (Wang et al., 2011). This sediment must come from the ebb-deltas or the neighbouring barrier islands, which affects the stability and safety of the barrier islands (Louters and Gerriten, 1994). An inability to supply this sand could lead to drowning of the basin. Uncertainties in the sediment transport capacity of the inlets and the sensitivity of the ebb-deltas, with an increased sea level, illustrates the need for accurate computational solutions.

2.2 Tidal inlet morphology and hydrodynamics

The main components of a tidal inlet (figure 2.3) are: the barrier islands, ebb-and flood-delta, inlet channels and the back barrier or basin. They are shaped by the interactions of waves, alongshore currents and tides (De Swart and Zimmerman, 2009). The local balance between the effect of the tides and the waves affects the overall morphology. Stronger waves tend to form more distinct flood-deltas whereas a tidal dominance is linked to more distinct ebb-deltas. A more detailed description of the separate morphologic units, specified to the Ameland inlet, is given below.

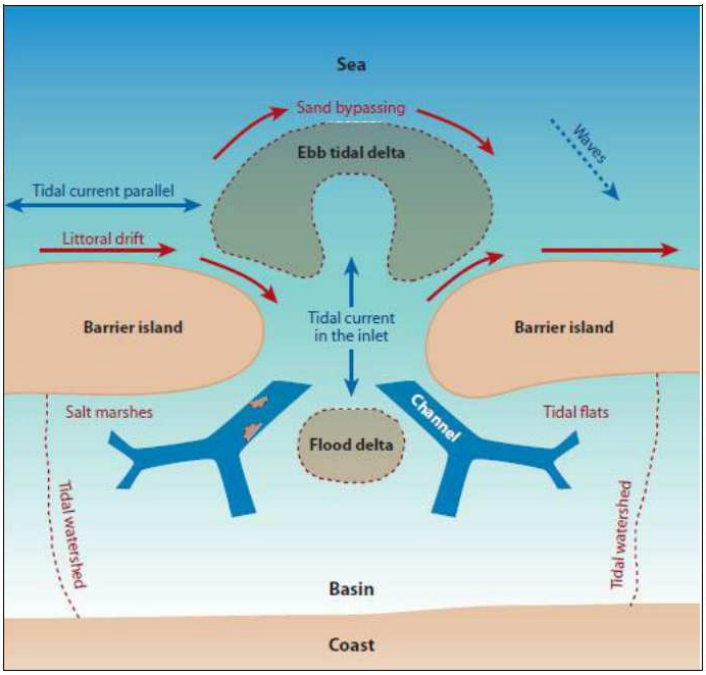

Figure 2.3. Schematized representation of an idealized tidal inlet system. The different morphological units, like the barrier islands, salt marshes, channels, and ebb-and flood delta are indicated. The main physical processes governing sediment transport are given (waves in the main wind direction, tidal current and littoral drift) (De Swart and Zimmerman, 2009).

2.2.1 Morphology

Ebb-delta

On the seaward side of the inlet lies the shallow ebb-tidal delta. This part of the inlet system formed by the jet like outgoing tide (Van der Vegt et al., 2006). It is usually submerged by just a few meters of water, but parts can rise above the mean sea level (De Swart and Zimmerman, 2009). In the Dutch Waddenzee the ebb-deltas are typically oriented to the west (Dissanayake, 2012). The shallow delta folds around the ebb-tidal channel and is comprised of several smaller migrating bars or shoals.
The migration of these shoals is referred to as cyclic bar behaviour, which indicates that sediment bypasses the inlet (Cheung et al., 2007, De Swart and Zimmerman, 2009). The total volume of the ebb-delta is defined by taking the total volume above the average coastline (Walton and Adams,1976), which results in an estimated volume of 130 Mm^3 for Ameland (Cheung et al., 2007).

Flood-delta and basin

On the opposite basin side of the ebb-delta a flood-delta can be present, formed by the radial character of the ingoing flood (Van der Vegt et al., 2006). The distal part of the inlet system is called the basin, back-barrier or lagoon. It houses several different morphologic features and is more muddy then the seaward part of the system. The main morphological features are the tidal channels that display a tree like branching into smaller units and intertidal areas. The intertidal areas are also referred to as tidal shoals, sand- and mud flats.

Tidal channels

Tidal channels transport water from the back-barrier to the sea on each tidal cycle. The transported volume of water is called the tidal prism, which is approximately 480 Mm^3 for the Ameland inlet (Cheung et al., 2007). The widest and deepest section of the tidal channel is situated between the two barrier islands and is called the gorge. In the basin, the channel branches out into smaller channels, where an ebb-and flood dominance can be distinguished (De Swart and Zimmerman, 2009).

Van Veen (1950) was the first to describe ebb-and flood dominated channels and distinguished three different forms in the Waddenzee. The flood channel is more open to the incoming flood and narrows in the basin direction. A sill can be present at the end (figure 2.4a). The ebb-channels display the opposite trend and are open to the ebb-current. The ebb and flood channels never meet and tend to evade each other. Instead they move laterally and approach each other's flanks.

The second type is formed when an ebb or flood channel splits into two smaller separate branches. This results in the embracing of the tip of the channel by the other one (figure 2.4b). The third type is a continuous main channel. In this channel the ebb and flood flow are usually confined to one side of the channel. Over time, when the channel becomes too wide, sediment can accumulate between the ebb and the flood directed flow that leads to the splitting of the system into two separate channels (figure 2.4c).

The Ameland inlet resembles the third type, but differs. It has a single main tidal channel without clear ebb and flood dominated channels (Cheung et al., 2007). Typical tidal flow velocities in the Ameland inlet gorge over a tidal cycle are in the order of ~1 m/s. Measurements of the discharge through the Ameland inlet indicated a maximum $30*10^3$ m^3/s magnitude in the ebb and flood direction over a single tide (Briek et al., 2003).

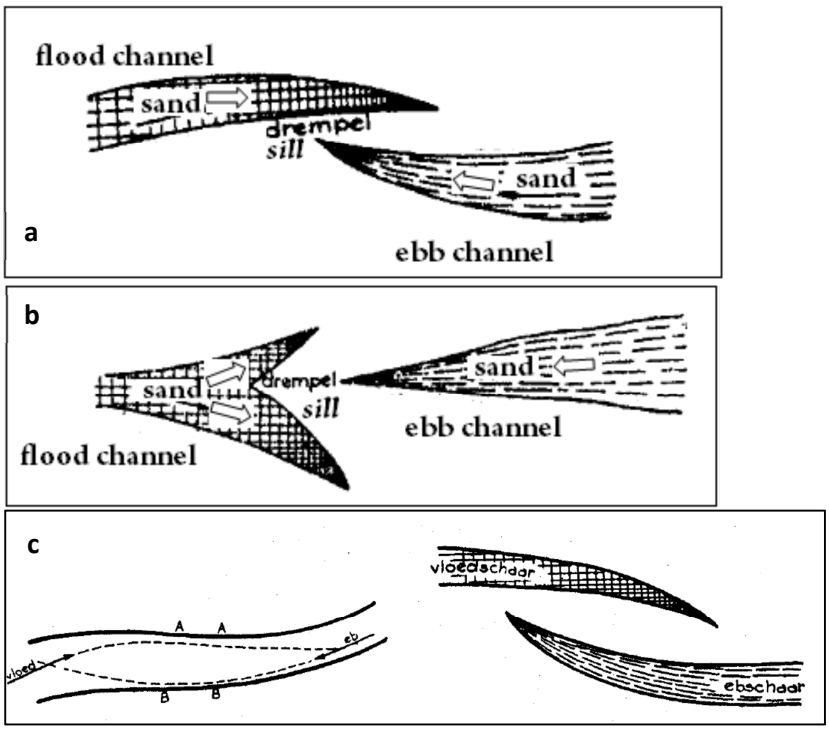

Figure 2.4. (a) Ebb-and flood channels (b) The splitting and embracing of a channel tip (c) Formation of ebb and flood channels by bend action (Van Veen, 1950).

Tidal channel dimensions

The dimensions of a channel can be expressed by the width depth ratio (w/h). In the neighbouring Vlie inlet the main channel w/h ratios were determined using bathymetric data (Terwisscha van Scheltinga, 2012). An overview of the w/h ratios is given in table 2.1. In the distal part of the Vlie inlet w/h ratios of 80-160 were found, whereas in the inlet gorge ratios of 80 are present.

Locally other factors could play a role in controlling the tidal channel geometry. Around the Texel inlet glacial deposits are present that form a boundary for the main inlet. It is hypothesized that the more resistant Pleistocene layers (figure 2.2) prevent incision and force the inlet channel to widen (Van der Spek, *personal communication*).

Channel section	YEAR	depth	width	W/D
Slenk B2	1930	14	600	43
	1950	9	500	56
	1970	6	500	83
	1990	7,5	300	40
	2010 (*)	8	275	34
Oosterom B4	1930	10	700	70
	1950	11	800	73
	1970	12	800	67
	1990	15	500	33
	2010	14	500	36
Oosterom B6	1930	5	400	80
	1950	6	500	83
	1970	5,5	400	73
	1990	7,5	250	33
	2010	6,5	200	31
Vliesloot E1'	1930	7	225	32
	1950	7,5	300	40
	1970	10	450	45
	1990	15	325	22
	2010	18	325	18
Blauwe Slenk D6	1930	10	700	70
	1950	10	1200	120
	1970	9	1500	167
	1990	10	1600	160
	2010	12	1600	133
Blauwe Slenk D7	1930	11	1200	109
	2010	12	1400	117
Inschot D5	1930	15	1300	87
	2010	13	450	35
Noordmeep C4	1930	17	600	35
	1950	15	600	40
	1970	18	700	39
	1990	21	600	29
	2010	20	700	35
Noorder Balgen C5	1930	6	300	50
	2010	12	400	33
Oostmeep Branch C6	1930	5	300	60
	2010	10	250	25
Oostmeep C7	1930	11	700	64
	2010	12	750	63
Inlet channel	2010	35	2800	80
	2010	38	3200	84

Table 2.1. Width depth ratios in the Vlie inlet over the past 80 year period (Terwisscha van Scheltinga, 2012).

Bedforms in tidal channels

The formation of a specific type of bedforms is dependent on the local flow environment (Van Rijn, 2007). Three different types of bedforms are distinguished: small ripples, larger mega-ripples and dunes. The dimensions of mega-ripples and dunes are dependent on the local flow conditions and water depth (Van Rijn, 2007, Bartholdy et al., 2010). The orientation of the major dune crests can be used to determine the dominant ebb and flood flow directions in inlets. Elias (2006) used such a technique to determine sediment transport direction in the Texel inlet. Howver the reversal of the dune crest orientation over a single tide has been found by Van den Berg et al. (1995). This indicates that the interpretation of the results has to be done with care.

For the Ameland inlet no bedform record is available, but they are likely to be present. In other inlets dunes were found of 1.9 m high and 145 m long (Gulf of Cadiz, Spain by Lobo et al., 2000). Sand waves of 85-130 cm high and 45 m long were present near Sapelo Island, Georgia (US) (Zarillo

et al., 1982). In the Danish Waddenzee dunes were 1-1.5 m high (Bartholdy et al., (2002). A description for the Nieuwe Schulpengat of the Texel inlet is given by Elias (2006). There dunes were 50 m long and 0.5 m high at the -15 m contour. In deeper sections of the Nieuwe Schulpengat larger sand waves were found with 200 m wavelengths and 4.25 m crest heights.

2.2.2 Hydrodynamics and sediment transport

The main hydrodynamic and sediment transport component in tidal inlet systems is the tide that propagates from west to east. The tidal average range is approximately 2 m near Ameland and is dominated by the lunar component (M_2). An overview of all the tidal components and amplitudes in the Ameland area is given in De Fockert (2008). In the shallow inlet area the lunar over tides (M_4 and M_6) are important, due to the effect on tidal asymmetry in shallow areas. The asymmetry of the tidal wave refers to the distortion of the tidal wave that alters the flood period in relation to the ebb period (Wang et al., 1999).

The linear interactions of two tidal components generate higher harmonic (M4, M6) tidal components. The main tidal constituent (M_2) and the M_4 harmonic interact and deform the tidal wave. Closer to the shore distortion of the tidal wave occurs because the propagation velocity of the tide (*c*) is given as a function of depth (*h*) and the gravitational constant (*g*) (equation 1). This means the tidal flow in shallow areas consists of a longer less strong ebb duration and a shorter stronger peak flood (Wang et al., 2012). The difference in phase duration and the interaction with the local topography tends to generate residual currents in tidal inlets.

$$(1)\ c = (gh)^{0.5}$$

Residual currents are defined as “time-independent current cells produced by nonlinear tidal rectification, particularly by the interaction of tidal currents and topography” (De Swart and Zimmerman, 2009). These currents have the potential to locally stir up and transport sediment (figure 2.5b). In ebb-dominated tidal inlets residual flow cells tend to form on either side of on the seawards inlet opening in (figure 2.5a) (De Swart and Zimmerman, 2009), due to the tidal phase difference. Oother factors such as grain size or fresh water discharge could play a dominant role in the residual sediment transport patterns (Wang et al., 2012).

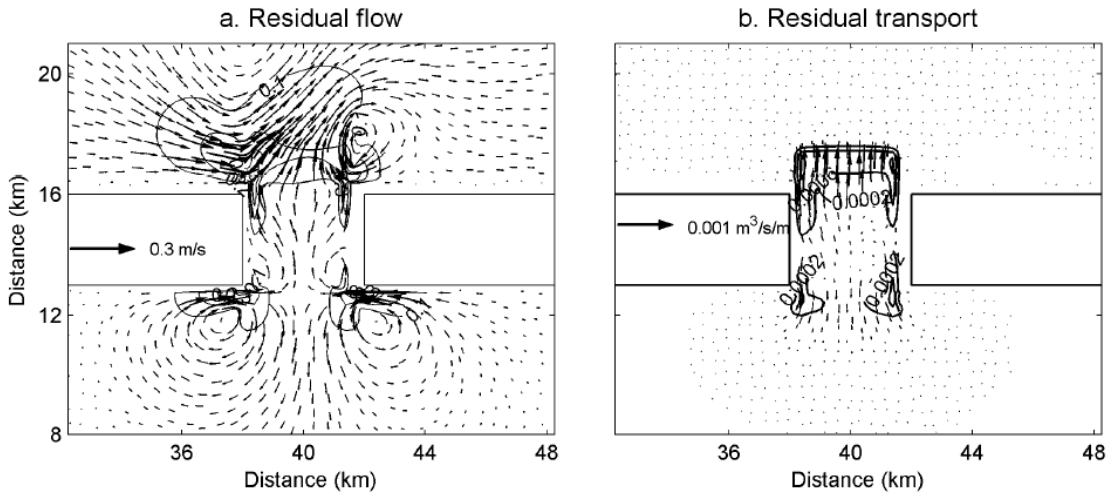

Figure 2.5. (a) Residual flow patterns in a schematized Ameland inlet model. (b) Corresponding residual transports (Dissanayake, 2012).

Tidal watersheds

As the tide propagates from west to east it enters the Waddenzee through the inlets. Due to a phase lag the tide propagating around the island and through the inlet meet in the basin. This location is called a tidal divide or watershed. It is characterised by the smallest variance in effective velocity present over a single tide (Wang et al., 2011). The low effective velocity promotes the settling of fines. The location of the tidal watershed is not stationary.

The closure of the Zuiderzee and Lauwerszee affected the tidal watersheds locations of the Texel, Vlieland and Schiermonnikoog inlets (Wang et al., 2011). The Ameland tidal divide remained relatively stable during these recent basin changes (Wang et al., 2011).

Waves

Incoming waves from the North-Sea dissipate the majority of their energy on the shallow ebb-delta. This reduces the wave related effects in the landward part of the system. It also means the effects of waves on sediment transport, and therefore the morphology, are the largest on the ebb-delta. The mean wave conditions on the Ameland coast are wind dominated with an average wave height of 1 m, while storm events can generate significantly larger wave heights and water levels (Swinkels and Bijlsma, 2011).

Sediment transport fluxes

The sediment transport through the Ameland inlet is tide driven and dominated by suspension. Locally waves stir up sediment and increase the transported sediment volumes (Van der Vegt et al., 2006). An overview of the sediment transport fluxes and directions is given in figure 2.6.

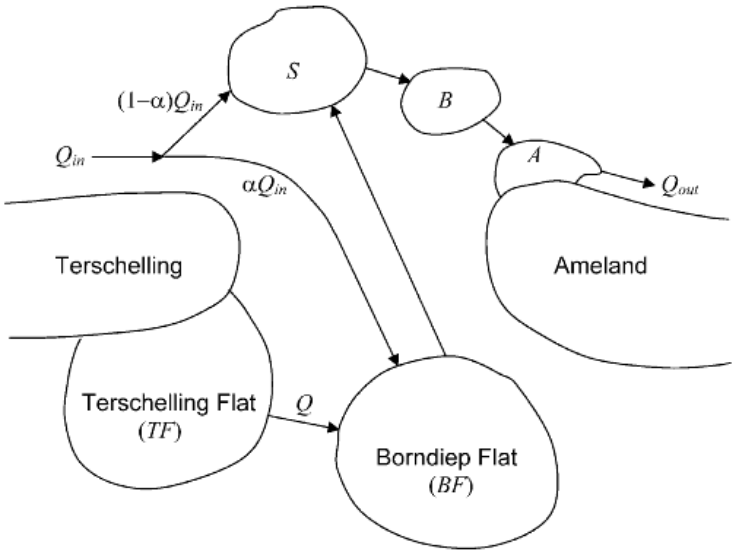

Figure 2.6. Sediment transport direction (indicated by the arrow) and bypassing in the Ameland inlet (Cheung et al., 2007).

The net longshore drift along the islands is from west to east due to the predominantly westerly wave climate. The oblique incoming waves generate a net alongshore current (~0.5-1.0 m/s) from west to east that transports sediment towards the Ameland inlet (Q_{in} figure 2.6). The amount of sediment coming from the updrift (Terschelling) location is estimated at 1 Mm^3/yr (Cheung et al., 2007). This sediment can be imported into the basin (*BF*) by the tidal current (αQ_{in}) or deposited ((1-α) Q_{in}) on the ebb-delta (*S* figure 2.6). Over time sediment is eroded from the basin flats by the lateral movement of channels (*BF* figure 2.6) and transported towards the ebb-delta. The cyclic migration of the ebb-delta (*B* and *A*) delivers sediment to the coast of the neighbouring Ameland barrier island. The sediment that moves in the downdrift direction has "bypassed" the inlet (Q_{out} figure2.6).

2.2.3 Long-term behaviour of the Ameland tidal inlet

Over longer periods the different morphological units and their interactions with the tidal flow, waves and alongshore currents gave rise to different arrangements of the Ameland inlet channels. The rearrangement of channels has been referred to as cyclic, due to a reoccurring lateral shift of the central inlet channels. The apparent cyclic development of the Ameland inlet is described by Israel and Dunsbergen (1999), who distinguished four phases over the past 100 years (figure 2.7).

In phase 1 there is a single channel (Borndiep) in the gorge that divides into two smaller channels on the seaward side, the Akkerpollegat and the Westgat. The orientation of these channels is to the west. In phase 2 the system changes to a two channel system in the gorge. The development of a two channel system in the 1980's meant the Borndiep flowed directly into the Akkerpollegat. This increased the sediment supply to the Bornrif, which increased the bypassing of sediment (Cheung et al., 2007). Phase 3 includes the formation of a small secondary Boschgat channel that flowed into the smaller Westgat. The larger Akkerpollegat was directly seaward oriented. The Bornrif had merged with Ameland. The final phase, phase 4, shows a shift towards the west of the Akkerpollegat. In addition the Boschgat had further reduced in size. The reduction of the Boschgat channel should promote the stability of the Boschplaat on the eastern tip of Terschelling (Elias and Bruens, 2012).

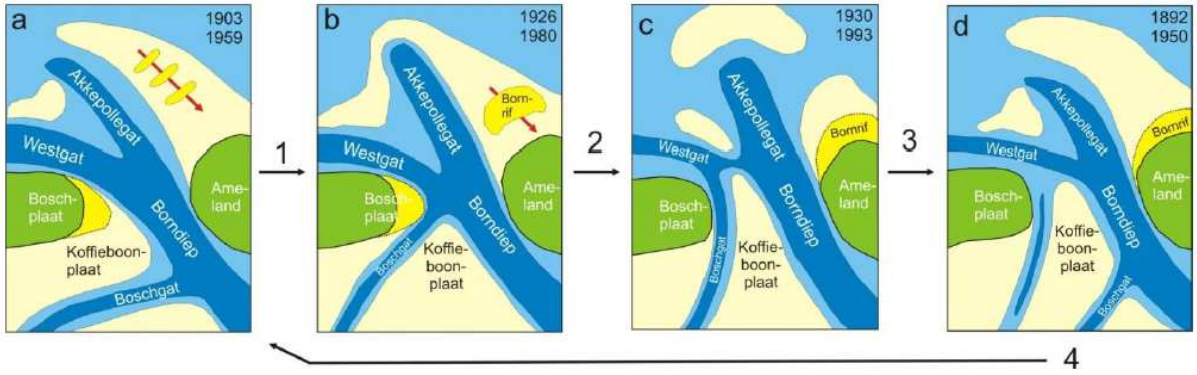

Figure 2.7. Apparent cyclic behaviour of the Ameland inlet (Israel and Dunsbergen, 1999).

2.3 Equilibrium of tidal inlets

In order to model a stable representation of the Ameland inlet a definition of equilibrium is required. Van de Vegt et al. (2006) suggest the equilibrium to be characterised by the absence of morphologic development in the system. However natural systems display a cyclic migration of bars, shoals and channels. This means a decay in the energy dissipation and residual transport could be found, but morphological development remains present (Van der Wegen, 2010). Therefore the stable state of an inlet is referred to as a dynamic equilibrium. The following indications are described for a system moving towards equilibrium (Van der Wegen, 2010):

-More equal ebb and flood durations.
-Phase difference between water levels and velocities of 90° out of phase to prevent Stokes drift.
-Stable tidal prism (*P*) and cross-section (*A*) relation

Empirical equilibrium relations

Stability analysis of tidal inlet systems led to the development of empirical equilibrium relations (Wang et al., 2011). These relations relate the volume of the tidal prism, area of tidal flats and the volume of the ebb-delta to each other. The tidal flat area above mean sea level (A_{fe}) is given by (Wang et al., 2011):

$$(2)\ \frac{A_{fe}}{A_b} = 1 - 2.5 * 10^{-5} A_b^{0.5}$$

where A_b is the basin area. The channel and delta volume relations are summarized by De Fockert (2008). The channel volume is given by:

$$(3)\ V_{channel} = \alpha P^{1.5}$$

with α a proportional constant and P the tidal prism in m^3.

The volume of the ebb-delta (V_{delta}) in m^3 is given by:

$$(4)\ V_{delta} = \alpha P^{1.23}$$

where $\alpha$is a proportional constant.

For the Ameland inlet some relations are summarized by Cheung et al. (2007) to determine the principal hydrodynamics. The main semi-empirical relationship for Waddenzee gorges is based on the mean tidal velocity V and the average depth h_{av}.

$$(5)\ V = 0.334 {h_{av}}^{1/4}$$

The mean tidal velocity can be expressed in terms of the cross-sectional area A of the gorge below mean sea level (m^2), the tidal period T (44.640 seconds for semi-diurnal tides) and the tidal prism P.

$$(6)\ V = \frac{2P}{TA}$$

The equation resulted in an estimated cross-sectional area of 32000-37000 m^2 for one and two channel configurations.

2.4 Delft 3D process-based modelling software

The conducted research for this traineeship focused on the process-based modelling of tidal inlet systems. These models were created with the state-of-the-art Delft3D software developed by Deltares and the Technical university of Delft. The software is based on interlinking separate components that together simulate flow, waves and sediment transport. An overview of the main parameters and components is given in this chapter.

2.4.1 FLOW-module

The basic hydrodynamics are computed in the Delft3D-FLOW module. The software can be used in a full 3D or 2D and 2DH (depth averaged) mode. In this report the 2DH mode is used. This means the shallow water equations, based on the Navier-Stokes equations, are solved. In 2DH mode the effects of the Coriolis force, density difference and wind are neglected. The corresponding continuity and momentum equations are solved in the *x* and *y* direction, given by (Lesser, 2009):

$$(7)\ \frac{\delta\zeta}{\delta t}+\frac{\partial[hU]}{\partial x}+\frac{\partial[hV]}{\partial y}=0$$

$$(8)\ \frac{\partial U}{\partial t}+U\frac{\partial U}{\partial x}+V\frac{\partial U}{\partial y}+g\frac{\delta\zeta}{\delta x}+c_f\frac{U\sqrt{U^{-2}+V^{-2}}}{h}-v_e\left(\frac{\partial^2 U}{\partial x^2}+\frac{\partial^2 U}{\partial y^2}\right)=0$$

$$(9)\ \frac{\partial V}{\partial t}+V\frac{\partial V}{\partial y}+U\frac{\partial V}{\partial x}+g\frac{\delta\zeta}{\delta y}+c_f\frac{V\sqrt{U^{-2}+V^{-2}}}{h}-v_e\left(\frac{\partial^2 V}{\partial x^2}+\frac{\partial^2 V}{\partial y^2}\right)=0$$

where ζ is water level (m), h is the water depth (m) ,v_e is the eddy viscosity, c_f is the friction coefficient and U and V are the depth averaged velocities in the x and y directions.

2.4.2 Transport and roughness

In natural environments sediment transport occurs when the shear stress of the flow exceeds the critical shear stress of the sediment bed. This can be expressed by the non-dimensional Shields value. The Shields number (equation 10) represents the balance between the drag force and lift on a sediment grain. Sediment transport occurs when $\theta_{flow} > \theta_{crit}$.

The required critical shear stress, for initiation of sediment transport, varies depending on the median grain size and the cohesiveness of the sediment. This means that for clay (<8 µm) and silt (<63 µm) a higher shields value is necessary to entrain sediment form the bed (Van Rijn, 2007) than for sand. The volume of transported sediment over a single computational time step can be estimated by a sediment transport equation (chapter2.4.3).

$$(10)\ \theta=\frac{\tau_b}{(\rho_s-\rho)D_{50}}$$

In equation 10 D_{50} is the median grain size and ρ_s and ρ_w are the density of sediment and water. The total shear stress (τ_b) is determined by a quadratic friction law in Delft3D (Hasselaar, 2012).

$$(11)\ \tau_b=\frac{\rho_w g U|U|}{C}$$

In this equation U is the depth averaged horizontal velocity and C the Chézy bed roughness coefficient ($m^{0.5}/s$), which is used in the friction coefficient term (c_f equation 14). The Chézy coefficient is calculated by the White-Colebrook (W-C) equation, which uses the depth (h) and Nikuradse roughness height (k_s) (equation 12). Larger Chézy values indicate a less rough environment and lower shear stress values. The incorporation of the c_f coefficient in the momentum equations (8 and 9) means larger velocities are present with larger (less rough) Chézy values. The larger flow velocities drive an increase in sediment transport (Hasselaar, 2012).

$$(12)\ C=18\log\left(\frac{12h}{k_s}\right)$$

$$(13)\ n=\frac{h^{1/3}S^{1/2}}{U}$$

$$(14)\ c_f=g\frac{n}{\sqrt[3]{h}}$$

In Delft3D the roughness of the bed can be specified using different methods. The first method is to use a spatially and temporally a fixed roughness value, for example Chézy or Manning (equation 13), for flow in the U and V directions. Instead of a fixed value a spatially variable roughness coefficient can be used. Alternatively roughness predictors, based on the presence of bedforms, are available to define a spatial and temporal variable roughness.

The use of a roughness predictor (trachytope function) means the roughness varies in space and time (Van Rijn, 2007). The trachytope roughness can be updated at every time step or over a number of time steps (D_t). The D_t needs to be a multiple of the model time step. It overrides any previously specified roughness value. The resulting related k_s value is used to compute the local roughness coefficient value. The combined quadratic bedform height (k_s) is given by:

$$(15)\ k_s = \min\left(\sqrt{k_{s,r}^2 + k_{s,mr}^2 + k_{s,d}^2}\,\frac{h}{2}\right)$$

where $k_{s,r}$, $k_{s,mr}$ and $k_{s,d}$, are the roughness heights for ripples, mega-ripples and dunes based on the Van Rijn (2007) formulations. The magnitude of a single component depends on the wave current interaction parameter (ψ). An example for the low flow regime current-related bedform height is given in equations 16-18. The equations for the higher and transitional flow regimes are given in the Delft3D-Flow manual and by Van Rijn (2004). For waves computation related friction similar D_{50} based relations are presented

$$(16)\ k_{s,r} = 150 D_{50} \qquad for 0 < \psi < 50$$

$$(17)\ k_{s,mr} = 0.00002 \psi h \quad for\ 0 < \psi < 50$$

$$(18)\ k_{s,d} = 0.0004\, \psi h \qquad for\ 0 < \psi < 100$$

$$(19)\ \psi = \frac{U_{w,c}^2}{(s-1) g D_{50}}\ with\ U_{w,c} = U_{\delta,r} + U$$

Where $U_{\delta r}$ is the representative peak orbital velocity near the bed and U is the depth averaged velocity. The current related frictions coefficient f_c is based on the Darcy-Weisbach formulations ($f=8g/C^2$).

$$(20)\ f_c = \frac{8g}{\left(18 \log\left(\frac{12h}{k_s}\right)\right)^2} = \frac{0.24}{\left(\log\left(\frac{12h}{k_s}\right)\right)^2}$$

The effect of a specific roughness component can be modified by changing a calibration factor α (*RpC*, *MrC* in Delft3D) that is a direct multiplication of the specific bedform roughness height ($k_{s.r}$). For mega-ripples a maximum of 0.2 m is assumed. Setting the calibration factor (*RpC*) to zero removes the roughness component from the computations. Furthermore a relaxation length (*RpR*) is used. A relaxation length of 1 equals 1 computational time step. The individual and combined roughness height terms can be written to the trim-file when *BdfOut* is incorporated in the MDF file. The k_{sr} term is also used by the Van Rijn (2007) sediment transport predictor (Van Rijn, 2004).

2.4.3 Sediment transport predictors

The total sediment transport is defined as the sum of the suspended load and bedload transport. The magnitude of sediment transport, for a specific flow condition, can be estimated by a sediment transport predictor. Various sediment transport predictors are available, but in this report the default Van Rijn (1993), VR93, and Van Rijn (2004, 2007), VR07, equations were used. These are able to implement the effects of waves and flow on sediment transport (Delft3D-FLOW manual).

In the Van Rijn (1993) formulations bedload is computed below a fixed reference height *a* and suspended load above height *a.* Bedload is given by (Van Rijn, 1993):

$$(22)\ S_b = 0.006 \rho_s w_s D_{50} M^{0.5} M_e^{0.7}$$

where:

S_b= bed load transport (kg/m/s)

w_s = settling velocity

M= is the mobility parameter due to waves and currents

M_e = the excess sediment mobility number

u_e =the effective velocity due to currents and waves

$$(23)\ M = \frac{u_e^2}{(s-1)gD_{50}}$$

$$(24)\ M_e = \frac{(u_e - u_{cr})^2}{(s-1)gD_{50}}$$

The suspended load over the depth is given by:

$$(25)\ q_s = \int_a^h uc\ dz$$

$$(26)\ q_s = \int_a^h vc\ dz$$

$$(27)\ c = c_a at\ z = a$$

$$(28)\ c_a = 0.015\rho_s \frac{D_{50}(T_a)^{1.5}}{a(D_*)^{0.3}}\ with\ c_{a,MAX} = 0.05\rho_s$$

in which:

qs = suspended load

u = current velocity (m/s) at height z above the bed in the velocity vector direction

v = wave induced velocity (m/s) at height z above the bed in the wave direction

c = sediment concentration (volume) at height z above the bed

a = reference level (m)

D_*= the dimensionless particle size

T_a= a combination of wave related shear stress expression given in Van Rijn (2004)

In addition more detailed predictors components are used to compute entrainment and settling. An overview is given in the Delft3D flow manual.

The main difference between the Van Rijn (1993) and the Van Rijn (2007) (TRANSPOR 2004) is a recalibration against new data, the extension of the model to incorporate the wave zone and the addition of a bottom roughness prediction. The Van Rijn (2007) bedload prediction is given below in order to illustrate the incorporation of a local roughness. A detailed overview of the suspended load computation is given in the TRANSPOR 2004 Delft3D release notes (Van Rijn, 2004). The bedload transport averaged over a single wave period is given by:

$$(29) S_b = 0.5\ \rho_s D_{50} D_*^{-0.3} \left(\frac{\tau_{b,cw}}{\rho}\right)^{1.2} \left(\frac{\max(\tau_{b,cw} - \tau_{b,cr})}{\tau_{b,cr}}\right)$$

where

$$(30)\ \tau_{b,cw} = 0.5\rho f_{cw} \left(U_{\delta,cws}\right)^2$$

$$(31)\ f_c = 0.24(\log\left(\frac{12h}{k_s}\right)^{-2}$$

$$(32)\ f_w = e^{-6+5.2\left(\frac{A_s}{k_s}\right)^{-0.39}}$$

$$(33)\ f_{c,w} = \alpha^{0.5}\beta_f f_c + (1-\alpha^{0.5}) f_w$$

$$(34)\ \alpha = \frac{\widehat{U}_\delta}{\widehat{U}_\delta + U}$$

in which U_δ is the peak orbital velocity at reference height a, $U_{\delta cw,s}$ is the instantaneous velocity due to current and wave motion at reference height *a*, A_δ is the preak orbital excursion, β_f is the coefficient related to the vertical structure of the velocity profile and $\tau_{c,cr}$ is the critical shields stress.

The reference concentration (c_a) is calculated in the same way as in VR93, but the T_a expression is recalibrated. Furthermore the reference level *a* is determined by:

$$(35)\ a = 0.2h, max(0.5k_{sc,r}, 0.5k_{scwr}, 0.01)$$

where k_{sc} and k_{sw} are the predicted (Van Rijn, 2007) ripple roughness height for currents and waves (chapter 2.4.2). Although a roughness is used for the sediment transport prediction the corresponding hydrodynamics are still sensitive to the specified definition of the roughness implementation.

In the majority of previously conducted long term modelling (Van der Wegen, 2010, Dissanayake, 2012) the Engelund-Hanssen (1967) predictor for total sediment transport is used. The sediment transport predictor gives a total sediment load (q_t) instead of a separate bedload and suspended load fraction.

$$(36)\ q_t = q_b + q_s = \frac{0.05\alpha q^5}{\sqrt{g}C^3\Delta^2 D_{50}}$$

q = the magnitude of the flow velocity
α = tuning parameter
Δ = relative density

2.4.4 Sediment

Sediment can be implemented in 2DH computations as a homogenous distribution of a single grain size or a graded composition of various sediment fractions. The incorporation of graded sediment is based on the concept of Hirano (1971, from Dastgheib, 2012). This concept consists of an active layer (*ThTrLyr*) from which sediment can be eroded and be deposited. Below the active layer additional bookkeeping layers are added (*MxNULy*), of a fixed thickness (*ThUnLyr*), that can be varied to mimic the local availability of sediment (Dastgheib, 2012).

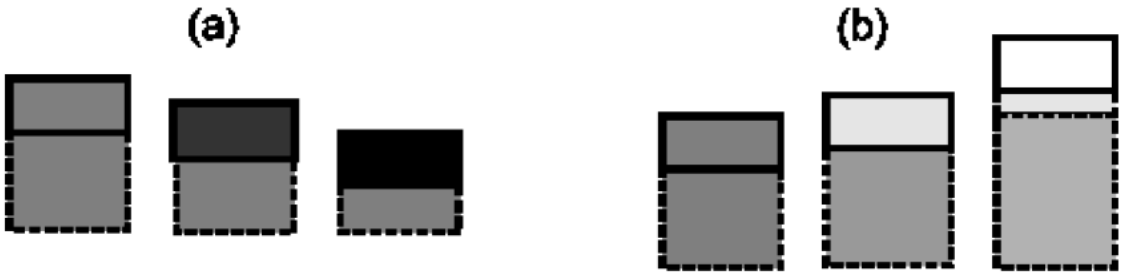

Figure 2.8. Transport layer concept in Delft 3D. (a) Erosion of a cell (b) Sedimentation in a cell. The solid lines represent the active layer and dotted lines the sediment layer. Darker colours are coarser sediments (Dastgheib, 2012).

In case of erosion fine sediment is taken from the active layer, this leads to a coarser layer (figure 2.8a). Sedimentation results in a finer active layer as well as a new book keeping layer that is coarser than the active layer, but finer than the original bookkeeping layers (figure 2.8b) (Dastgheib, 2012).
The incorporation of graded sediment is sensitive to the thickness of the active layer. The layer thickness acts as a controlling factor on the grain size distribution and morphologic development (Sloff and Ottevanger, 2008). Smaller active layers result in a rapid coarsening of the system. This coarser bed in turns affects the composition of the bookkeeping layer and the overall morphologic development. The use of a thicker active layer allows a better representative distribution, with a more realistic morphologic development. An example of this effect is given by Sloff and Ottevanger (2008) on the river Waal, where it was suggested to scale the active layer thickness to the dune height of the system.

2.4.5 Transverse bedslope

The non-cohesive bedload transport in the model is affected in the longitudinal and transverse direction by bedslope effect definitions. These definitions represent a gradient in the initial direction of sediment transport. The longitudinal transport is defined according to Bagnold (1966) by default

and Van Rijn (1993) is used for the transverse direction. The magnitude of the transport can be increased by a factor *AlfaBs* in the longitudinal and *AlfaBn* in the transverse direction (equation 31).

$$(31)\ S_{bmodel} = \alpha_s * S_{btransport\ formula}$$

A different bedslope definition is that of Koch-Flockstra (1980) (K-F), which is used in fluvial modelling and has not been implemented in tidal inlet environments. The required description for implementing K-F is given in appendix III. The addition of the KF bedslope prediction is a modified direction (φ_s) of the original main sediment transport component (φ_t) (equation 37). The Koch-Flokstra (1980) equation also allows the tuning of the *AlfaBn* factor, but in practice it should be set to default (Sloff, *personal communication*).

$$(37)\ tan(\varphi_s) = \frac{sin(\varphi_t) + \frac{1}{f(\theta)}\frac{\partial z_b}{\partial y}}{cos(\varphi_t) + \frac{1}{f(\theta)}\frac{\partial z_b}{\partial x}}$$

The magnitude of transverse transport depends on a weight function of the Shields number (θ, equation 10), which is given by the Talmon et al. (1995):

$$(38)\ f(\theta) = 9\left(\frac{D_{50}}{h}\right)^{0.3}\sqrt{\theta}$$

given in Delft3D by:

$$(39)\ f(\theta) = A_{sh}\theta^{B_{sh}}\left(\frac{D_i}{H}\right)^{C_{sh}}\left(\frac{D_i}{D_m}\right)^{D_{sh}}$$

The terms A_{sh}, B_{sh}, C_{sh} and D_{sh} are tuning parameters. A_{sh} (*Ashld* keyword in Delft3D) is the main tuning parameter and determines the effect of gravity on the grains. The lower range of values 0.35-0.5 should result in shallower wider channels whereas the upper range 1.0-1.5 generates deeper narrower channels. B_{sh} is set to 0.5 by default. The other parameter C_{sh} is a tuning value for the bedform effect. The last variable D_{sh} is the hiding exposure tuning parameter (Van Breemen, 2011).

2.4.6 Morphologic development

A fixed bathymetry can be maintained to determine the sediment transport fluxes in a system. Alternatively sediment transport can be combined with updating of the model bed, in order to allow morphologic development. With morphologic change the bed is updated after every flow computation step. The flow module first determines the magnitude of sediment transport in a single cell. This is then corrected for the cell interfaces and the transverse bedslope. The change in the local bed level is determined at the centre of the computational cell. The corresponding hydrodynamics are computed for the same cell centre (*Mor* setting). The *Mor* setting is an important factor to consider when comparing the model to those validated for hydrodynamics (*Mean* setting).
The morphologic module of Delft3D is fitted with a morphological acceleration factor (equation 35. This factor reduces the time required to model morphologic development, by multiplying the bed development over a single computational step (equation 35). The basic validity of the *MORFAC* factor depends on an absence of irreversible changes in the system over one computational step. A detailed evaluation of the MORFAC in modelling applications is given by Lesser (2004).

$$(35)\ \Delta t_{morphodynamic} = MORFAC * \Delta t_{hydrodynamic}$$

Mormerge

The Delft3D *MorMerge* method uses a multi-core approach to solve a range of forcing conditions and combine the effects in the morphologic updating of the bed (Roelvink, 2006). An example of such a variable is the use of multiple wave conditions from multiple incidence angles. The net effect of the all the wave related sediment transport is used in the morphologic updating scheme.

2.5 Tidal inlet modelling

Models of tidal inlets can be divided into two different groups. The first group are physical scale experimental representations (Reynolds, 1887, Kleinhans et al., 2012). The second are process-based models (Lesser, 2009, Dastgheib, 2012 Dissanayake, 2012). In this chapter an overview of both types of studies is presented.

2.5.1 Physical scale experiments

Since the early work of Reynolds (1887) there have been several attempts at creating scaled down representations of natural systems. Tambroni et al. (2005) used a laboratory setup where an erodible channel was connected to a tidal sea. The water level in the sea was controlled by filling and emptying the basin, similar to the early experiments of Reynolds (1887). The resulting morphology resembled concave beach profiles and tidal bar like bedforms that agreed with theoretical predictions. However the experiments were affected by the formation of ripples. Stefanon et al. (2009) conducted a similar series of laboratory experiments, aimed at investigating the initial tidal network formation, which also suffered from similar unwanted bedform formation.

Recently experiments were carried out that successfully created scale experimental meandering rivers (Van Dijk et al., 2012). The strategy of these experiments was to scale down the system in terms of sediment mobility. In order to ensure a realistic mobility, steep longitudinal slopes and hydraulic rough flow conditions were deemed essential. The sediment mobility based approach led to the tidal experiments by Kleinhans et al. (2012), where the basin was tilted to drive the flow in the ebb-and flood direction.

When regarding figure 2.9 the main features of tidal inlets can be observed in the scaled-down system. The ebb-tidal delta is the lobe like feature on the bottom left of the image. The barrier islands were formed by fixed elements. The basin area displays the branching of the central channel into smaller tidal channels. Equilibrium in the inlet development was observed as a shift in morphologic development from the entire basin and inlet to the inlet. It was suggested that this could be either a scale effect or that in natural systems perturbations (RSLR, storms and biological processes) are required to maintain a dynamic system.

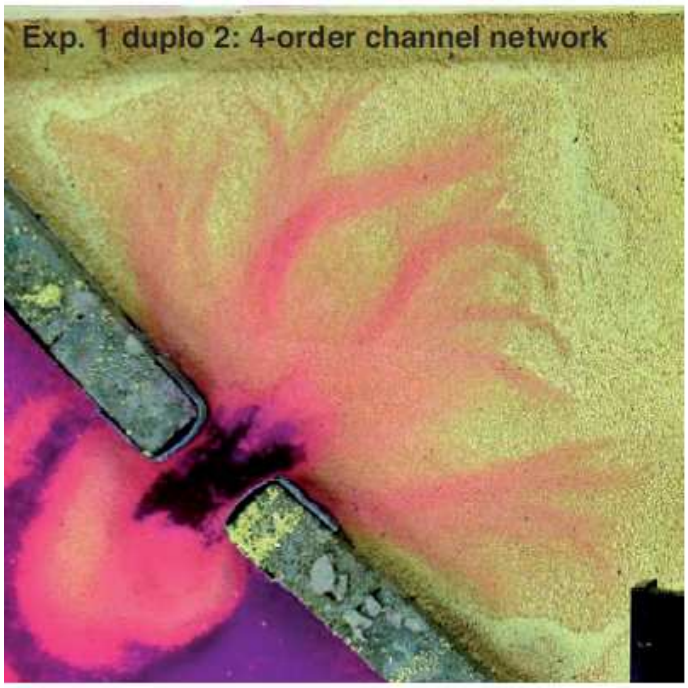

Figure 2.9. Physical scale model representation of a tidal inlet system (Kleinhans et al., 2012).

2.5.2 Process based models

Process-based models are based on solving the Navier-Stokes shallow water equations (chapter 2.4). The idea behind long term process-based morphological modelling is that, by incorporating enough of the physics into a model, eventually the most important features of the morphological behaviour will come out, even at longer time scales. The validation of Delft3D process based morphological models, for a range of scenarios, is discussed in detail in the work of Lesser (2009).

Delft3D process-based studies were carried out with two different aims. The first is related to reproducing the short term (days-months) hydrodynamic behaviour (Swinkels and Bijlsma, 2011) and sediment transport patterns of tidal inlets (Elias, 2006). The second group investigated the morphologic development of tidal inlet systems on long terms. The long term studies can be divided into timescales of decades (De Fockert, 2008), a century (Dastgheib, 2012, Dissanayake, 2012 and millennia (Van der Wegen, 2010). Furthermore the long term studies can be dividend in for- and hindcasts of natural systems and conceptual models.

Short term studies

The hydrodynamic characteristics of tidal inlets are reproduced in various modelling studies. A short term model of the Texel inlet (Elias, 2006) reproduced validated flow patterns. Water levels and flow velocities can also be successfully modelled for storm events, as was done for the Ameland inlet (Swinkels and Bijlsma, 2011). The hydro-dynamically valid models allowed the addition of sediment transport, without morphologic bed updating, in order to model transport directions and magnitudes in the inlet (Schouten and Van der Hout, 2009). The model output generated insights in the detailed sediment transport processes in unmonitored parts of the inlet (Elias, 2006). The information gained from the model data in the short term simulations illustrates the potential of long term process-based models in understanding tidal inlets.

Medium term studies

De Fockert (2008) modelled the morphologic development of the Ameland inlet between 1993 and 1999 (figure 2.10). This was done by using the Van Rijn (2007), TRANSPOR2004, sediment transport prediction with the corresponding bedform roughness height prediction for ripples and mega-ripples in combination with a single fraction 260 µm sediment bed.

With just the principle tidal conditions the hindcast was subjected to incision along the central channel. The addition of a parallel computed wave conditions (*MorMerge*) reduced the central channel erosion. In other studies the magnitude of the wave effect was determined by the balance between the tidal range and the wave height. A more pronounced wave influence resulted in a less pronounced the ebb-delta (Dissanayake, 2012). The model with waves was characterised by an unrealistic seaward outbuilding of the ebb-delta.

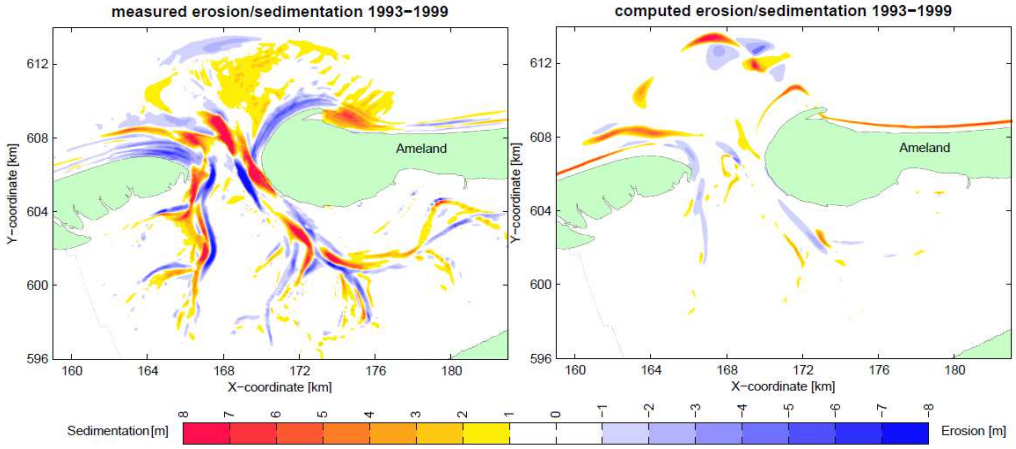

Figure 2.10. Sedimentation/erosion patterns in the natural inlet and a hindcast with combined flow and waves (De Fockert, 2008).

Long term studies

The model of De Fockert (2008) incorporated the hydrodynamic and bathymetric characteristics of the natural inlet over a 10 year interval. Dastgheib (2012) investigated the Waddenzee development on a longer (200 year) scale in order to determine the ability of process-based models to represent natural systems. It was found that the representation of the system was valid for local sections and specific processes, for example sediment exchange.
Often schematizations are made to model the long term behaviour. The schematizations consist of using an idealized bathymetry, principal tidal and wave components, total load Engelund-Hanssen (1966) sediment transport prediction and a fixed homogenous roughness value. The longest term schematized model setup simulations (Van der Wegen, 2010) simulated periods up to 8000 years. The models created dynamic systems from an initial flat bathymetry. The development of these idealized environments led to the formation of dynamic equilibriums.

2.5.3 Channel stability

The long term morphologic modelling studies of the Waddenzee tidal inlets were characterised by an unrealistic incision of the main tidal channels. Several different methods were used to produce more stable channels (Van der Wegen, 2010, Dastgheib, 2012, Dissanayake, 2012).
The slope of the banks is an important factor to consider, for steep banks imply cohesive banks. This means the height of the banks must not be too high to prevent gradients larger than the angle of repose (Van der Wegen, 2010). In order to correct this transverse bedlope effect was increased. The effect of increasing the transverse effect on the cross-sectional development is given in figure 2.11a.The default value (*AlfaBn* 1.5) led to unrealistic channels, whereas larger *AlfaBn* of values promoted wider and shallower channels (Dissanayake, 2012). It should be noted that larger transverse bedslopes increase the morphological wavelength, a relation between bar lengths and the tidal prism, in long term schematized environments (Van der Wegen, 2010).

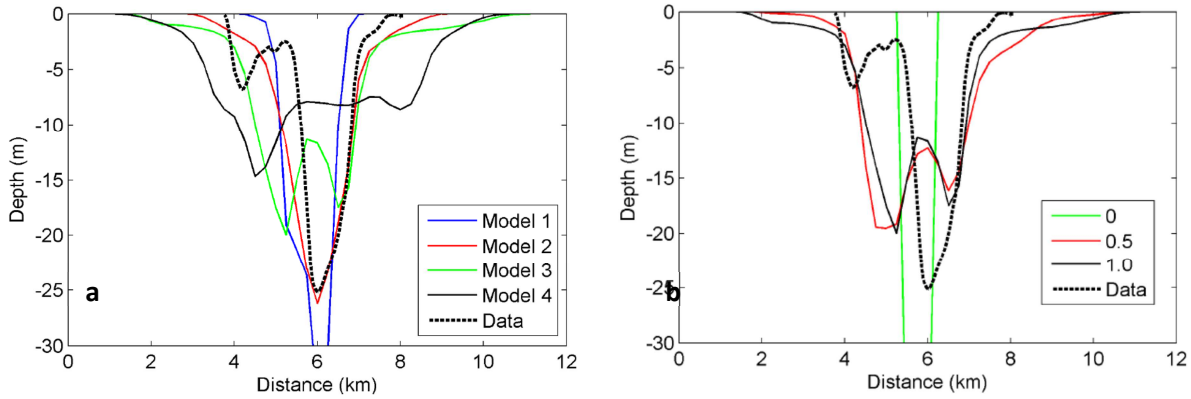

Figure 2.11. (a) Incised tidal inlet channels in the schematized model of Dissanayake (2012). The corresponding AlfaBn values are (model 1) 1 (model 2) 20 (model 3) 50 (model 4) 100. (b) The corresponding Dry cell erosion values are given in the legend.

The dry cell erosion factor (DCE, *ThetSd* keyword in Delft3D) promotes the erosion and sedimentation in dry neighbouring cells in order to simulate bank erosion (Van der Wegen, 2010). A default value of 0 means no erosion and sedimentation takes place in neighbouring dry cells. A DCE of 1 means all the erosion and sedimentation takes place in the neighbouring cells. The default value of 0 led to unrealistic channels that incised to large depths (figure 2.11 b). The use of larger 0.5 (50% of erosion in neighbouring dry cell) and 1 values improved the morphology of the channels. Furthermore large cell erosion factors produced better representations of the ebb-delta compared to low values that led to an increased seaward extended delta in long term simulations (Dissanayake, 2012).
Alternatively the response as a result of a graded sediment bed (chapter 2.4.2) and initial distribution were investigated (Dastgheib, 2012). The graded bed approach maintained the same D_{50}

as the natural system (0.250 µm), but a combination of fine and coarse sediment fractions was used. The initial grain sizes fractions are given in table 2.2 for a minimum and maximum size scenario. In Delft3D 5 underlayers of 2 m thickness were used with an active layer of 1.5 m. The total amount of sediment available below the initial bed was set at 65 m.
The inlet channel response improved compared to a homogeneous sediment initial flat bed (250 µm) with the Engelund-Hanssen (1967) sediment transport prediction. The improved channel response is given in the cross-sectional profile in figure 2.12b and the corresponding grain size is given in figure 2.12a.

Fraction	Minimum size (mm)	Maximum size (mm)
1	0.075	0.150
2	0.150	0.300
3	0.300	0.425
4	0.425	0.600
5	0.600	1.180
6	1.180	2.360

Table 2.2 Sediment classes incorporated by Dastgheib (2012).

Instead of an initial uniform graded distribution an optimal initial sediment size was determined (Dastgheib, 2012) using the sediment fractions listed in table 2.2. This was done by using a hydrodynamics run and correlating the D_{50} value to the shear stress. The resulting bathymetry of the tidal inlets channels displayed better agreement with measurements in a 70 year hind cast of the Dutch Waddenzee. It is suggested that this method solves the unrealistic incision in Waddenzee inlet models.
It should be noted that the D_{50} value in the centre of the channel peaks at 1.4 mm (figure 2.12a), which was the largest D_{50} fraction incorporated in the model (table 2.2). Although these grain sizes are found in the Pleistocene sub-layers of the Texel inlet (Elias, 2006) the D_{50} value is approximately 3 times larger than is present in the Ameland inlet (SedimentAtlas). Since the Ameland area was part of the model by Dastgheib (2012) the validity of the used grain size fractions in the Ameland is questionable.

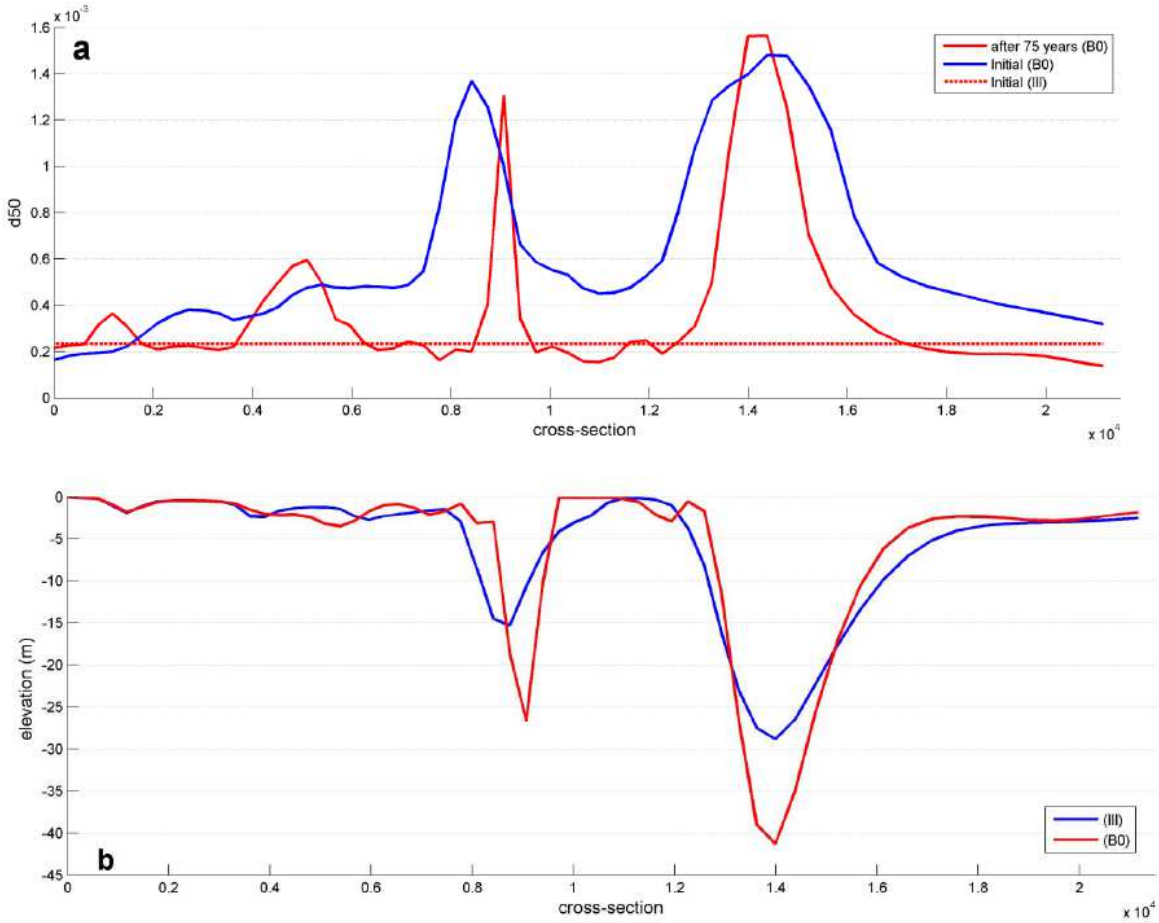

Figure 2.12.(a) Spatially varied D_{50} the initial model bed profile (B0), homogeneous sediment bed (II) and final bed grain size are given (Dastgheib, 2012). (b) Bed development with a spatially varying D_{50} for the space varying model run (B0) (Dastgheib, 2012).

Summary of process based modelling

It can be summarized that tidal inlet representations can be divided into two different types of models. The first are those that accurately represent the hydrodynamics in which morphologic development is left out and a fixed bathymetry is used (Swinkels and Bijlsma, 2011). The second group are models with the addition of morphologic development and sediment transport on short (Elias, 2006) and longer terms (Dastgheib, 2012).

The long-term morphodynamic model display an unrealistic incision of the tidal channels. This has been corrected by using spatial grain size distributions (Dastgheib, 2012), increased transverse bedslopes and dry cell erosion effects (Dissanayake, 2012).

3. Synthesis and research questions

The presented selection of literature illustrates the main morphologic components and hydrodynamic interactions in the Ameland inlet system. Furthermore the long term process-based modelling studies (chapter 2.4.3) indicate that in process-based models the main inlet channel might not be stable and various additional approaches are necessary to reduce the unrealistic incision. This knowledge is combined in order to develop a more stable long term model of the Ameland inlet.

Ameland inlet morphology and development

The Ameland inlet consists of a large shallow ebb-delta on the seaward side. The basin area consists of a large tidal channel that branches out into several smaller channels. The Waddenzee inlets are dominated by the influence of the semi-diurnal tides (Dissanayake, 2012). The small-scale morphology of the ebb-delta is largely determined by the local wave climate (De Swart and Zimmerman, 2009). The waves redistribute the sediment, supplied by the tides, along the coast, and drive the alongshore transport towards the east (Cheung et al., 2007). The long-term natural development of the Ameland inlet is characterised by an apparent cyclic shift in the main channel location and ebb-delta development (Israel and Dunsbergen, 1999). This cycle can be observed twice in the past 90 years.

Process-based models

Recent studies have shown that the complex flows in tidal inlets can be reproduced well (Elias, 2006, Swinkels and Bijlsma, 2012). This suggests that models should be able to model the morphologic development of tidal inlet systems. However in previous long term process-based tidal inlet modelling studies a severe incision of the central inlet channel was present (Dastgheib, 2012, Dissanayake, 2012). The severe incision led to irreversible changes in the model and an alternate equilibrium state not comparable to nature. Several methods used to correct this model artefact were summarized in chapter 2.5. These methods do not address the cause of the channel instability, but only address the effects.

The common approaches in long term modelling are:

1: "Concrete" layers

The use of an un-erodible "concrete" layer forces the model to limit itself to a certain depth. A drawback of this model setup is that channels become too wide and scour holes can be found at the end of the non-erodible or armoured layer.

2: Coarse and graded sediment beds

A coarse grain size reduces the sediment transport and creates more realistic channels (Dastgheib, 2012). The use of this method might present unwanted effects on the ebb-delta due to the incorporation of unrealistic grain sizes, because of the large D_{50} values that were used compared to the natural Ameland grain sizes.

3a: Increased transverse Bedslope effect

An increase in the transverse bedslope created more realistic channels (Van der Wegen, 2010, Dissanayake, 2012). It is uncertain how these larger downslope effects aggect the morphologic development outside the channels. The mobility of the ebb-tidal delta shoals could be reduced.

3b: Increased Dry cell erosion factor

Van der Wegen (2010) and Dissanayake (2012) increased the dry cell erosion factor to 1 in order to produce stable channels by simulating bank erosion of dry cells. It should be noted that this means all bank erosion and sedimentation occurs in the neighbouring cell.

4: Homogeneous roughness representation

It is suggested that using a homogeneous roughness value is valid in long term simulations (Van der Wegen, 2010), because seasonal variations should not affect the long term development. However in short term hydrodynamic models detailed fixed spatial roughness definitions are used (Swinkels and Bijlsma (2012).

5: Engelund Hanssen and Van Rijn (1993) sediment transport predictions
Long-term modelling studies often use the Engelund and Hanssen (1967) equation, which only gives the total load representation (Dissanayake, 2012) and does not include additional wave-driven transports. The default Van Rijn (1993) equation can be used to model waves and suspended transport, however it also resulted in deeply incised channels (Dissanayake, 2012).

3.1 Research questions
Although recent research has modelled the long term development of tidal inlets (Dastgheib, 2012 Dissanayake 2012), the main inlet channels rapidly incised to unrealistic depths and presented an unrealistic equilibrium (Dastgheib, 2012). The main aim of this traineeship report is to investigate what morphological boundary conditions are required to create an equilibrium process-based model of the Ameland tidal inlet.

Question 1
The evaluation of the model assumes stable channels in the natural Ameland system over the past 100 year period. The question is:
What is the natural Ameland inlet channel development in the previous 90 years and what are the corresponding width depth ratios?

Question 2
The design of a stable process-based model makes it necessary to perform a basic sensitivity analysis of different parameters. In order to conserve computational time the following questions is:
On what timescale are morphological boundary conditions to be evaluated?

Question 3
Previous long term modelling studies used the Engelund-Hanssen (1967) transport predictor (Van der Wegen, 2010, Dastgheib, 2012). The main drawback is an inability to take suspended sediment and waves into account. The conventional default suspended sediment transport predictor yielded unstable channels (Dissanayake, 2012, Dastgheib, 2012)). The next question is:
What is the difference between the default (Van Rijn, 1993) and the Van Rijn (2007) sediment transport prediction on the morphologic development?

Question 4
The work of Dastgheib (2012) illustrated that the addition of a graded sediment bed reduced the depth of the inlet channels in long term simulations.
What is the effect of a homogenously distributed single and graded sediment fractions on the long term stability of the channels?

Question 5
It is suggested that the seasonal effects can be neglected and a homogenous value should produce a representative morphology (Van der Wegen, 2010), whilst short term research used a local bedform roughness prediction (De Fockert, 2008).
What is the effect using a fixed homogenous roughness compared to a space depended bedform based roughness value on the long term morphologic development?

Question 6
Conventional tidal inlet models are manipulated into stable states by increasing the transverse bedslope effect (Dissanayake, 2012). Other expressions, used in fluvial research (Sloff and Ottevanger, 2008), could improve the tidal inlet stability in long-term simulations. The final question is:
What is the effect of increasing the transverse bedslope and incorporating the Koch-Flokstra (1980) transverse bedslope correction compared to the default response?

4. Methodology and Methods

4.1 Methodology

The main aim of this report is to investigate the required settings to create an equilibrium representation of the Ameland inlet channels in a process-based model. The morphological boundary conditions to be evaluated in this report include the sediment transport prediction, definition of the bed roughness, transverse bed slope effects, dry cell erosion factor, MORFAC value and grain size characteristics and distributions. These morphological boundaries will be evaluated in an idealized representation of the Ameland inlet.

Modelling strategy
First measured bathymetric data of the inlet will be used to determine the natural development over the past 90 years in order to create a frame of reference for the model evaluation (figure 4.1). The second step is the development of a model of the Ameland inlet. This model will be designed to have a short runtime to allow a rapid evaluation of different settings and morphological boundary conditions. The numerical complexity will be reduced by neglecting the effects of wind and waves and a using coarse gird cell size. The last step will be the evaluation of different morphological boundary conditions on the long term (100 year) development of the Ameland inlet.

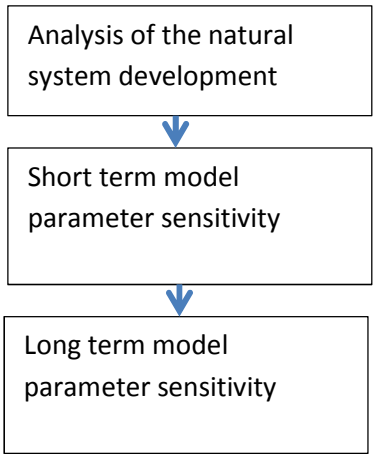

Figure 4.1. Conceptual order of the modelling approach and model development used in this report.

4.2 Methods

In this chapter the collection and analysis of the natural inlet data is presented. Next, the used Delft3D (chapter 2.4) model setup and boundary condition are presented. Last the analysis techniques and strategies of the model output are given.

4.2.1 Natural Ameland inlet data

Local parameters are required to evaluate the natural system behaviour. Measurements of such parameters, the local bathymetry and grain size characteristics, are available via the shared information system OpenEarth.

Bathymetry and cross-sectional profiles

Bathymetric surveys have been conducted, by Rijkswaterstaat, since 1925. The bathymetric survey data is divided into 10x12.5 km blocks, known as Vaklodingen. The Vaklodingen of the Ameland inlet were used study the natural channel development. They are repeated at regular intervals since 1971 and together these measurements create a database spanning the period from 1925 to 2011 for the Dutch coast and Waddenzee. Measurements prior to 1985 have a 250x250 m resolution and 20x20 m since.

The natural channel development was monitored qualitatively by plotting Digital Elevation Maps (DEM) of the bathymetry. The detailed changes between the time steps were determined by creating erosion/sedimentation maps. Finally cross-sectional channel profiles were drawn at various locations in the system.

The selected cross-sectional locations were chosen to be as perpendicular to the channel as possible over all the available time steps (1925-2008) (figure 2.4). The emphasis of the cross-sectional profiles lies on the development of the main tidal channels (Borndiep and Dantziggat). The width of the channel in the cross-sections was determined by using a -5 m NAP threshold. The intersection of the channel profiles with this depth threshold, on either channel side, marked the width of the channel. The corresponding depth was chosen at the maximum depth for a specific profile.

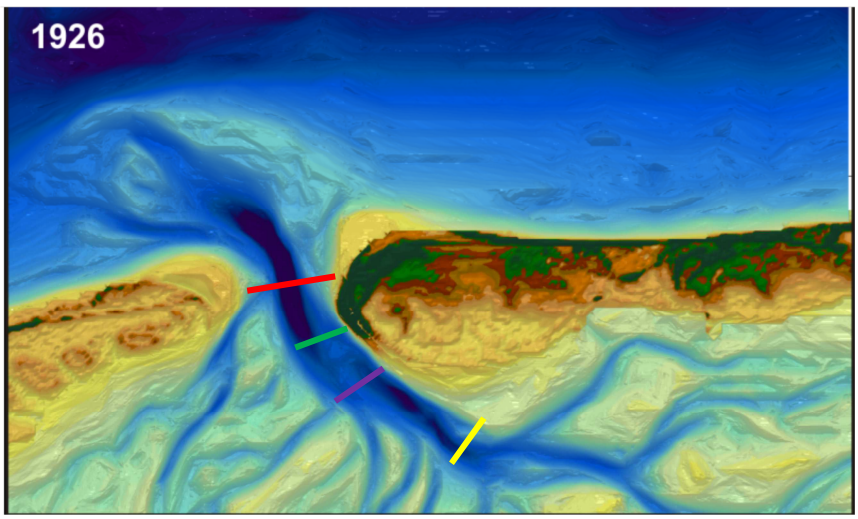

Cross-section (colour)	**Reference name**
Red(1)	Borndiep1
Green(2)	Borndiep2
Purple(3)	Borndiep3
Yellow(4)	Dantziggat

Figure 4.2. Overview of the cross-sectional profile locations in the Ameland inlet and the names used in the rest of the report.

Sedimentatlas

The same OpenEarth database was used to import the sediment characteristics of the area. This dataset, known as the "Sedimentatlas" contains grain size distributions of the Waddenzee. An overview of the grain sizes in the Waddenzee is given in figure 4.3. The average D_{50} in the Ameland inlet intertidal areas is around 200 µm. The Borndiep and Boschgat channels are coarser with sizes between 240 and 300 µm with local maxima of 400 µm.

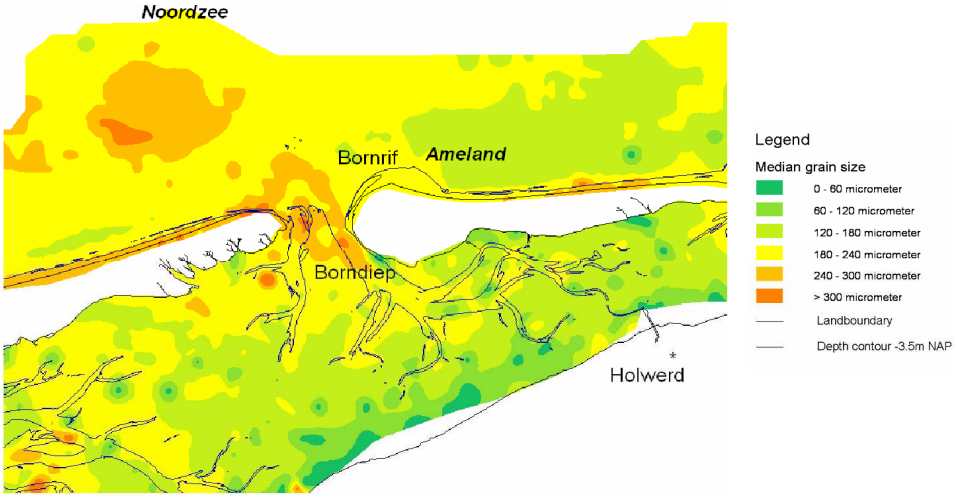

Figure 4.3. Sedimentatlas grain size data of the Waddenzee. The corresponding D_{50} values, in millimetres, are given in the legend (De Fockert, 2008).

4.2.2 Model setup

The models in this study were used to evaluate effects of different morphological boundary conditions and simulate the long term morphological development of the Ameland inlet. The same model formed the basis for the short term (2 year) trials and long term (100 year) runs.

Model domain

The basis of the model was the grid of the Ameland inlet (figure 4.4), based on the 2005 Vaklodingen). The size of the grid cells on the distal parts of the model was 300x300 m. In the central gorge the grid cell size refined to 200x200 m (figure 4.4).

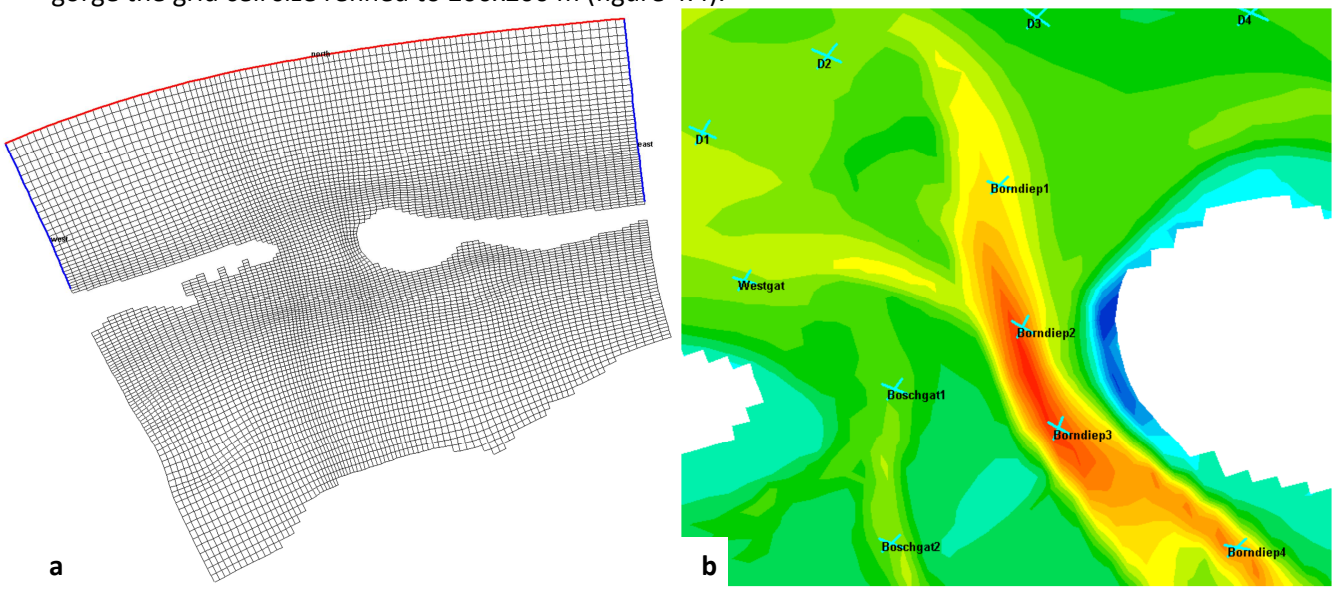

Figure 4.4.(a) Model grid and boundaries (b)observation stations of the model used in this report.

The boundary conditions were taken from Dissanayake (2012), who used a similar model setup. An overview for the harmonic North Sea water level forcing is given in table 4.1. The Western and Eastern open sea boundaries were set to Neumann boundaries with a gradient. The Waddenzee boundaries coincided with the tidal divides and were closed boundaries. The sediment transport exchange over the boundaries was set to 0 kg/s for all runs presented in this report.

These boundary conditions are a close approximation of the required tidal flow condition of this model. They are not validated against measurements. The Ameland environment is chosen in order to generate a frame of reference to test morphologic response to different morphological boundary conditions. This means a direct comparison with Ameland in terms of morphological development and sediment transport magnitudes should not be made. Only the relative responses of the model runs should be compared with each other.

Tidal component	**Frequency** (*deg/hr*)	**Amplitude west** (*m*)	**Phase west** (*deg*)	**Amplitude east** (*m*)	**Phase** (*deg*)
M_2	28.9933	0.8450	20.2	0.9200	53.3
M_4	57.9866	0.0938	259.5	0.861	304.4

Table 4.1. Boundary conditions along the seaward edge of the model (north) indicated in figure 4.4b.

The selected time step in model computations depends on the Courant number (*Cr*). The courant number is given by:

$$(36)\ Cr = c\frac{\Delta t}{\Delta x}\ with\ 0{,}1 < Cr < 10$$

where c is the wave celerity, Δt (s) is the computational time step and Δx the grid cell size (m). For the model grid (figure 4.4b) a computational time step of 1 minute was within the Courant number boundaries and used in all model runs. The models are started from initial uniform conditions (water level =0). A spin-up time of 900 minutes was used to ensure stable hydrodynamics prior to stating the bed updating. The basis of the model is the given in Appendix (I). An overview of the corresponding model parameters of the runs in the results section of this report is given in the Appendices (II and III).

Sediment transport and roughness

The sediment transport predictions of Van Rijn (2007) and the default Van Rijn (1993) were used (chapter 2.5). The roughness was defined with a homogenous Chézy value (65 $m^{0.5}/s$) or Mannings value (0.021), a space varying Manning value (Swinkels and Bijlsma, 2012) (figure 4.5) or by the VR07 bedform roughness height prediction (chapter 2.5). The required components for the implementation of a bedform roughness prediction are given in Appendix II.

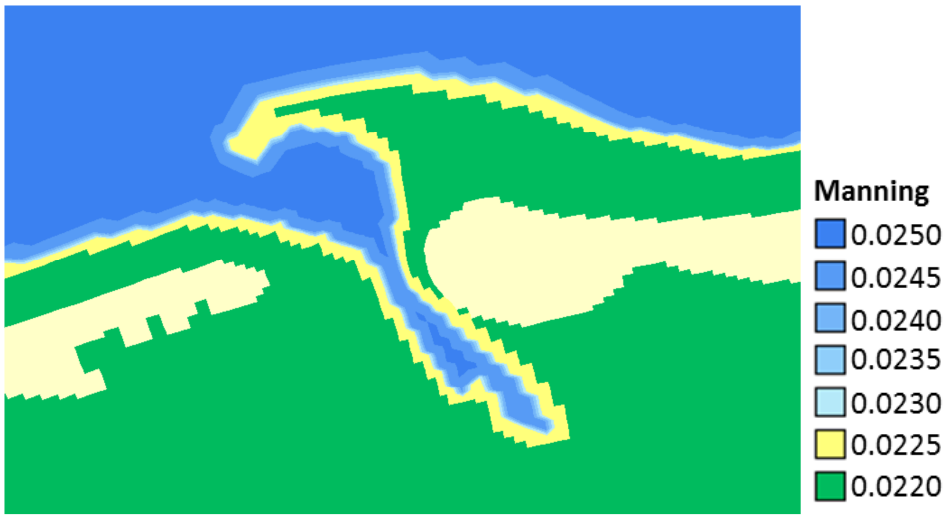

Figure 4.5. Space variable Manning roughness file used in the modelling.

Sediment

Different sediment bed scenarios were incorporated in the model that ranged from different size homogeneous sediment to graded beds. The corresponding graded bed grain sizes are given in table 4.2 for a realistic scenario and with an increased D_{50} (I, II) due to addition of a single coarse layer.

Realistic case (μm)	400	300	200	100
Increased I (μm)	1000	300	200	100
Increased II (μm)	1000	400	300	200

Table 4.2. Overview of the used realistic and increased sediment fractions.

The initial layer composition was varied to isolate the effects of fine and coarse layers on the morphological development and investigate the response to a variable layer definition (table 4.3).

	Finest (m)			**Coarsest** (m)
Equal layer	10	10	10	10
Reduced fine I	2	10	10	10
Reduced fine II	2	2	10	10

Table 4.3. Overview of the sediment composition scenarios.

4.2.3 Analysis and comparison of model results

In order to determine the performance of a model, different analysis techniques were used. The qualitative performance of the model was determined by visually comparing the generated morphology against other model output as well as the natural inlet. The main definition of equilibrium in the model output was a limited incision of the main channel. The incision was checked at the gorge and in the basin against the initial channel profile.

Volumetric change

The volumetric change in the basin and seaward part of the model was determined by multiplying the sedimentation/erosion with the area to get a volume. Positive and negative changes are separated based on a >0 and <0 criteria within a predefined polygon. The polygons are chosen to incorporate all of the morphologic features in the model, but exclude the disturbances along the boundaries.

5. Results

In this chapter the development of the main Ameland inlet channel over the period 1925-2008 is presented (chapter 5.1). This is followed by the output of the model for different parameter setting for a short (2 year) (chapter 5.2) and long (100 year) period (chapter 5.3).

5.1 Natural channel development

When regarding the channel development over time (figure 5.1) it can be seen that the deepest part of the inlet was located between the barrier islands over the entire 85 year interval. On the seaward part of the inlet the central channel was oriented to the west in 1925 and 1971. Between 1971 and 1993 an eastward rotation of seaward part of the channel was present. In this period the eastern shoal of the ebb-delta (Bornrif) migrated towards Ameland. After 1993 the seaward channel started to curve towards the west. Additionally a smaller second inlet channel (Boschgat) formed in 1971, which curved around Terschelling to the west. It migrated slightly eastward and remained active up to 2011.

In the basin changes occurred in the main channel location between 1925 and 1971. In this period the deepest part of the gorge moved east and the southern part of the main channel became more curved. Between 1971 and 1993 the basin part of the main channel did not display large developments. Later maps (1999-2011) indicate a reduction in depth for the distal part of the Borndiep. More detailed channel development trends can be observed in the sedimentation erosion maps of the area (figure 5.2).

The erosion (blue areas) and sedimentation (red areas) zones are highlighted in figure 5.2 for the period 1975-2011. Between 1975 and 1989 there were only small zones of local erosion and sedimentation present in the basin part of the main Borndiep and smaller tidal channel branches. After 1989 the central channel displayed several changes. The gorge eroded on the Ameland side and sedimentation occurred on the Terschelling side. In the basin erosion along the length of the Borndiep was present. In the smaller distal tidal channel branches a lateral shift can be observed between 1989 and 1999. This shift is indicated by erosion on one side of the channel and sedimentation on the opposite channel bank margin. In the final figure (e) a similar lateral displacement of the Dantziggat was present, whilst the gorge remained stable.

The seaward part of the system displayed an erosion zone on the eastern part of the ebb-delta (Bornrif) that migrated towards the Ameland island head (1981-2008). On the downdrift side sedimentation, was present along the Ameland coast (1989-2008). On the central ebb-delta the largest changes in bathymetry were found on the previous flow paths of migrating tidal channel. West of the inlet the changes coincided with the development of the secondary Boschgat channel. The westward expansion of the channel marked erosion of the Terschelling barrier island tail in the period 1979-1981. In later stages 1981-1993 sedimentation was present in the Boschgat. The intertidal flats did not display large areas of erosion or sedimentation. The effects of in channel erosion and sedimentation are studied in detail by regarding several cross-sectional profiles.

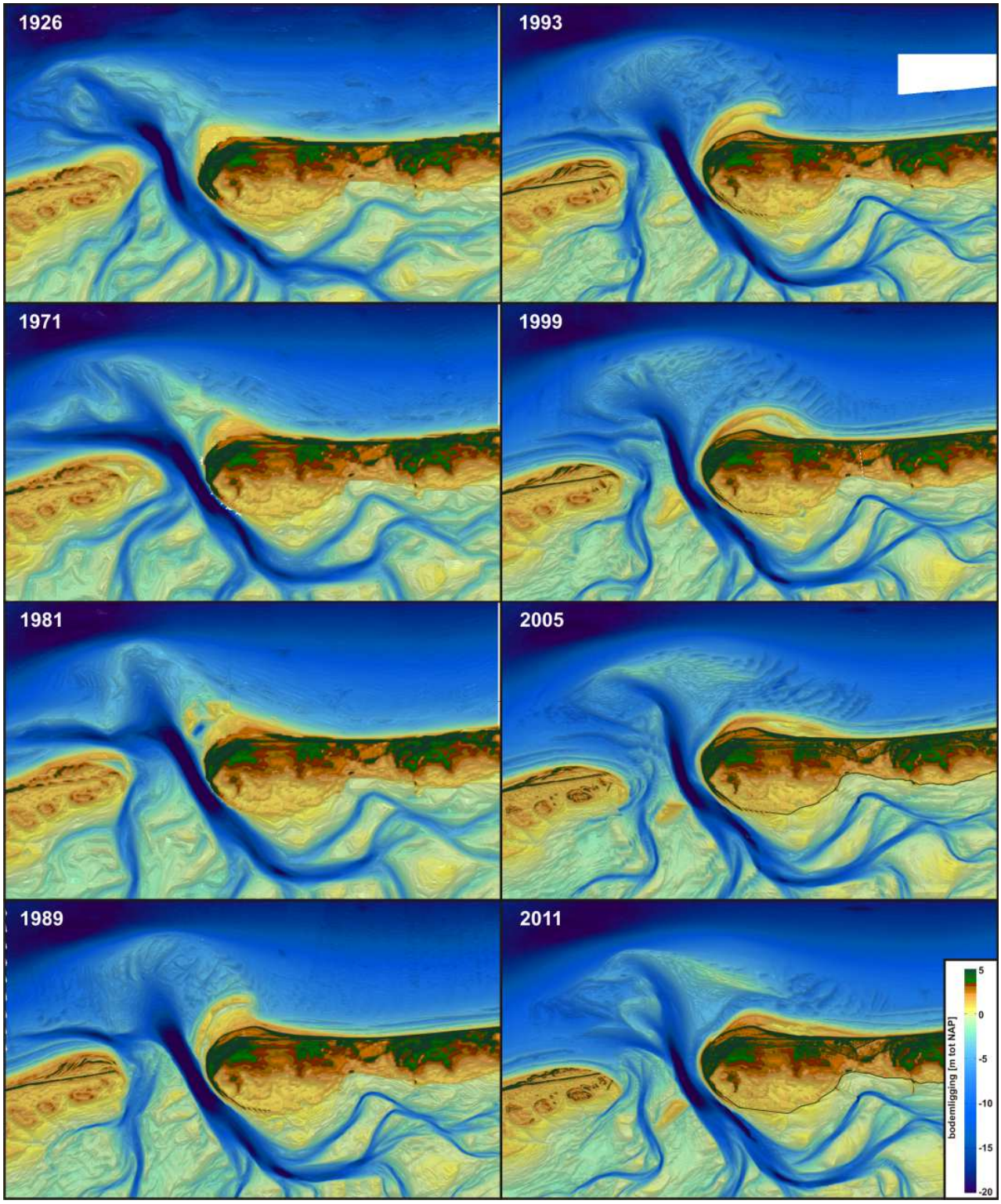

Figure 5.1 Overview of the historical development of the Ameland inlet based on bathymetric surveys (Beheerbibliotheek KPP, 2013).

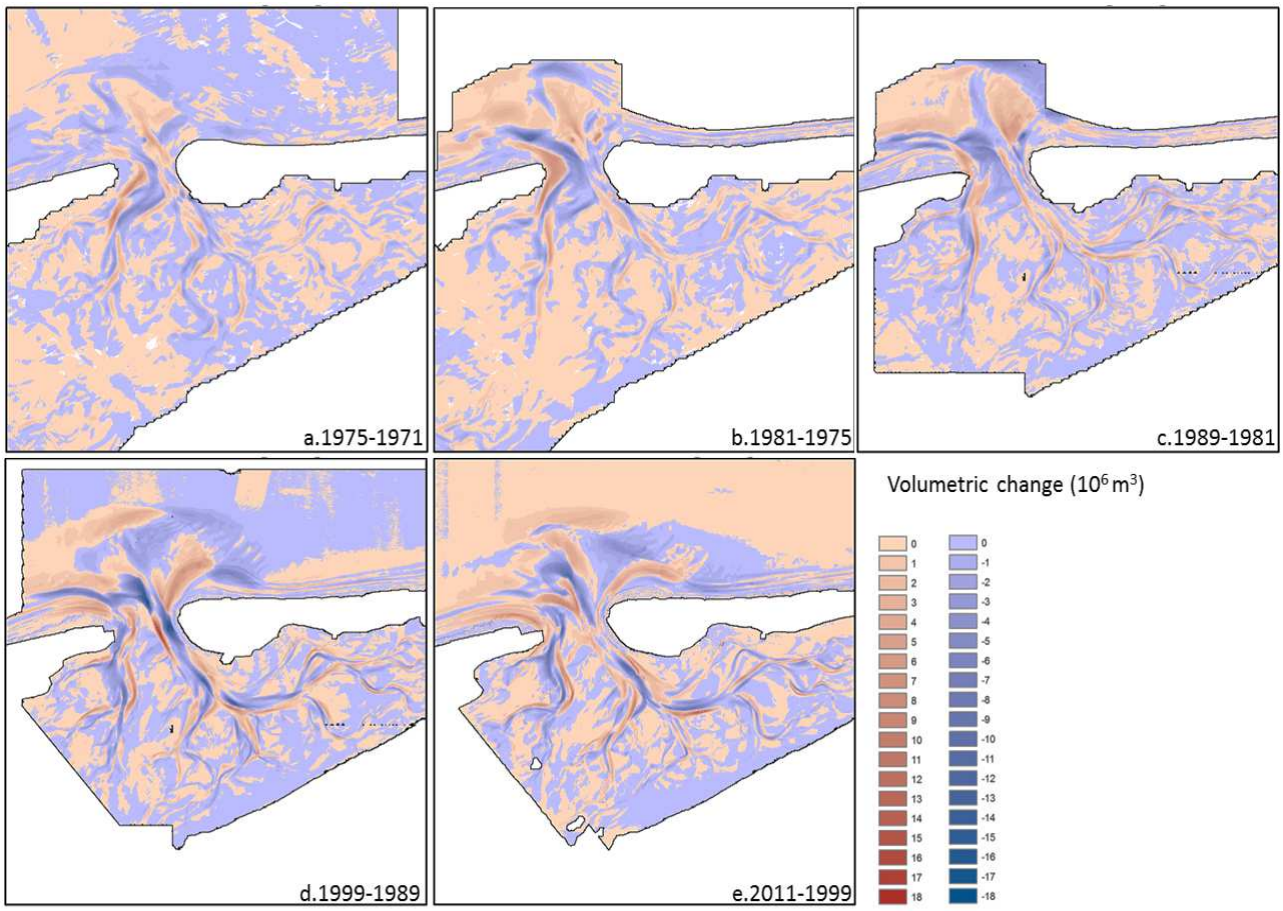

Figure 5.2. Erosion and deposition between two consecutive bathymetric surveys. Red indicates sedimentation and blue erosion. The corresponding magnitude is given in the legend (based on Willemsen, 2013).

Cross-sectional profiles and width depth ratios of the Ameland inlet

In table 5.1 the corresponding w/h ratios are given of the cross-sectional profiles, with a -5 m channel margin threshold (chapter 4.2). The detailed difference in channel dimensions and locations (1925-2008) allows for several observations to be made (figure 5.3a).

The largest change in the central Borndiep profile occurred between the 1925 and 1975. The channel shifted eastward, widened and reduced in depth from -27 to -25 m. This increased the w/h ratio from 57 to 99. The development from 1975 onward indicated a stationary channel that narrowed and deepened, -25 m in 1975 to -28 m in 1993. This reduced the w/h ratio to 37 in 1993. In 2008 the channel was located further east and had a reduced -24 m depth.

In the basin part of the Borndiep (figure 5.3b) the 1925-1975 development was characterised by an eastward shift and an increase in depth to -27 m NAP. Variations in width and depth were limited (1975-1981) and w/h ratios around 45 were present. After 1981 a reduction in depth and a westward directed lateral displacement could be observed. This reduction in depth and westward directed lateral displacement continued up to 2008.

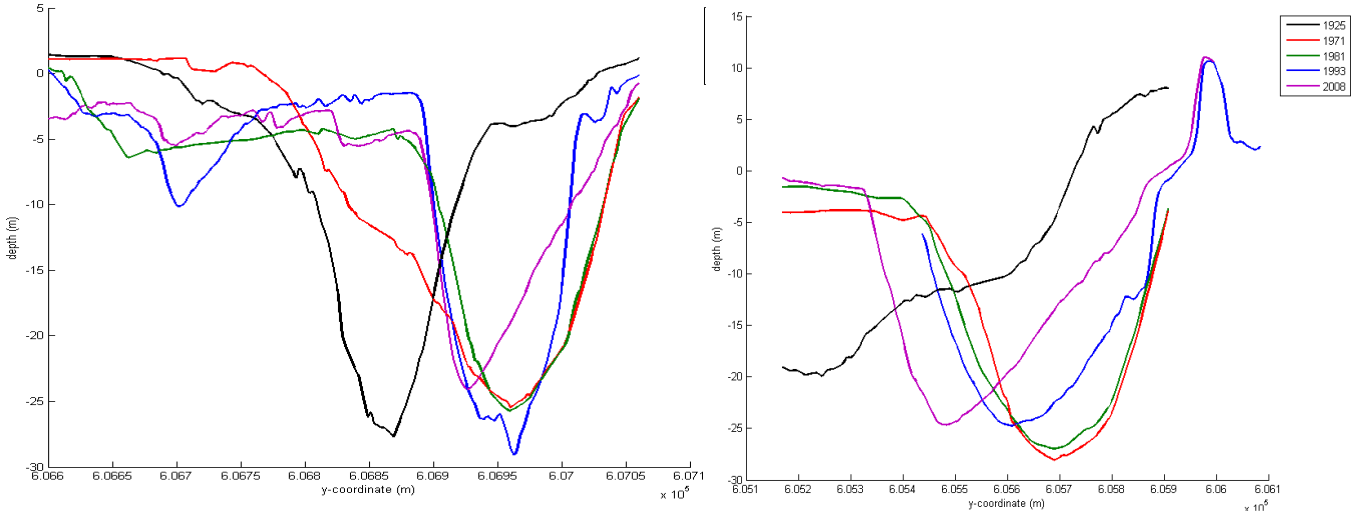

Figure 5.3. (a) Cross-sectional profiles in the Borndiep(1) between the barrier islands.(b) Cross-sectional profiles in the basin part of the Borndiep(2) (figure 4.2). Ameland is on the right in both images.

In the more distal Dantziggat the response displayed a lateral shift and increase in depth that reduced the w/h ratio from 144 to 104 between 1925 and 1975. After 1975 the system progressively increased in depth to -23 m in 1993. This reduced the w/h ratio from 144 to 76. Similar to the Borndiep the 2008 profile displayed a lateral displacement and a reduction in depth to -15 m NAP (figure 5.3) that increased the w/h to 135.

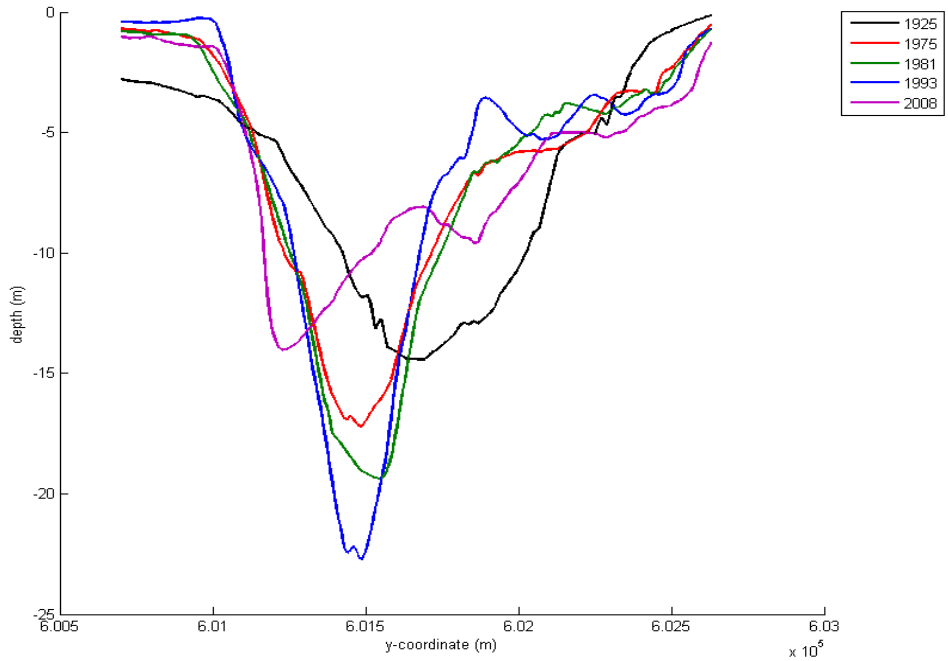

Figure 5.4. Cross-sectional profiles in the Dantziggat(4) figure (4.2). Ameland is located on the right.

Summary channel development

The overall trends of the channel are a large lateral shift and increase in depth between 1925 and 1975. From 1975 to 1981 the development was stable. 1981 marked the start of the incision and narrowing of the channel throughout the basin. The incision reached the maximum extent in 1993 after which a reduction in depth and a westward directed lateral shift were present.

cross-section	year	depth (m)	width (m)	w/h
Borndiep	1925	27.7	1303	57
	1971	25.5	1811	99
	1981	25.7	1403	67
	1993	29.1	905	37
	2008	24.7	1204	63
Borndiep (2)	1971	28.1	1029	45
	1981	26.9	984	44
	1993	24.8	984	49
	2008	25.2	1118	56
Borndiep (3)	1925	18.9	1720	123
	1971	19.2	1272	89
	1981	15.9	1581	144
	1993	18.1	1581	120
	2008	19.0	1561	112
Dantziggat(4)	1925	14.4	1360	144
	1971	16.6	1220	104
	1981	19.1	1081	76
	1993	22.6	860	80
	2008	14.0	1220	135

Table 5.1. The widths and depths for the Ameland inlet based on the -5 m width threshold (chapter 4.2). The presented depth values are not corrected for the channel margin threshold.

5.2 Short term model

In this section the basic hydrodynamics of the model are presented (chapter 5.2.1). This is followed by the morphologic development as a result of different parameters setting during the short 2 year simulation period (chapter 5.2.2).

5.2.1 Hydrodynamics

The semi-diurnal tide drove the flow in the model. The water level and the corresponding velocity magnitude in for are given in figure 5.5a for the model with the bedform predicted roughness. The maximum velocity (1.1 m/s) coincided with the ebb part of the water level signal. Flood velocities were slightly lower at 0.9 (m/s). The roughness prediction and space variable Manning file velocity signals are identical. In the more distal parts and seaward part of the system the velocities reduced. The combined *m*- and *n*–direction velocity magnitude in the gorge had local maxima of 1.6 m/s over a single tide. The corresponding instantaneous discharge maximum over a single tide through the inlet was approximately $30*10^3$ m^3/s in the flood and $-30*10^3$ m^3/s in the ebb-direction (figure 5.5b).

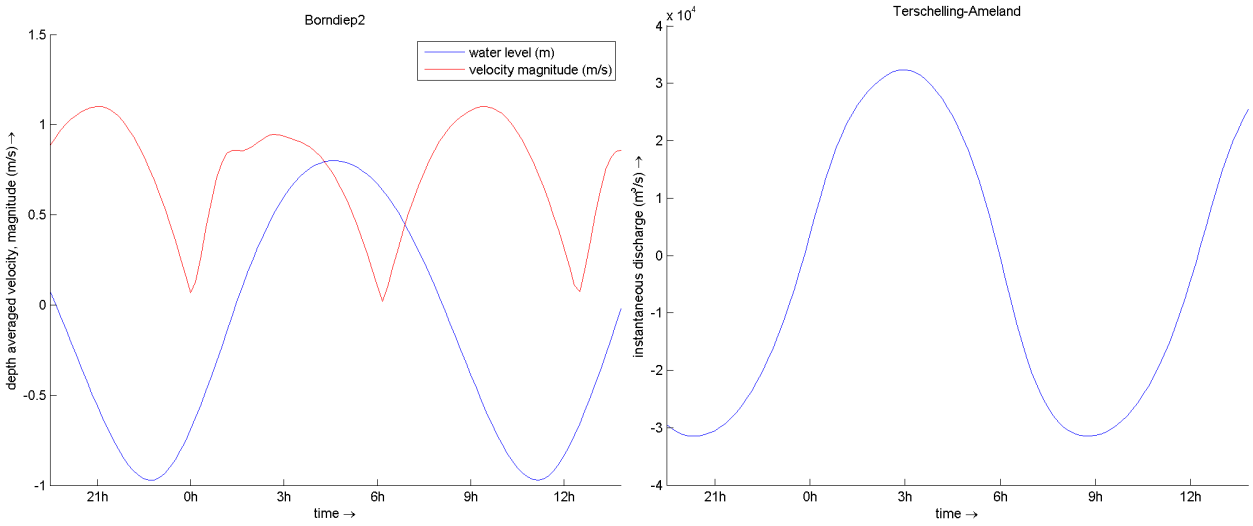

Figure 5.5. (a) Water level (m) velocity magnitude (m/s) in the gorge. (b) Instantaneous discharge (m3/s) between both islands over a single tide.

5.2.2 Morphologic development

In order to evaluate the model results on short time periods the same cross-sectional, Borndiep and Borndiep (2) locations indicated in figure 4.2, are plotted for the different scenarios. The default model settings are given in appendix I.

Default sediment transport predictor

The default sediment prediction (Van Rijn, 1993) was used to investigate the effect of varying the grain size of a homogenous sediment bed on the channel development. In figure 5.6a the cross-sectional bed development is given. In all scenarios there was incision of the central channel and the formation of an additional channel on the left of the profiles. The largest incision of the bed level (-3 m) was present for the 200 µm sediment bed. The incision reduced for increasingly coarse beds. The largest (1000 µm) fraction profile development was limited to 30 cm of incision. The bed profile response trends are the same for the channel in the basin (figure 5.6b).

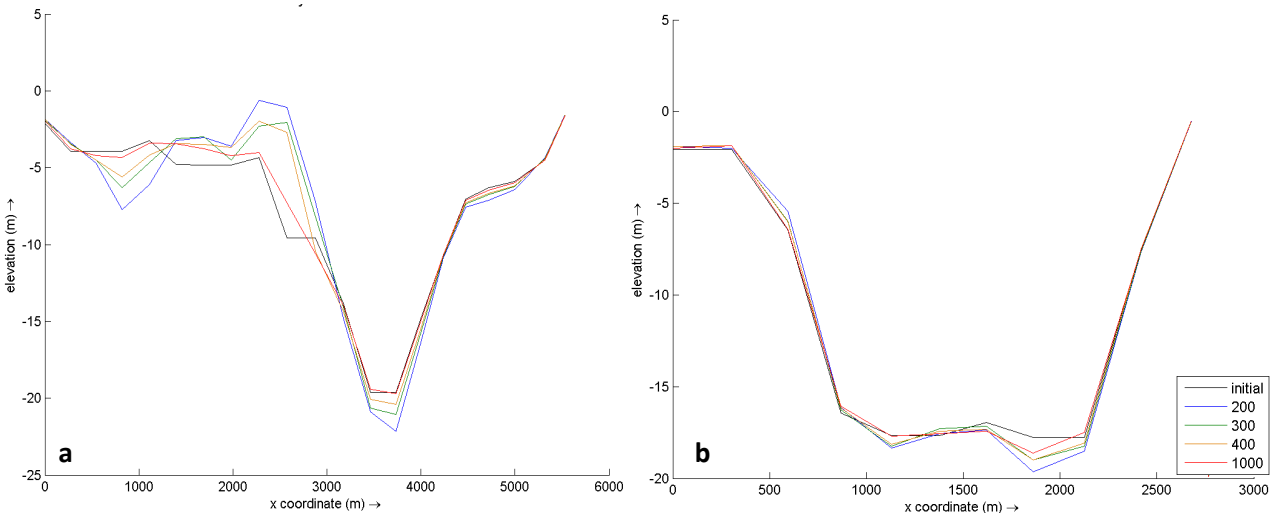

Figure 5.6. Cross-sectional bed development for different grain sizes (a) in the gorge (b) in the basin. On the left is Terschelling and on the right is Ameland. The sediment fraction size is presented in the legend in µm.

Van Rijn (2007) sediment transport predictor

A different sediment transport prediction (VR07) altered the development of the system compared to the VR93 prediction (figure 5.7). In both the 200 µm and 300 µm runs there was a reduction of the main channel incision compared to the VR93 morphology. The incised depth of the 300 µm VR07 run closely resembled the 1000 µm VR93 prediction (figure 5.6a). With the VR07 prediction the largest reduction in incision (-1.5 m) was found by increasing the sediment bed from 200 to 300 µm. An increase in grain size to larger fractions, 400 µm and 600 µm, further reduced the incision but did not halt the channel depth development. On the left bank of the tidal channel a different development was present. The lower grain sizes had an accumulation of sediment on top of the bank and steeper channel margin with both the VR93 and VR07 transport formula.

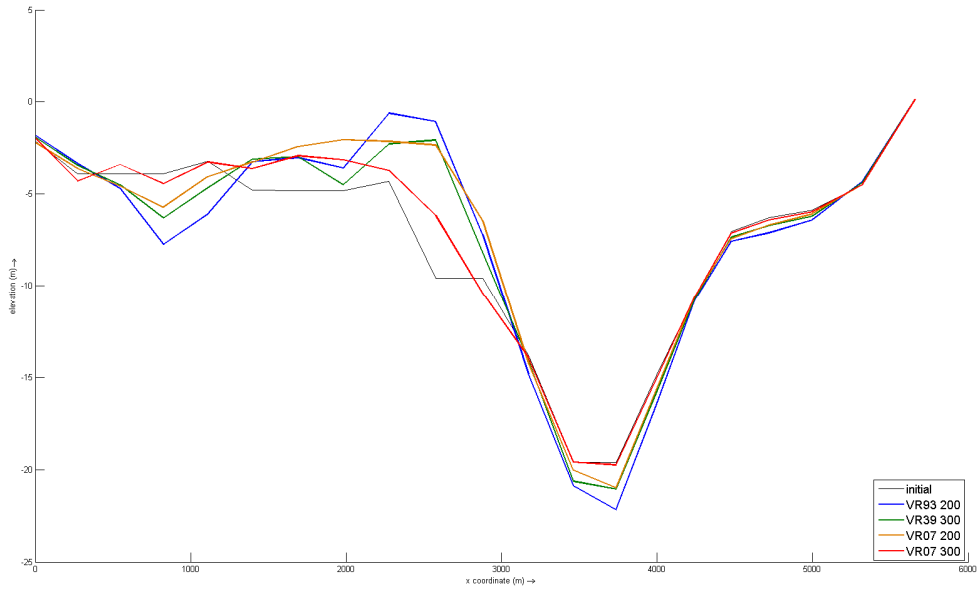

Figure 5.7. Cross-sectional profile between Terschelling and Ameland. Given is the bed development over the 2 year interval for the default VR93 and VR07 sediment transport predictions with a 200 and 300 µm sediment bed.

Roughness definition

The gorge profile morphologies differed for the implemented roughness definitions. This is illustrated in figure 5.8a for the gorge and the basin (figure 5.8b). The incorporation of a space variable bedform roughness (chapter 2.4) limited the incision of the bed compared to the homogeneous Chézy (65 $m^{0.5}$/s) and space varying Manning file roughness.

The Van Rijn (2007) bedform roughness prediction module requires several additional parameters (*RpC*, *RpR*, *MpC* and *MpR*). With different *RpC* an *MrC* tuning parameter settings (0.5-1.5) no differences in the cross-sectional morphologic development were present in the 2 year runs. The addition of dunes (*DnC* >0) resulted in errors in the flow module and are therefore left out of the model runs.

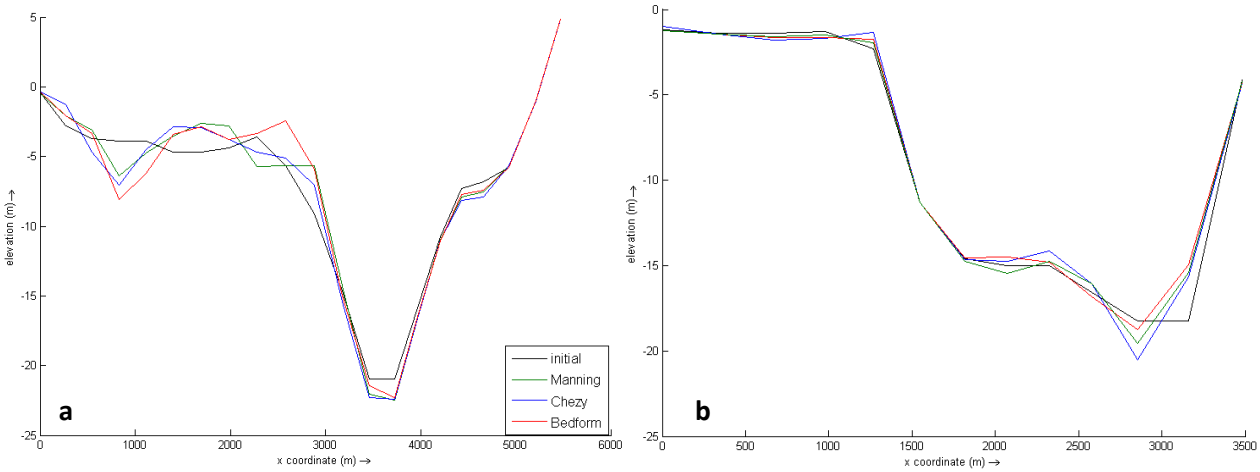

Figure 5.8. The cross-sectional profile bed development in the (a) gorge and (b) basin for the homogeneous Chézy (65 $m^{0.5}$/s) VR07, space variable Manning and bedform roughness run.

Transverse bedslope parameter

The effects of the transverse bed slope (chapter 2.4) were investigated for the default Van Rijn (1993) *AlfaBn* and Koch and Flokstra (1980) definitions with a homogenous 200 µm and 300 µm sediment bed. The corresponding gorge profile responses are given in figure 5.9a and b respectively.

A larger *AlfaBn* bedslope parameter reduced the incision of the main channel at the gorge location for both sediment sizes. With a 300 µm sediment the *AlfaBn* 20 run closely resembled the initial bathymetry in both the gorge and basin. The 200 µm sediment bed runs indicated a different range of sensitivity to the transverse bedslope parameter. The main channel incised to the default (1.5 *AlfaBn*) profile for the value range <25. Increased *AlfaBn* (>25) resulted in a reduced depth of the main channel in the gorge and basin locations.

The incorporation of Koch-Flokstra (1980) did not alter the development compared to the default *AlfaBn* 1.5 200 and 300 µm sediment bed morphology. Furthermore the tuning parameter *Ashld* (0.35, 0.7 and 1.5) did not result in changed cross-sectional profiles over the modelled 2 year period.

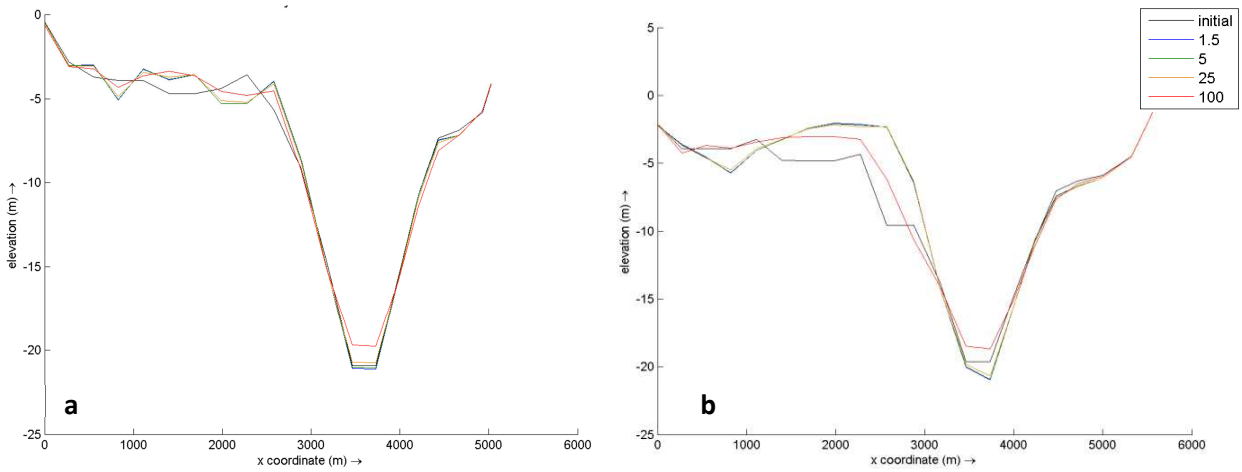

Figure 5.9. Cross-sectional profile of the bed development with (a) 300 µm (b) 200 µm sediment bed. The range of AlfaBn values in combination with the default transverse besdlope effect is given in the legend.

MORFAC parameter

Before running long term simulations the sensitivity and stability of the model to increasingly large *MORFAC* values was investigated. The same cross-sectional development bed was present with increasingly higher *MORFAC* values after an equivalent period of simulated time. The response of a single bed location displayed the same trend up to *MORFAC* values of 50. The largest *MORFAC* (100) bed response indicated a strong semi-diurnal tide driven response signal with instabilities superimposed on the signal (figure 5.10). The stable bed response led to the selection of *MORFAC* 50 for the long term runs.

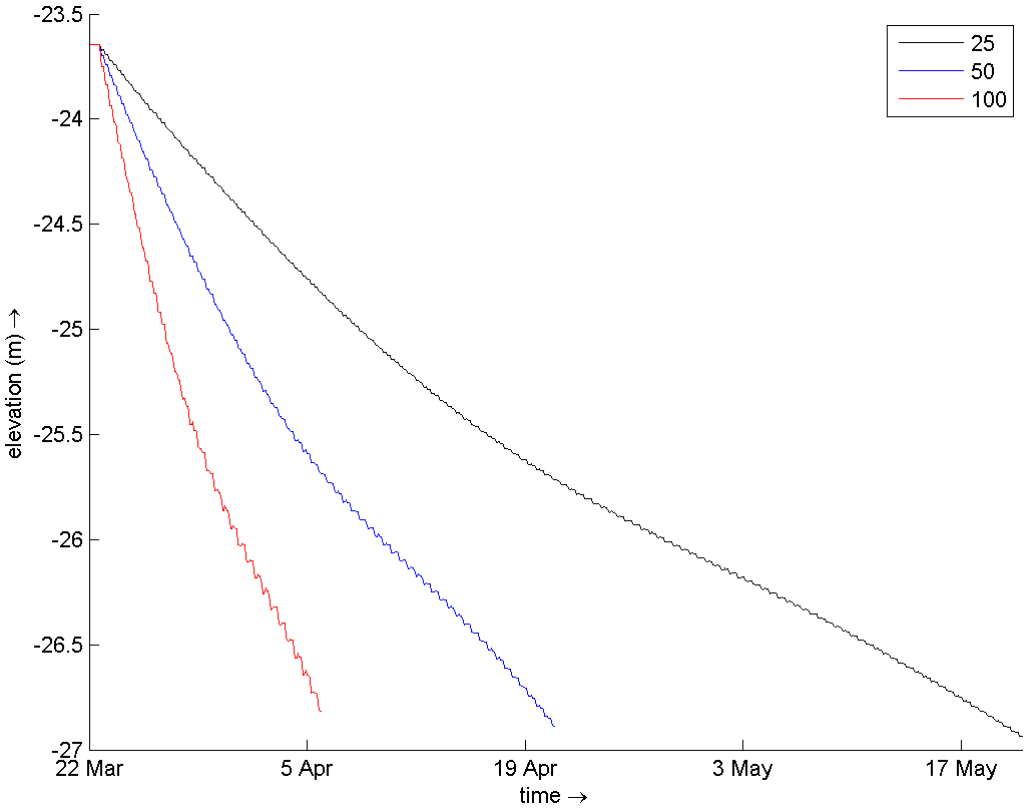

Figure 5.10. The bed development in a single location for a MORFAC of 25, 50 and 100. The bed development time is 2 years for all scenarios. The MORFAC is given in the legend.

Summary short model runs

The above presented results indicated that in order to stabilize the 2 year run main inlet channel with the VR93 sediment transport prediction large sediment fractions were necessary. A large reduction in the incision of the central channel was present after changing to the VR07 transport prediction. The difference between the Manning and Chézy roughness definition was a slight reduction in channel incision. The addition of space variable bedform roughness resulted in a larger reduction of the cross-sectional profile incision. Further adjustment of the VR07 transport *RpC* parameters did not alter the short term morphological development

The most prominent changes occurred by varying the transverse bedslope (*AlfaBn*) to values of 25 with 300 µm and higher (50-100) with 200 µm sediment bed. The more complex K-F transverse bedslope effect did not affect the morphology. The apparent insensitivity of the morphologic response to some morphological boundary condition parameter values led to the evaluation of these parameters in long term simulations.

5.3 Long term model

The long term model runs (100 years using a *MORFAC* of 50) allowed the identification of the effects of the morphologic boundary conditions on the channel stability and morphology over 100 years. The basic model setup settings are listed in appendix I. First the default VR93 sediment transport response is given for a homogenous Chézy and space varying bedform roughness. This is followed by the VR07 sediment transport predictor and the homogeneous sediment bed grain size sensitivity. Next the bedform roughness height definition sensitivity and the overall morphologic response of the system is presented. The optimal trachytope roughness response model is used to illustrate the effect of using multiple sediment fractions and compositions. Finally the long term effects of the transverse bedslope, K-F and dry cell erosion are given.

5.3.1 Van Rijn (1993)

The default sediment predictor, with a homogeneous 300 µm sediment bed, morphology was characterised by the formation of deeper channels in the distal and central part of the basin. The incision started between the 10 year and 20 year mark. After 80 years the tidal channels incised to depths of -50 m (figure 5.11a). The ebb-delta displayed a seaward directed outbuilding in the first 10 years that continued up to the end of the run. The resulting ebb-delta morphology reached the northern model boundary. The addition of a bedform roughness resulted in a different morphology. With the bedform predicted roughness the seaward ebb-delta extension was less compared to the homogeneous roughness runs (figure 5.10b). Furthermore, instead of a large central channel on the ebb-delta, multiple smaller channels were formed after 10 years with elongated shoals between them. The same reduced seaward outbuilding was found for the Boschgat channel. The main channel incised less, but still reached local maxima of -50 m. The channels in the distal part of the basin displayed a similar incising trend. It should be noted that the initial sediment layer thickness was 25 m, so locally the base of the sediment bed was reached in both roughness runs.

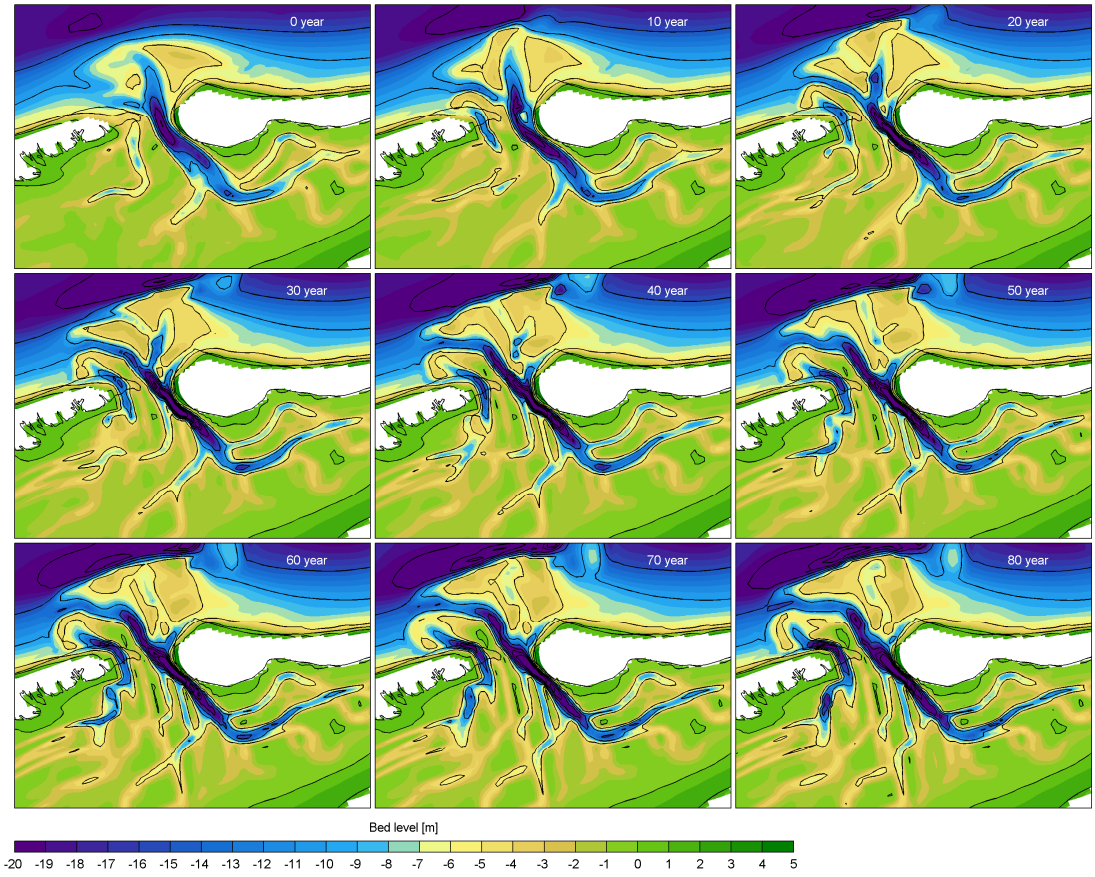

Figure 5.11. (a) The 80 year morphologic development with the default Van Rijn (1993) sediment transport prediction and a constant C=65 $m^{0.5}$/s roughness.

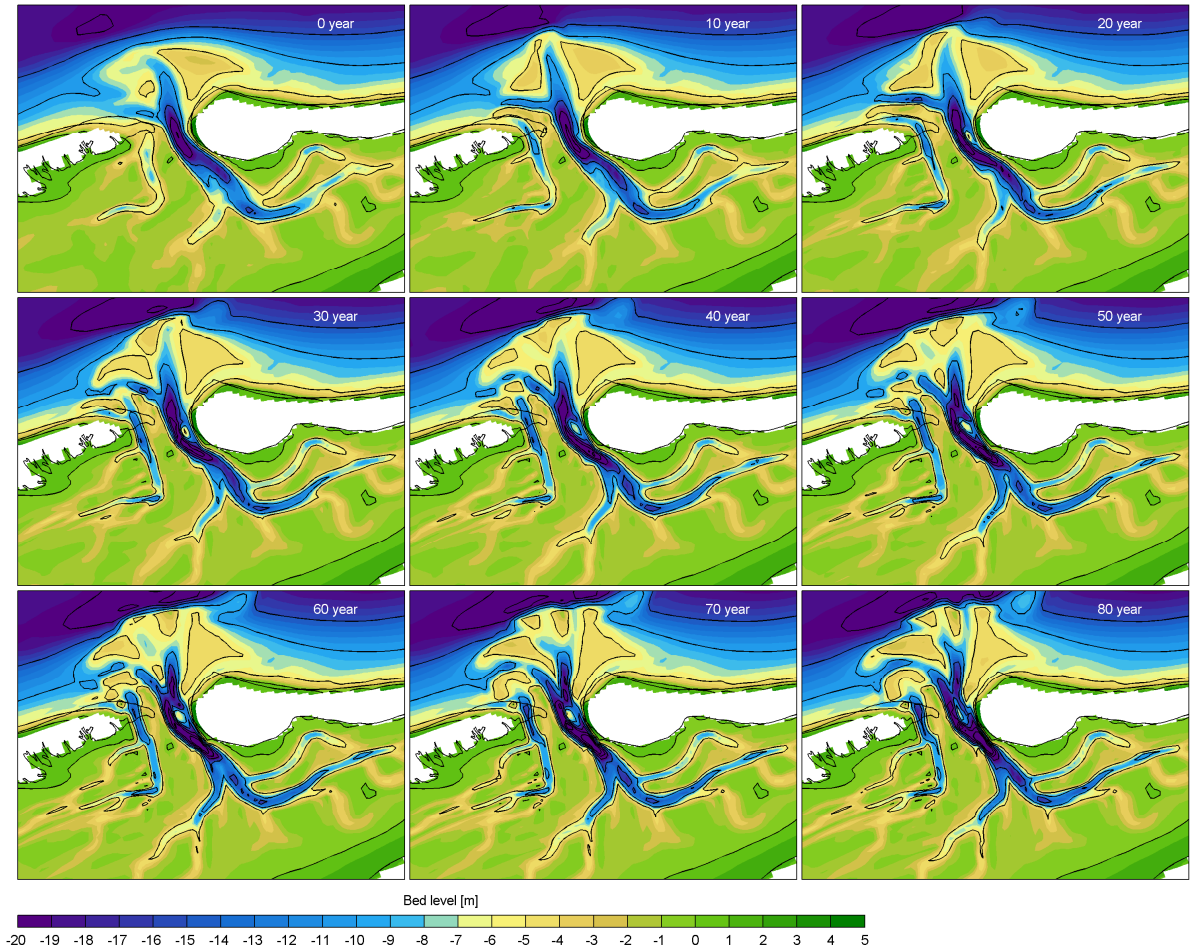

Figure 5.11. (b) The morphologic development with the default Van Rijn (1993) sediment transport prediction and a space variable Van Rijn (2007) bedform roughness.

The volumetric change in the basis, for the homogenous roughness run, displays a gradual net export in the seaward direction. The positive change levelled out at $1.5*10^8$ m^3 and the negative change was $-2.8*10^8$ m^3. The seaward part displays (figure 5.12a) a non-steady net increase in sediment in the first 40 years. In the last 20 year a slight reduction was present. The unsteady response of the delta volume is due to increased outbuilding that reaches the boundary of the polygon.

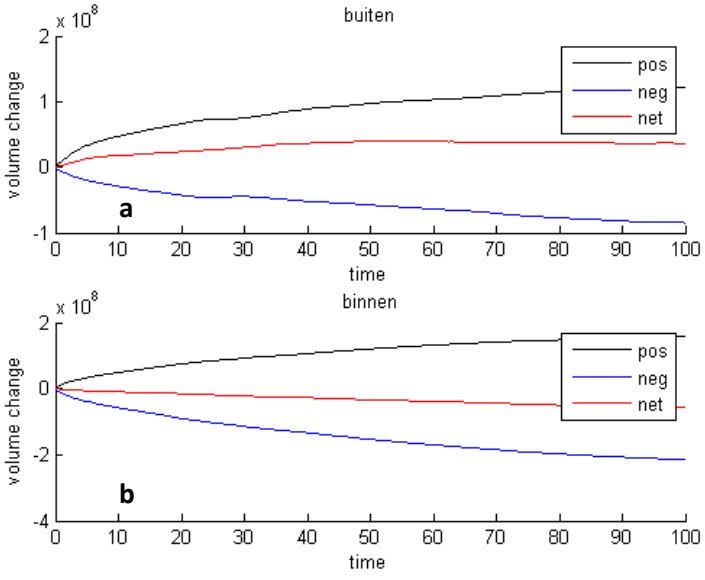

Figure 5.12. Volumetric change in the basin and seaward part of the model with the VR93 C(65) setting.

5.3.2 Van Rijn (2007) homogenous sediment bed grain size variation

The model was run with the VR07 transport formula, the Manning roughness file and a varying homogenous sediment bed grain size. The morphological development over the 80 year period is given in figure 5.13a-e. The smaller (100-200 µm) sediment runs led to large changes in the system. The most severe system developments were found with 100 µm (figure 5.13a). In both fine sediment environments the morphodynamic development was characterised by a large seaward directed outbuilding of the ebb-delta, up to the North Sea model boundary. The channels in the basin locally eroded through the sediment layer and displayed bends with 90° angles. The 100 year morphology no longer represented the initial bathymetry. More coarse sediment beds (300-600 µm) provided more stable system responses (figures 5.13c, d and e).

The 300 µm run channel incised to -40 m in the basin whilst the gorge depth remained comparable to the initial -21 m depth. The ebb-delta was incised by a rotation of the main inlet channel to the west. The seaward extension of the delta was reduced compared to the fine sediment runs. In the basin little changes were present in the smaller channels. The Larger fractions (400 and 600 µm) resembled the 300 µm run trends, but the development was less pronounced. This manifested itself by a reduced seaward ebb-delta expansion. The larger fractions did not reduce the incision of the main channel. At the basin location depths similar to the 300 µm run were present. All below presented runs use a homogenous 300 µm sediment bed.

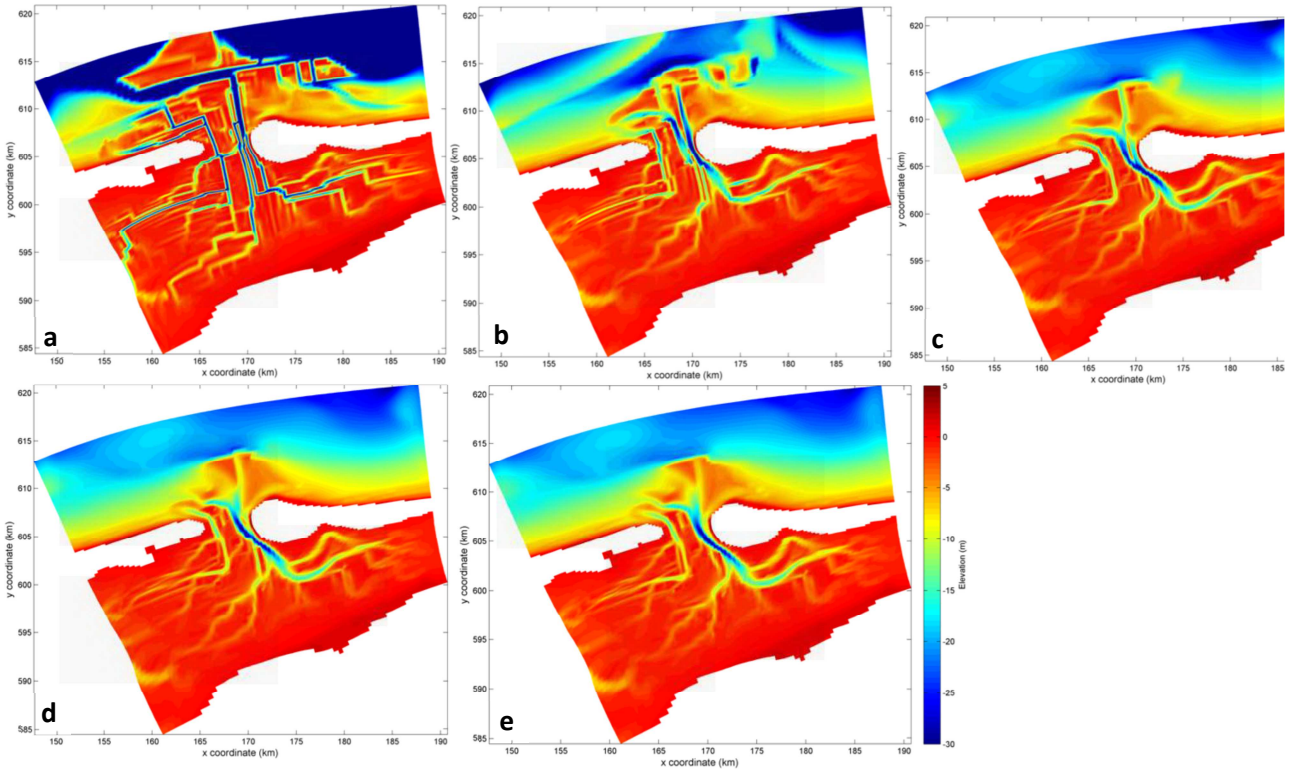

Figure 5.13. 80 year morphology of the Ameland model inlet. (a) 100 µm (b) 200 µm (c) 300 µm (d) 400 µm (e) 600 µm

5.3.3 Homogenous and space variable roughness definitions

With a homogeneous Chézy value (65 $m^{0.5}/s$) (figure 5.16) the ebb-delta extended slightly in the seaward direction within the first 30 years. The seaward outbuilding continued during the run. The 80 year delta extended further seaward than the with a fixed and spatially variable Manning roughness (figure 5.15c). The morphologic response with a homogenous Manning roughness indicated that a value of 0.026, equivalent to a Chézy of 65 for h=25 m, resulted in a reduced development of the ebb-delta and channel. The 100 year morphology resembled the space variable

Manning roughness response in terms of channel and ebb-delta development (figure 5.14a). A lower 0.021 Manning roughness (same velocity and discharge as Chézy 65) led to a non-realistic morphology with narrow channels and a strong seaward outbuilding of the ebb-delta (figure 5.14b)

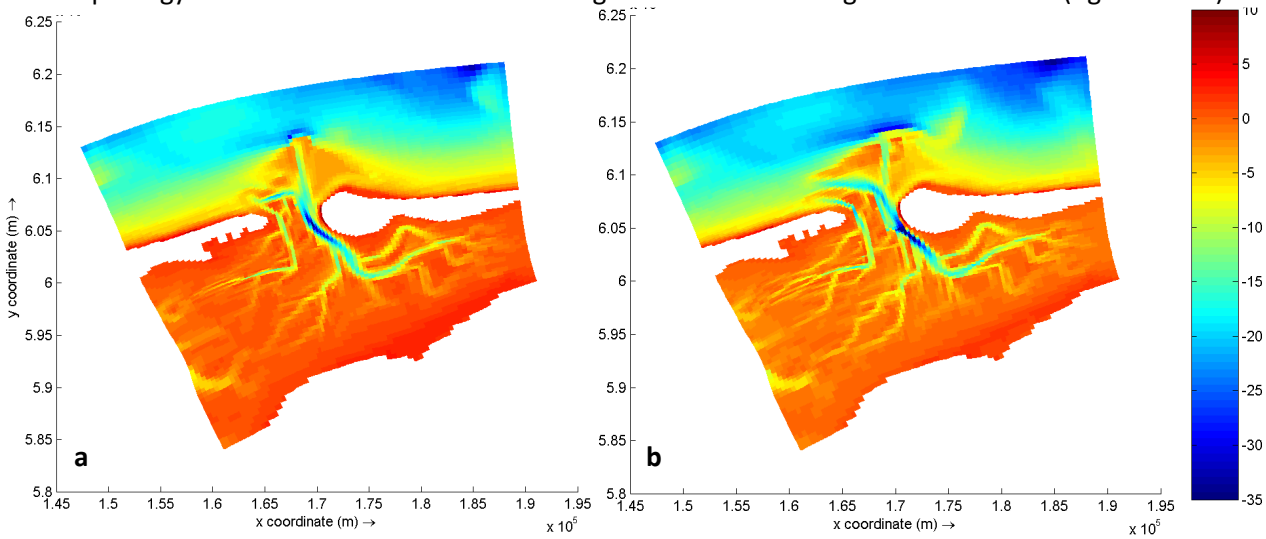

Figure 5.14. 100 year morphology for a Manning value of (a) 0.026 (b) 0.021.

The Incision of the main channel, with the spatial Manning roughness, was –23 m in the gorge and -35 m in the basin. The Chézy channel incised to larger depths in the gorge (-32 m) and similar depths in the basin (-35 m). The volumetric change of the ebb-delta and basin is characterised by an increase in the net sediment export from the basin over the entire 100 year period (figure 5.15) for both roughness runs. The degree of positive and negative change is larger for the Chézy based run than the Manning file response. The final net volumetric response indicates the same trend.

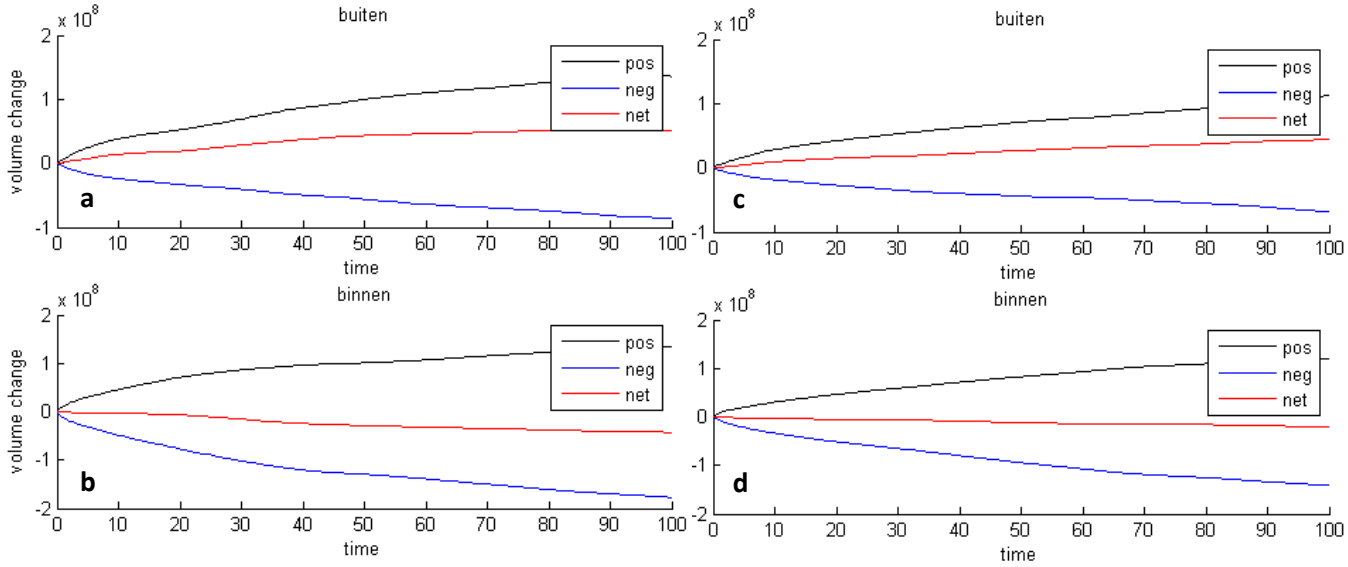

Figure 5.15. Volumetric change of the delta (a and b) Chézy (c and d) Manning file.

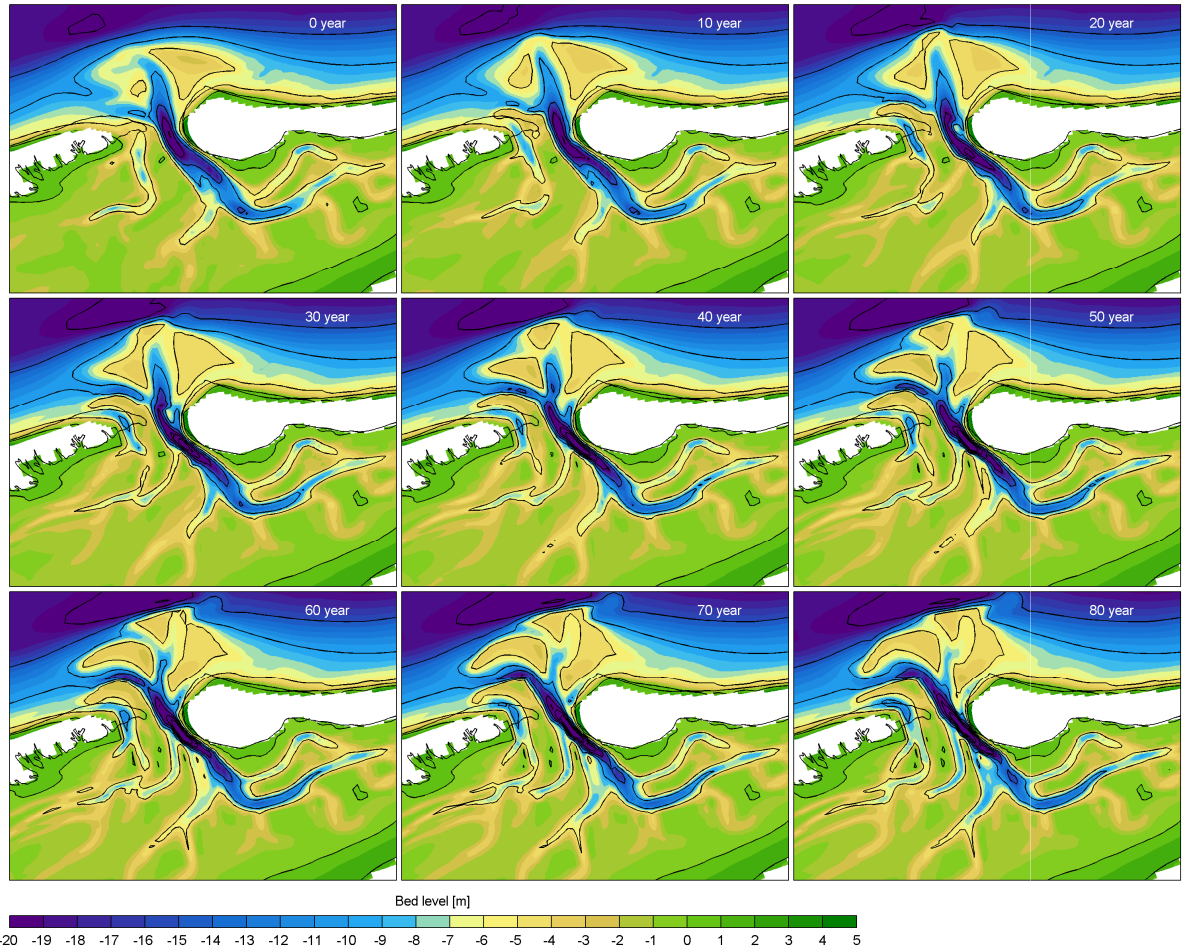

Figure 5.16. The 80 year model morphology with a Chézy (65 $m^{0.5}/s$) roughness definition and a homogenous 300 µm sediment bed.

5.3.4 Van Rijn (2007) bedform roughness

In the short term models the cross-sectional profiles, as a result of the trachytope or bedform roughness parameter sensitivity range, were similar. The long term run effects are more pronounced and depend on the specified tuning parameters (*RpC*, *MrC*). First the sensitivity of the bedform roughness height prediction is presented. This is followed by the morphologic development of a realistic and extreme bedform roughness setting.

Predicted roughness height

The space variable bedform roughness prediction (chapter 2.4) was implemented in combination with a 300 µm homogeneous sediment bed. The bedform roughness prediction is space varying. The ripple term (*RpC* 1) affected the roughness height in all parts of the system (figure 5.17a). The roughness height was 0.01 m along the landward margin of the basin and increased towards the channels. In the small branches of the basin the ripple roughness height had a 0.045 m maximum. The maximum value was also found on the seaward side of the inlet. The gorge and main tidal channel had lower values similar to the distal basin.

The predicted presence of mega-ripples (figure 5.17b) was tied to the central channel with maximum values of 0.2 m in the gorge. In the rest of the Borndiep lower values, between 0.08-0.12 m, were found. In the distal part of the basin, the intertidal flats, the effect of the mega-ripples was fixed at 0.02 m. The seawards edge of the model was continuously characterised by the maximum 0.21 combined roughness height value. Over a single tide the roughness varied both in space and magnitude, the above described trends remained present. The ripple and mega-ripple maximum

roughness height values for a range of *RpC* and *MrC* values is given in table 5.2 together with the maximum velocity in the gorge.

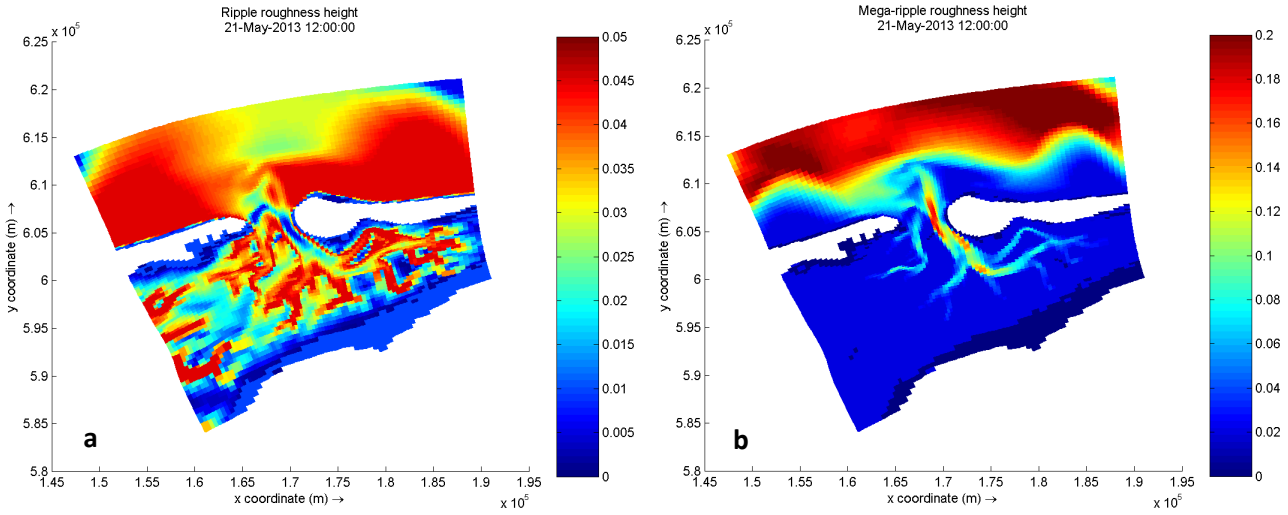

Figure 5.17. Roughness heights for (a) ripples (b) mega-ripples during flood (RpC = 1).

Over a single tide the largest roughness values remain focussed at the deepest part of the gorge and reduce in the seaward and landward direction (figure 5.17c). The smaller tidal channels have a lower similar roughness.

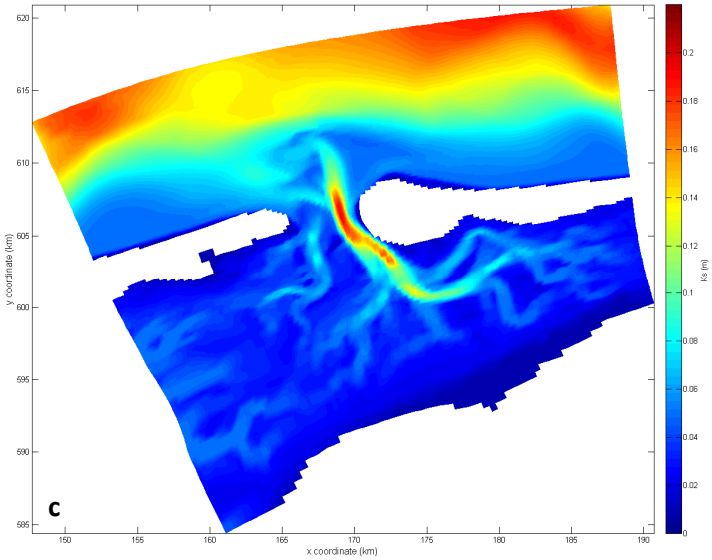

Figure 5.17. (c) The predicted roughness averaged over a single tide. The combined k_s roughness height is given in the legend.

The 100 year model output for relaxation length scenarios (*RpR*, *MrR* 0-1) yielded identical cross-sectional profiles in the gorge and basin. In the remainder of the runs a default value of 1 was selected for the relaxation lengths. The upper limit of the model sensitivity, in terms of hydrodynamics and morphodynamics, to the *RpC* and *MrC* parameters was investigated by increasing the parameter values.

An increase of the tuning parameter for mega-ripples (*MrC*) did not correspond to an increase in the roughness height for values larger than *MrC* > 1.The maximum 0.2 m (k_{mr}) value was the main contributor to the combined roughness for the lower range of the tuning parameter. The ripple roughness tuning coefficient displayed a different trend and allowed *RpC* >1 coefficients. The ripple height increased in magnitude for larger values; with 0.045 m for *RpC* is 1.0 and 1.0 m for an *RpC* of 24.0. The increased ripple parameter altered the combined roughness height contribution from

mega-ripples to ripples. Since the roughness height is a site specific prediction the contribution increased ripple roughness height affected the red areas in figure 5.16a.
The response of the gorge velocity magnitude, of the Borndiep(1) observation point, to a combined roughness height is given in table 5.2. The low range of the bedform roughness predicted velocity values was similar to the Chézy predicted 1.0 m/s and identical to the Manning file 0.95 m/s. The response to larger tuning values consisted of an overall maximum velocity reduction for increased *RpC* values. The instantaneous discharge through the inlet reduced to $2.3*10^4$ m^3 for the roughest (*RpC* 24) environment.

RpC	**MrC**	$\mathbf{k_r}$	$\mathbf{k_{mr}}$	$\mathbf{k_s}$	$\mathbf{U_{max}}$ (m/s)
0.5	0.5	0.022	0.16	0.16	0.95
1.0	1.0	0.045	0.20	0.21	0.88
2.0	2.0	0.090	0.20	0.23	0.82
3.0	3.0	0.110	0.20	0.23	0.82
6.0	6.0	0.130	0.20	0.25	0.82
9.0	9.0	0.400	0.20	0.45	0.78
12.0	12.0	0.500	0.20	0.55	0.75
24.0	24.0	1.000	0.20	1.00	0.60

Table 5.2. Roughness height and velocity maxima for increasing bedform tuning parameters. The velocity location is the seaward part of the main tidal channel Borndiep(1).

Bedform roughness morphology
The detailed morphologic development of the model with a local bedform roughness prediction and the VR07 transport prediction (*RpC 1, MrC 1*) displayed a stable development characterised by a limited delta outbuilding (figure 5.18) and channel incision during the first 40 years (figure 5.18a and b). The same trends were observed with lower, *RpC 0.5* and *MrC 0.5,* parameters. The development in the first 40 years consisted of the straightening of the Akkerpollegat to flow directly in the seaward direction. The Bornrif extended in the seaward direction and became shallower. In the Borndiep there was limited incision and a slight narrowing of the central channel (figure 5.18b). The basin displayed local incision and maintained the original width (figure 5.18c). The largest change was found at the Boschgat, where a seaward expansion and incision were found. After the first 40 years the continued development of the Boschgat resulted in a two channel system after which the morphologic change in the system increased.
On the seaward margin of the Boschgat a sedimentary lobe expanded seaward. The Akkerpollegat rotated towards the west, closing of the previous flow path. The deepest part of the main channel expanded in the basin direction and incised to a depth of -35 m NAP (figure 5.18b). The gorge profile remained relatively stable with a minor additional increase in depth (figure 5.18a).

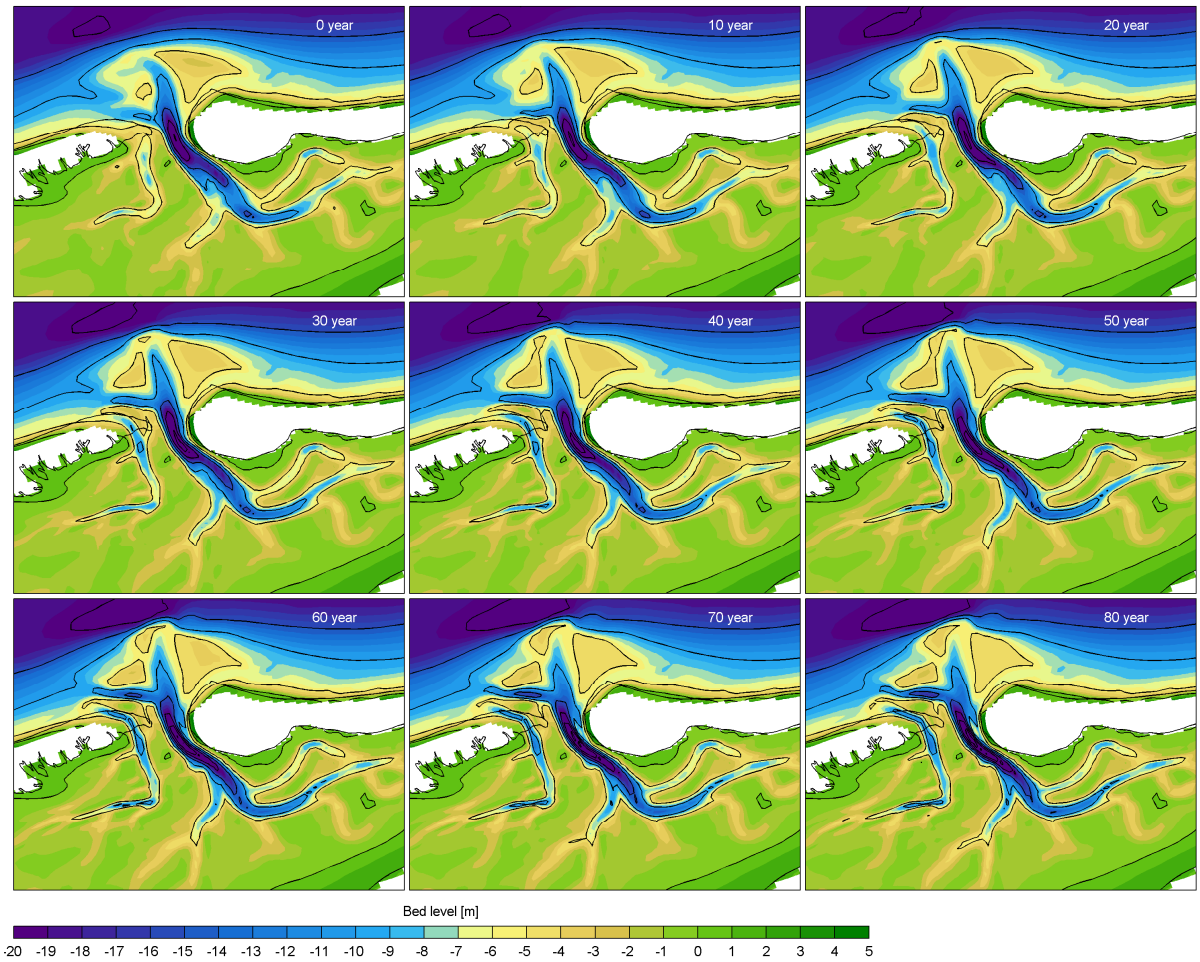

Figure 5.18.(a) The 80 development of the model with a bedform based roughness prediction and a homogenous 300 µm sediment bed.

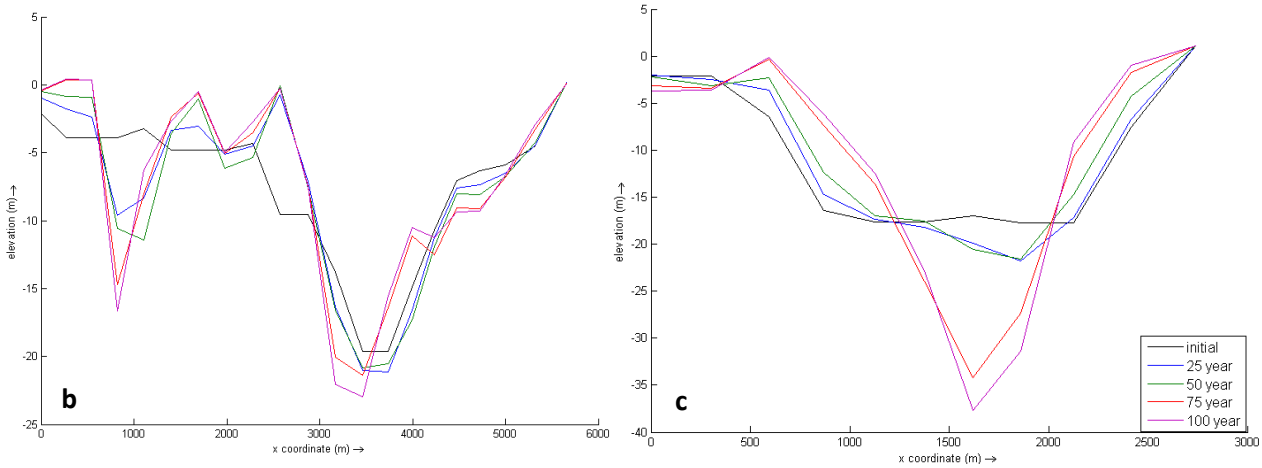

Figure 5.18. The cross-sectional profile development of the (a) gorge and (b) basin with the bedform roughness definition. In the legend the time steps are given 0, 25, 50, 75 and 100 years.

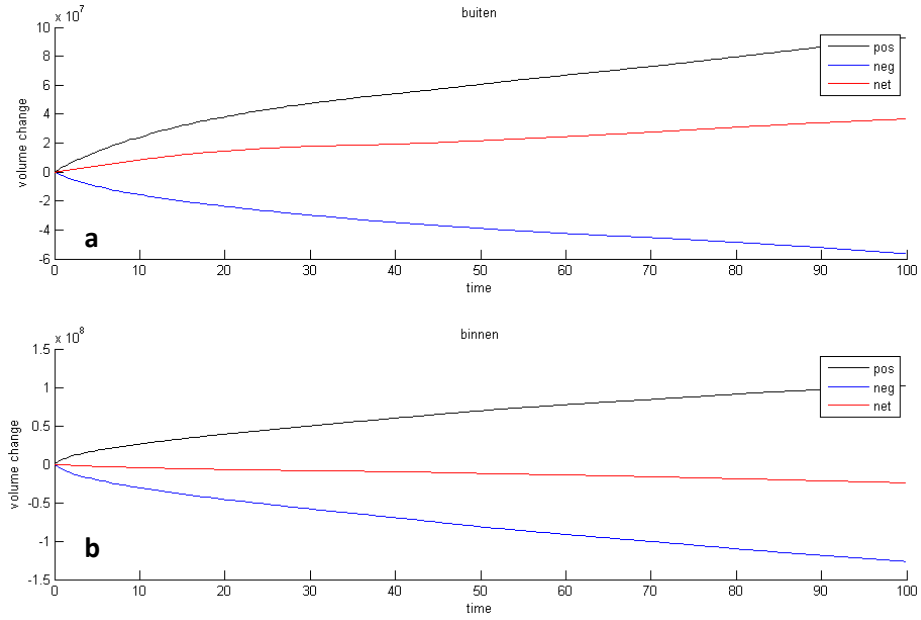

Figure 5.19. The volumetric change in the (a) seaward and (b) basin part of the model.

The volumetric change in the basin (figure 5.19a) and seaward part of the model (figure 5.19b) indicate that the system exported sediment to the sea over time. In the first 15 years the net volumetric change in the basin displayed a small fluctuation before levelling out up to the 40 year mark. After 40 years the net export of sediment increased. The seaward margin displays the opposite trend that consisted of an increase in the sediment volume.

Throughout the run the cumulative suspended sediment load was larger than the bedload through the gorge (figure 5.20). The increase in morphodynamic development after 40 years coincided with an increase in the suspended load cumulative transport (figure 5.20). The bedload rate was characterised by a gradual increase in the cumulative transport throughout the run.

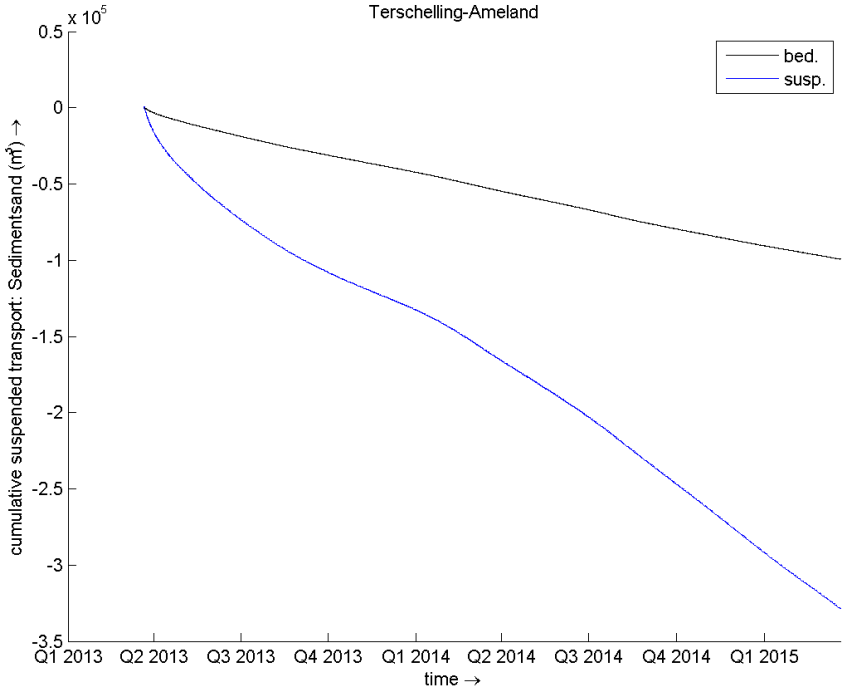

Figure 5.20. Cumulative suspended load and bed-load transport through the inlet for the 100 year model run.

Maximum bedform roughness morphology

The morphologic development of the maximum roughness height (*RpC* 24.0) had a very limited morphological development compared to the default ripple and mega-ripple case (*RpC* 1.0). In the maximum roughness run the Bornrif did not undergo significant morphologic development during the 100 year period. This mean the ebb-delta did not extent in the seaward direction. The Akkerpollegat and Boschgat both maintained the original flow direction and did not display a rotation of the channel. The basin channel morphology of the Borndiep and Boschgat remained stable. The increased k_s height did not only reduce the flow velocities (table 5.2), but also the cumulative sediment transport through the gorge (figure 5.21). The largest reduction in sediment transport is found for the highest *RpC* values.

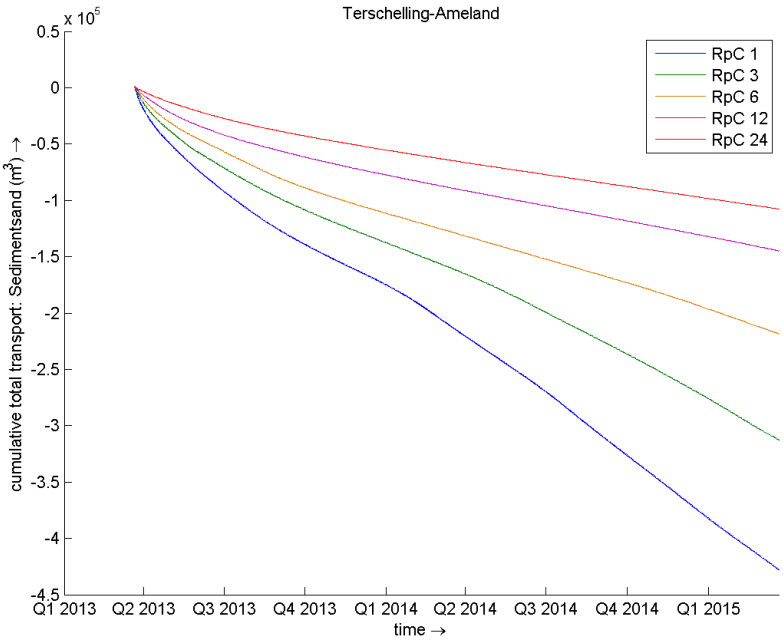

Figure 5.21. Cumulative total sediment transport through the gorge over the 100 year run for a range of RpC parameter values.

5.3.5 Van Rijn (2007) graded sediment without morphologic development

The active layer depth is a key feature in controlling the spatial distribution of sediment (Sloff and Ottevanger, 2008). The difference in the final sediment distribution, without morphologic updating, for an active layer thickness of 0.10 and 1.00 m is presented first. This is followed by the grain size distribution and sediment transport through the gorge. Finally the graded sediment sorting patterns is given.

In figure 5.22 the difference in the grain size after 100 years is given between a 1.00 m and a 0.10 m layer thickness. There was a difference in the final sediment distribution between both active layer runs. The smaller layer overall system was more coarse (blue areas) in the basin, along the barrier island coasts and on the north-western part of the ebb-delta. With a thick layer the channels and parts of the ebb-delta were coarser. Furthermore the most distal basin regions indicate an increased grain size with a thick active layer. The seaward part of the model displayed large local differences in the average grain size. In the main part of the inlet system the mean grain size variation was small +/- 0.02 mm. Locally larger changes in the order of 0.05-0.1 mm were present, which translate to a single initial sediment class fraction.

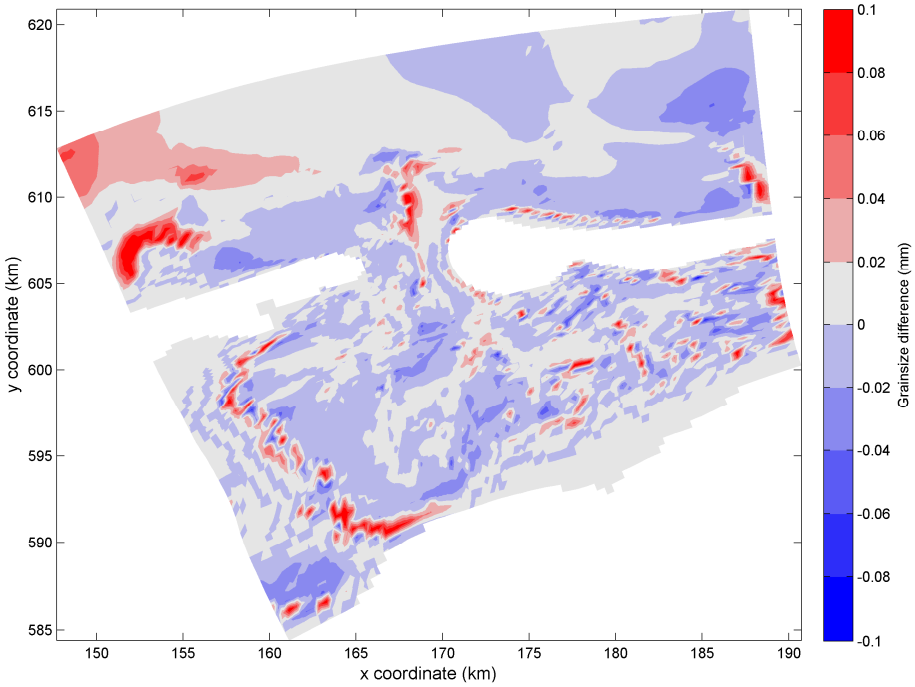

Figure 5.22. The difference in grain size (m) between a 1 m and a 0.10 m thick active layer after 100 years. The red colours indicate coarser sediment with a thick (1.00 m) active layer. The blue areas indicate a more coarse bed with a small (0.10 m) active layer.

The system was suspension dominated with a 100 year cumulative total of $14*10^5$ m^3 suspended load compared to $6*10^4$ m^3 for bed load. The cumulative total transport through the inlet, for the different sediment fractions and active layer thickness, is given in figure 5.23. The largest effect of the active layer thickness is found in the fine sediment fractions 100 µm and 200 µm, where a larger active layer resulted in increased fine fraction transport. The larger 300 µm and 400 µm sediment classes produced similar results for both layer thicknesses.

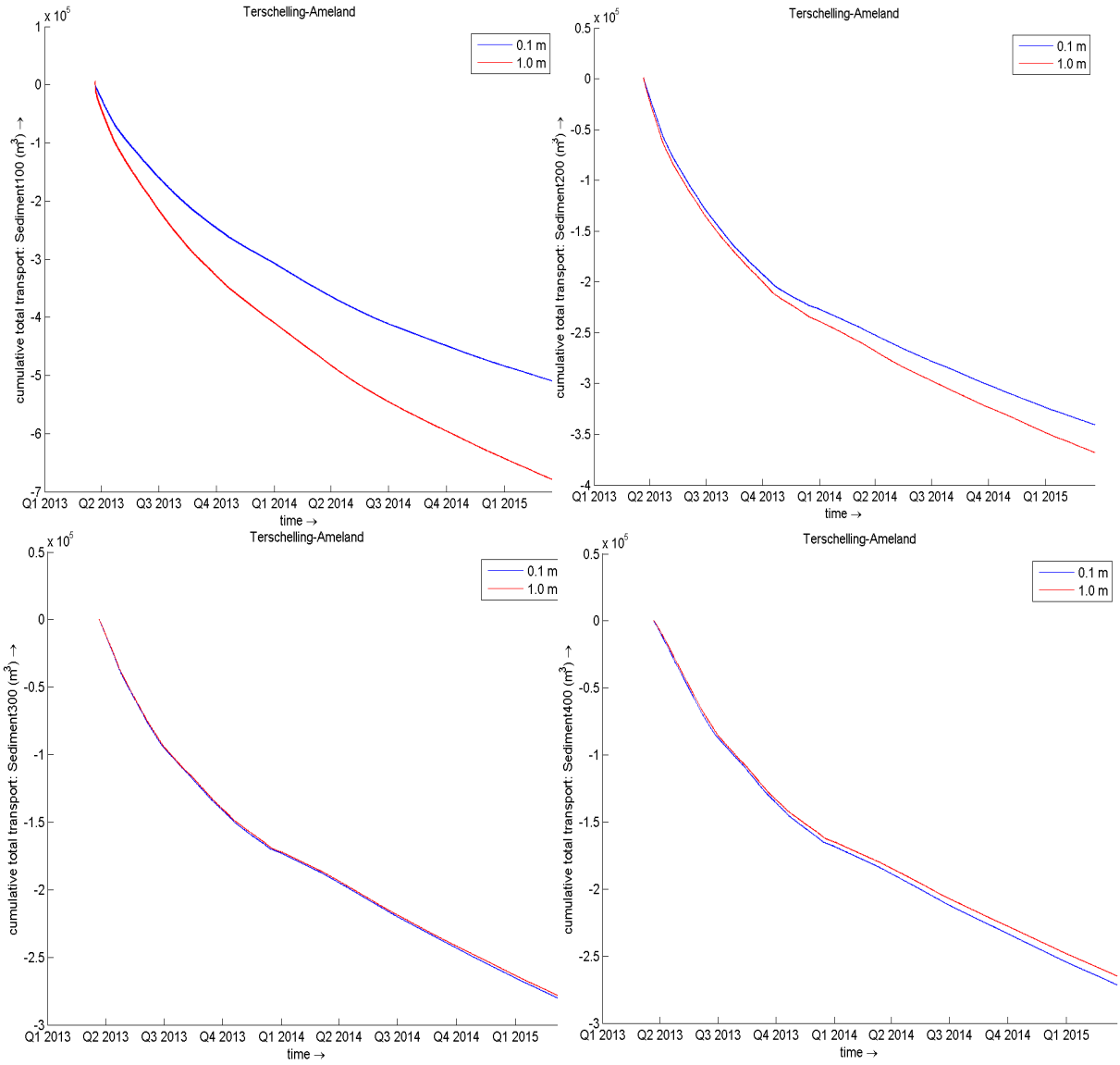

Figure 5.23. Cumulative sediment transport through the inlet for an active layer thickness of 0.1 and 1.0 m for all the used realistic grain size fractions.

The distribution of the 1 m active layer arithmetic D_{50} change over time indicates that the initial sediment sorting pattern developed within the first 25 years (figure 5.24a) and did not undergo large changes in the additional 75 year run time (figure 5.24b). The 100 year grain size distribution is characterised by the following trends:

-The gorge is the coarsest part of the inlet (350 µm) and more distal basin parts of the main inlet channel were finer (300 µm).

-The basin became rougher compared to the initial mean D_{50}, with the largest grains in the channels (300 µm) and finer sediment on the intertidal shoals (250 µm).

- Fining of the initial sediment occurred on the north-eastern and eastern sides of the ebb delta (150 µm).

-The North Sea margin displayed both local fining and coarsening.

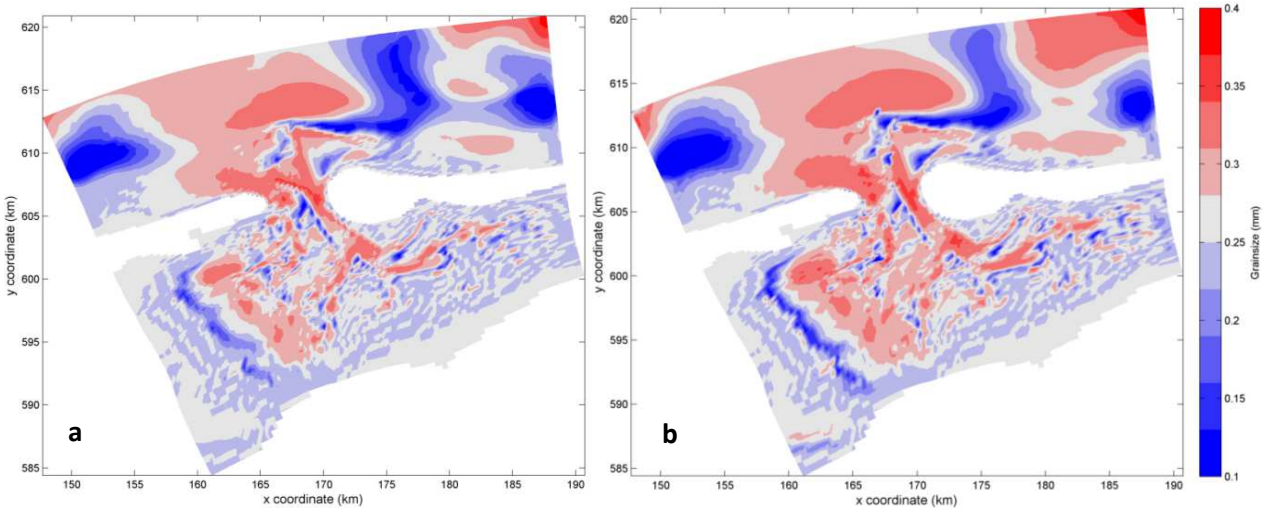

Figure 5.24. Spatial grain size distribution after (a) 25 and (b) 100 years with a 1.00 m thick active layer.

5.3.6 Van Rijn (2007) graded sediment with morphologic development

The development of the model with four sediment fractions and morphologic updating can be divided in two sections. First the overall morphologic development is presented for different initial layer and sediment fraction combinations. This is followed by the spatial sediment distribution and sediment transport trends.

10 m equal layer realistic sorting

With 10 m thick initial sediment layers and realistic sediment fractions the initial mean D_{50} was 0.250 µm. The morphologic development was characterised by a strong seaward outbuilding of the ebb-delta after 20 years (figure5.25). This outbuilding continued and led to the development of a large shallow ebb-delta with the main inlet channel curving to the west. The central channel incised to -28 m in the gorge (figure5.26a) and -40 m in the basin (figure 5.26b). The basin development was limited to incision of the tidal channels.

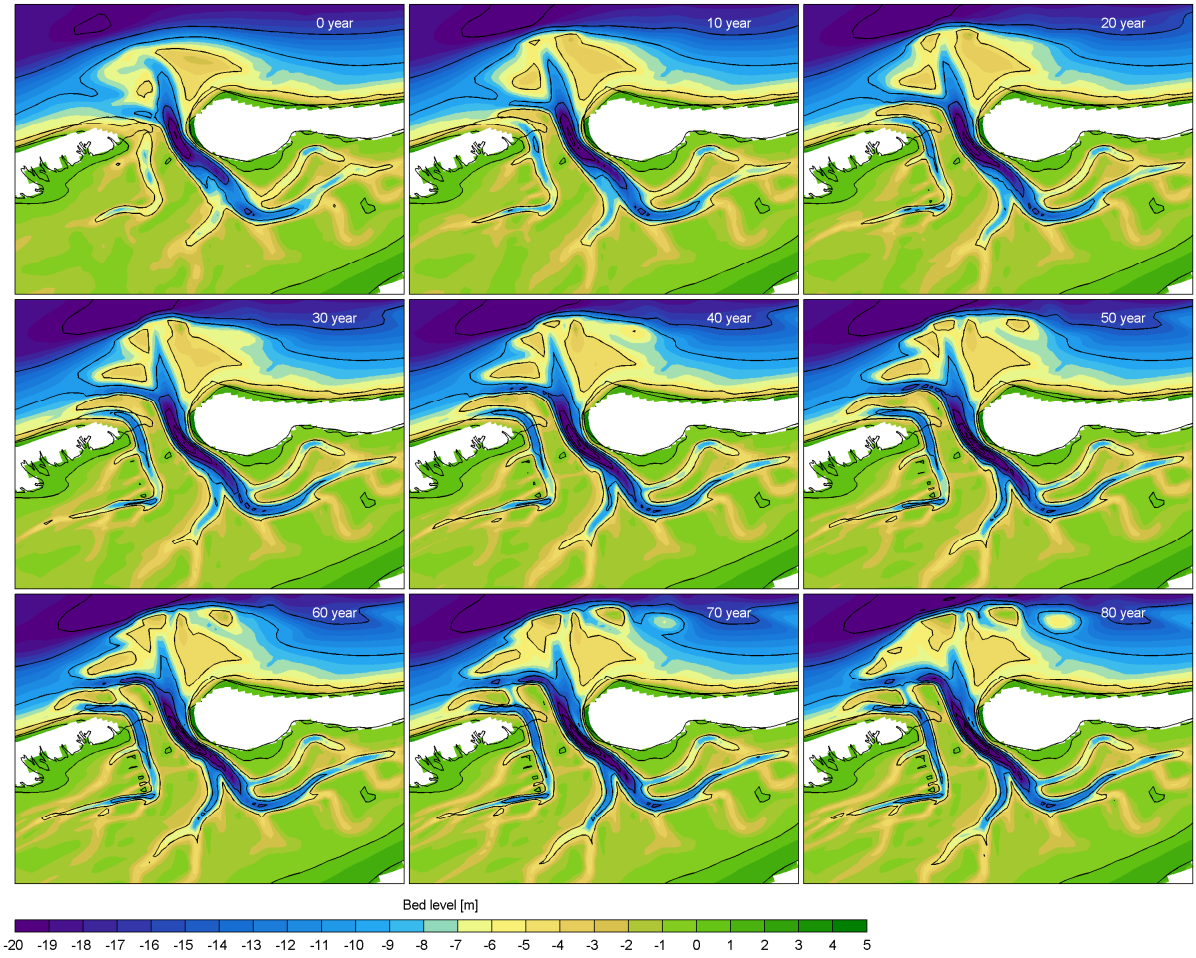

Figure 5.25. Morphologic development of the realistic graded sediment bed run (10 m layers).

Increased grain size

The addition of a single coarse fraction, 1 mm instead of 100 µm (Increased II), led to a larger average D_{50} of 420 µm instead of 280 µm. The gorge profile response (figure 5.26a) consisted of a limited incision compared to the realistic run profile. In the basin only a slight reduction in the incision was present with a -35 m maximum depth compared to the -40 m of the fine fraction run (figure 5.26b). The overall channel response in the basin indicated a reduction in the incised depth compared to the realistic sediment bed run (figure 5.27a). The reduced incision was also found along the Boschgat channels. The overall morphologic response displayed a reduction of the seaward ebb-delta extension.

An increase in the coarsest sediment fraction, 1mm instead of 400 µm (Increased I), increased the initial D_{50} to 400 µm. The ebb-delta outbuilding was similar to the realistic graded sediment composition (figure 5.27b). Along the Akkerpollegat a lateral channel displacement compared to the standard run can be observed. In the rest of the inlet only local differences were present such as the slight reduction in depth of the distal tidal channels.

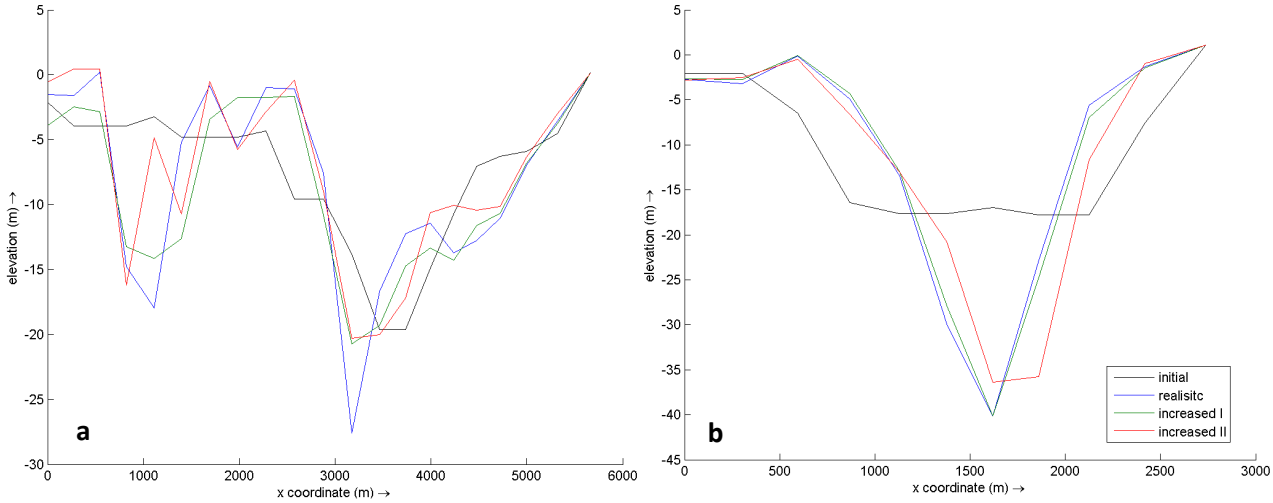

Figure 5.26. Cross-sectional profile of the (a) gorge and (b) with a realistic and increased (I, II) coarse fraction equal layer thickness sediment composition.

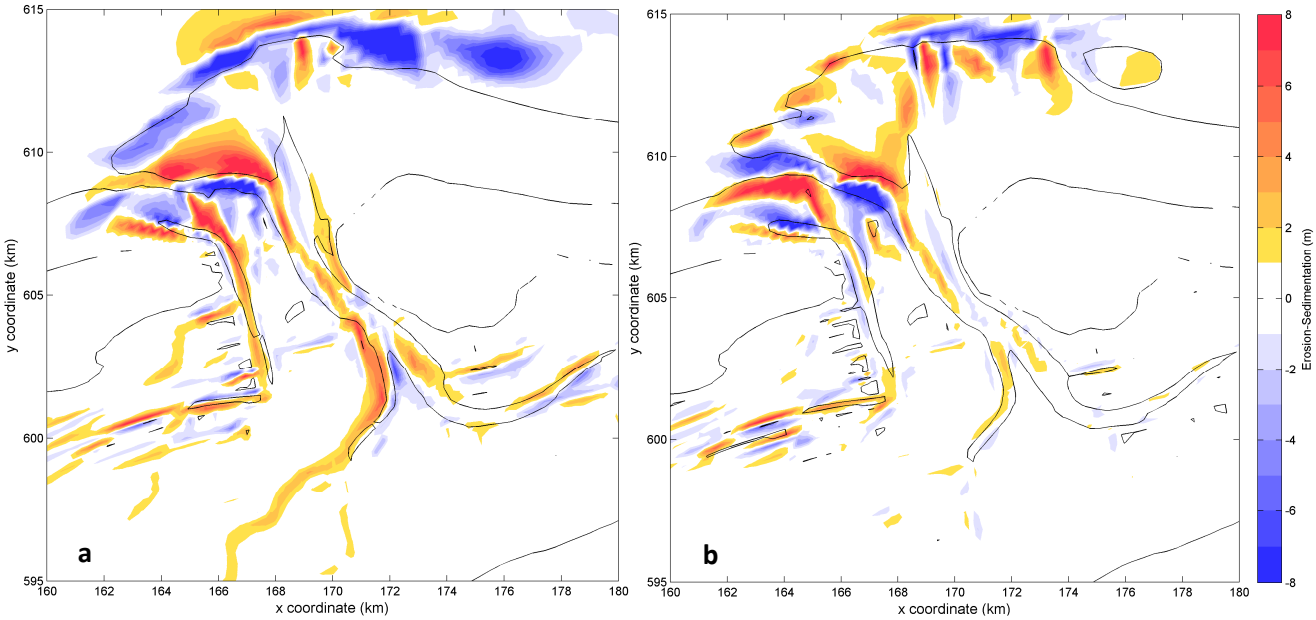

Figure 5.27. Erosion sedimentation difference plots after 75 years between the (a) Increased II and (b) Increased I distribution in comparison to the realistic bed composition Red indicates a less deep bed and blue a deeper bed in comparison to the realistic sorting run. The 0 and -10 m depth contour lines are given.

Reduction fine fractions layer thickness

Smaller initial fine sediment fraction layers (100 µm 2 m) increased the initial D_{50} to 280 µm. The resulting morphology was characterised by a reduced outbuilding of the ebb-delta compared to the standard distribution (figure 5.28a). The channels in the basin had a similar depth. The incorporation of an additional thinner (2 m) 200 µm layer increased the D_{50} to 310 µm. The overall response indicated a further reduced seaward directed ebb-delta development (figure 5.28b) similar to figure 5.27a. In the basin the main Borndiep and smaller Boschgat channels reduced in depth along their lengths.

It should be noted that the combined layer thickness must remain of sufficient thickness in order to prevent erosion through all layers. A reduction of all layer thicknesses to equal 2 m sets and realistic sediment fractions led to a reduction of the gorge incision from -26 m to -22 m and fixed the incision in the basin at -25 m. This means incision of the basin (10 m) is the same as the total amount of available sediment (4 classes x 2 m = 10 m).

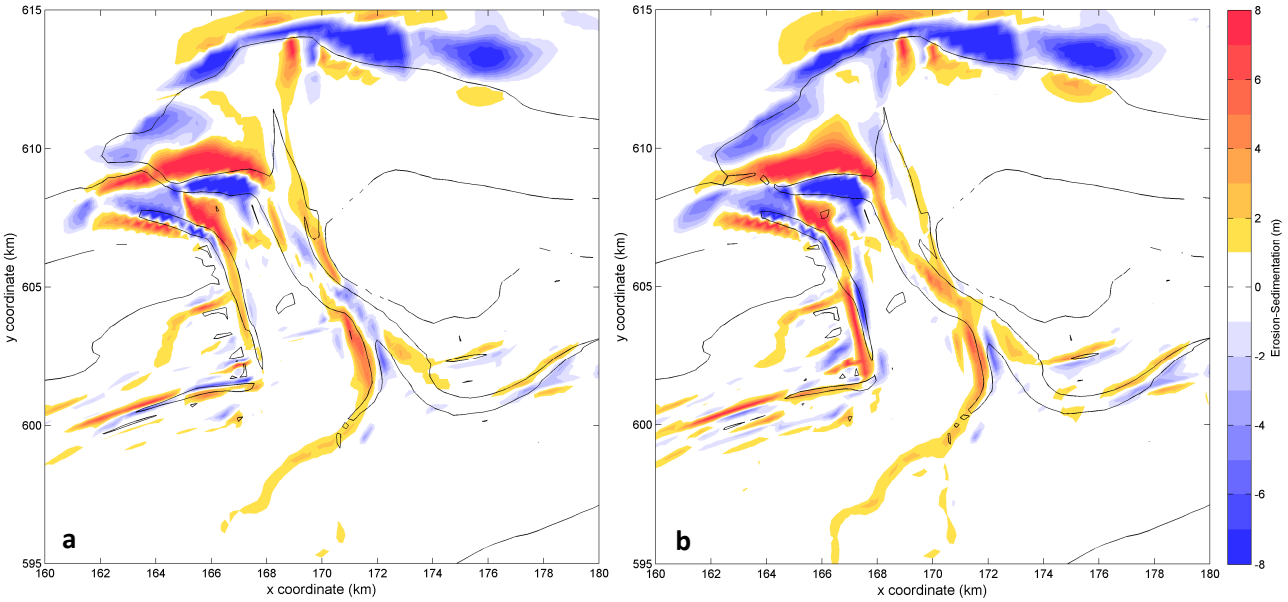

Figure 5.28. Sedimentation erosion difference patterns after 75 years between (a) 2m 100 µm and 10m equal layer (b) 2m 100 and 200 µm and 10 m equal layer. The 0 and -10 m depth contour lines are given.

Sediment distribution

The initial sediment layer thickness controlled the overall D_{50} and thus the size of the sediment fractions in the sorting patterns at the end of the model run (figure 5.29). The same sediment distribution trends are found for all size combinations and are similar to the trends without morphologic development. The trends became less pronounced for runs with an initial D_{50} close to the coarsest sediment fraction. The overall trends consist of:

-Main tidal channels are the coarsest parts of the system
-Basin channels show fining in the distal parts
-Intertidal flats are undisturbed
-Western part of the ebb-delta shows coarsening
-Local fining on the eastern part of the ebb-delta
-North Sea displays local fining and coarsening

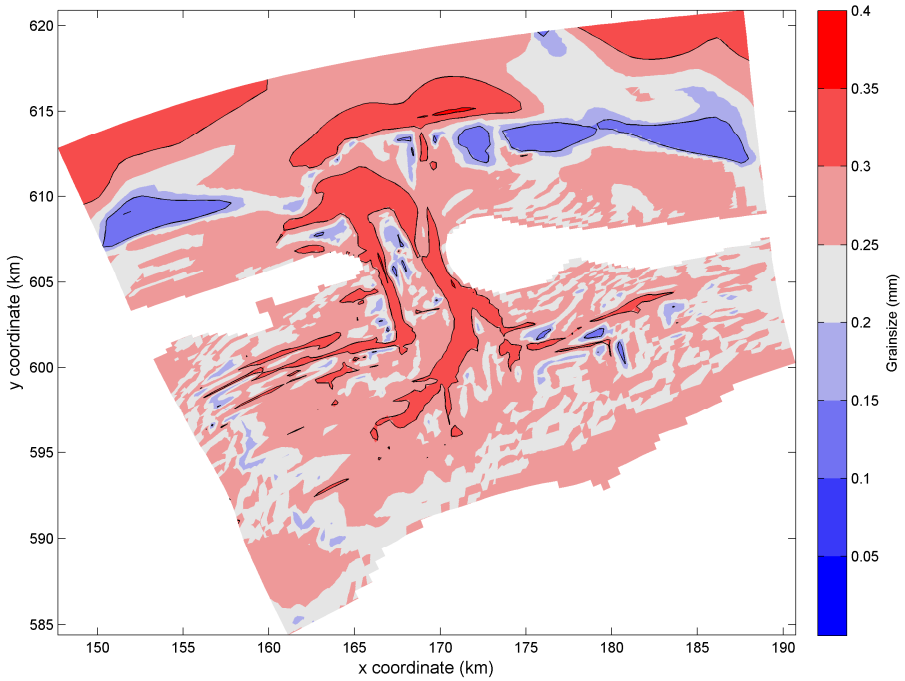

Figure 5.29. Sorting after 100 years for the realistic distribution with equal initial sediment layers.

Summary of graded sediment

The presence of fines controls the magnitude of seaward delta expansion. A reduction in the fine layer thickness reduces the ebb-delta outbuilding and the incision of the central and distal tidal channels. The incorporation of a single coarser fraction creates a reduction in incision only if the amount of fines is reduced. An increase of just the coarse fraction only provides a limited additional stability.

5.3.7 Van Rijn (2007) Dry cell erosion factor

The use of a larger dry cell erosion factor (DCE) increases the erosion and sedimentation in neighbouring cells (chapter 2.4). The effect on the overall long-term morphology was investigated by increasing the erosion factor. The resulting 75 year morphology was compared with the default run morphology. The figures 5.30a and b indicate that the difference between the standard and progressively larger dry cell erosion runs resulted in an altered development that was similar for both increased DCE runs.

The effects were found along the main channel in the basin part and on the ebb-delta. The magnitude of the difference along the channel illustrated that changes in the order of +/-4 m were present that indicate a slight lateral displacement compared to the default run. The maximum depth of the channels did not vary significantly.

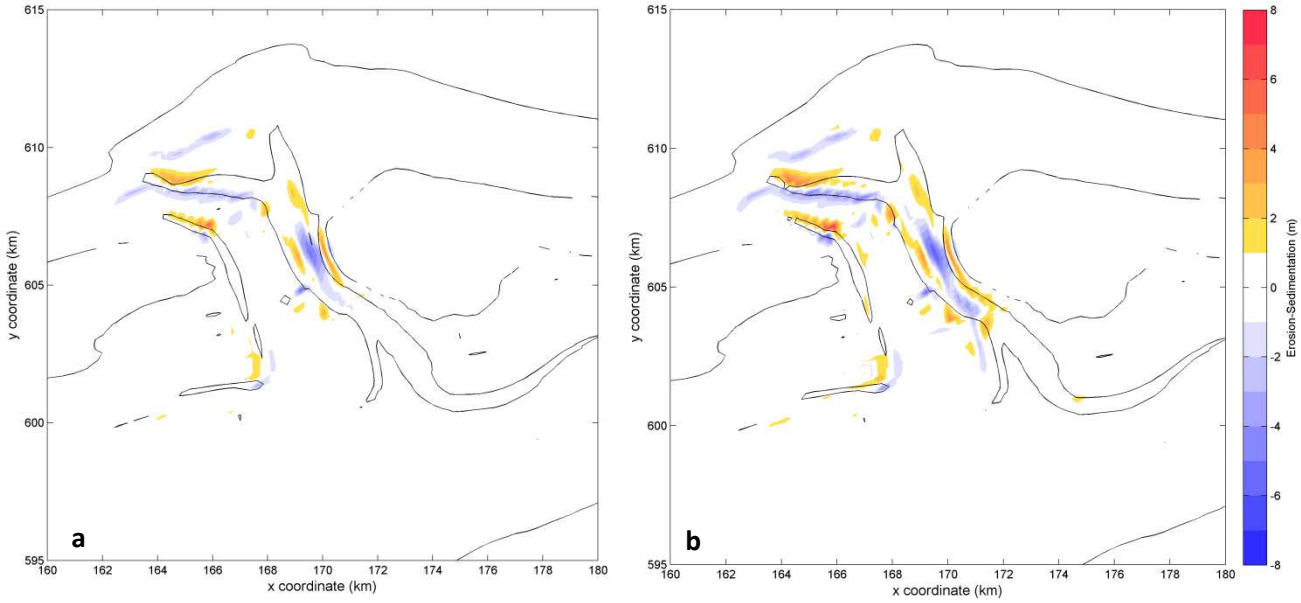

Figure 5.30. Difference in 75 year bathymetry. (a) DCE 0.2-0 (b) DCE 1.0-0. The corresponding 0 and -10m contour lines are plotted. The 0 and -10 m depth contour lines are given.

5.3.8 Van Rijn (2007) transverse bedslope

Two different transverse bedslopes effect were implemented. First the conventional increased *AlfaBn* effect on the channel and overall system morphology is presented. Secondly the Koch-Flokstra (1980) response is given for a range of *Ashld* tuning parameter values.

Conventional bedslope calibration

The model output for a larger transverse bedslope effect displayed more infilling of the central channel for a higher *AlfaBn* values. This led to a small reduction of the depth in the gorge (figure 5.31a) for the 3 and 5 *AlfaBn* runs. In the basin the increase in *AlfaBn* reduced the incision slightly with a value of 5. The morphology of the ebb-delta did not vary significantly for the low range of *AlfaBn* values compared to the default (*AlfaBn* 1.5) run.

The increased 25 run widened and reduced the depth of the tidal channels. This is indicated in figure 5.32b profile by sedimentation in the centre and erosion along the channel margins. The larger 25 morphology displayed a similar ebb-delta shape and outbuilding with a reduced channel depth compared to the 1.5 run. In the gorge the reduction in depth resulted in an unrealistic morphology (figure 5.31a).

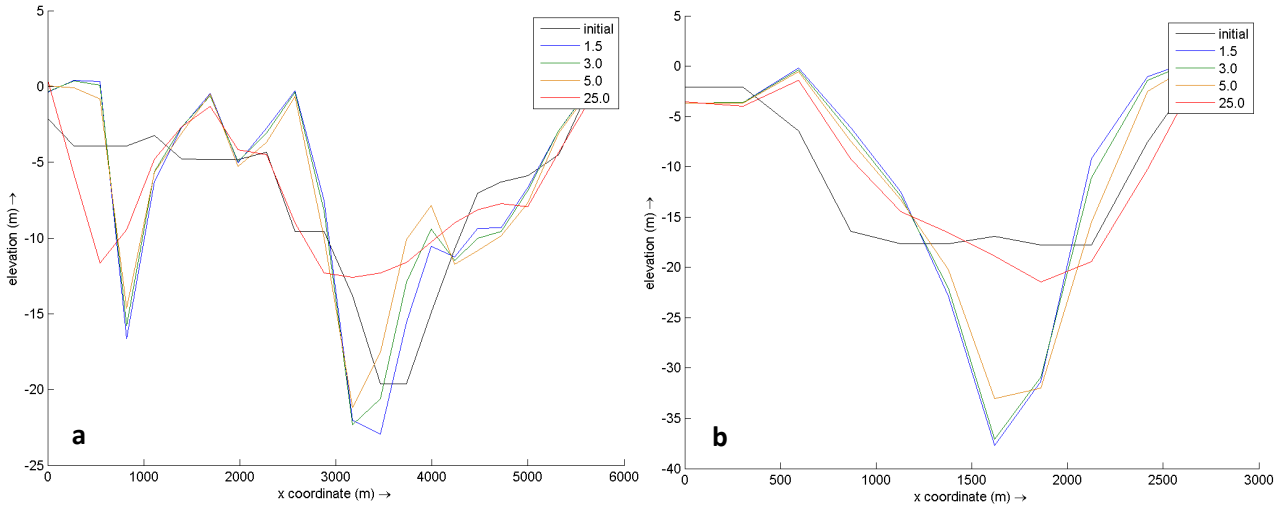

Figure 5.31. Cross-sectional profiles in the (a) gorge and (b) basin for a range of AlfaBn values.

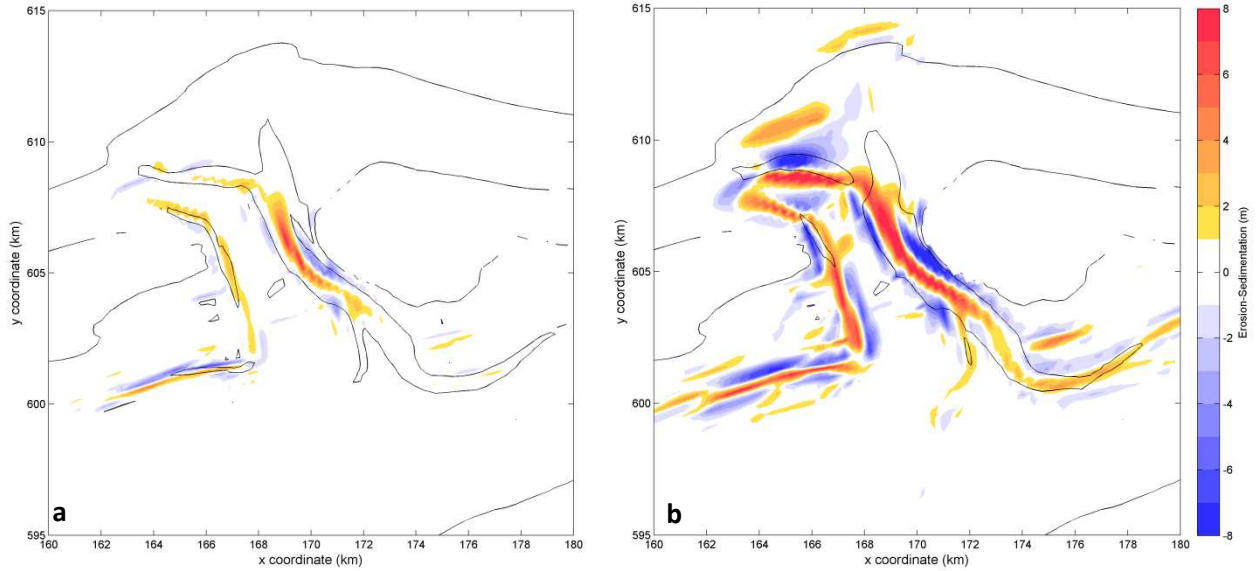

Figure 5.32. Difference in bed morphology given as sedimentation and erosion after 75 years for (a) AlfaBn 5-1.5 and (b) AlfaBn 25-1.5. The 0 and -10 m depth contour lines are given.

Koch-Flokstra (1980)

The most prominent change, compared to the standard trachytope run, was found on the ebb-delta. The ebb-delta extended in the seaward direction with a westward orientation. The resulting delta front was steep compared to the original profile and created a sharp boundary between the shallow delta and deep sea. On the seafloor base of the ebb-delta front incision of the bed was observed. The range of *Ashld* (0.35-1.5) did not significantly alter the overall delta development. And only minor variations were present in the degree of ebb-delta outbuilding.

In the main channels a reduction in the incision was present with a -30m Nap for all *Ashld* conditions compared to the default bedlope -38 m. Furthermore the incised area of the basin channel was located out of the centre and more towards Ameland. This can be seen by comparing the cross-sectional profiles of figure 5.33b and figure5.31b. The channel response differed for different *Ashld* parameter values.

In the gorge the initial profile depth was maintained for all *Ashld* runs (figure 5.33a). In the basin a reduced incision was present with a maximum -30 m depth with *Ashld* 0.7 (figure 5.33b). The basin profile response is not representative for the overall model trends. A better representation of the changes is given in the difference plots (figures 5.34a and b). A smaller *Ashld* 0.35 reduced the

incision of the main tidal channel and Boschgat compared to the 0.7 run. A larger tuning parameter value (1.5) increased the incision compared to *Ashld* 0.7. The widths of the main channels were similar for all *Ashld* runs. The ebb-delta did not undergo large changes for the presented parameter range.

K-F graded sediment bed

In a complex scenario, with multiple sediment fractions, incorporating and varying the KF parameter did not affect the ebb-delta outbuilding in contrast to the homogenous sediment bed runs. The main effect of the K-F incorporation was a reduction in the channel depth compared to the standard 4 class sediment fraction run. Varying the *Ashld* magnitude affected the Borndiep and Boschgat channels. Lower values of *Ashld* only controlled the depth and resulted in shallower channels in both the gorge and basin.

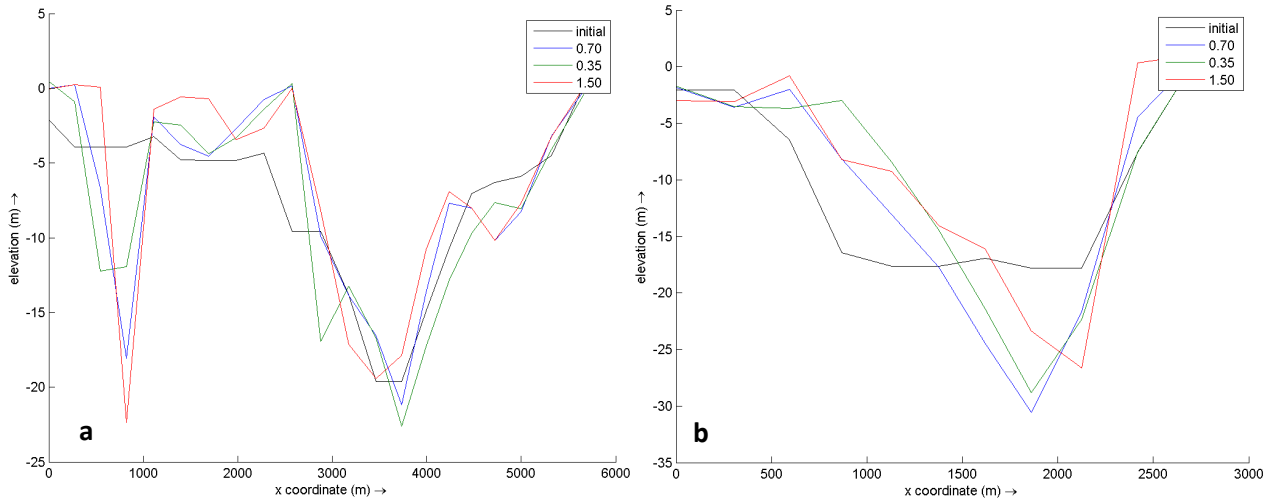

Figure 5.33. The cross-sectional profiles after 100 years for the Ashld range in the legend for the (a) gorge (b) basin.

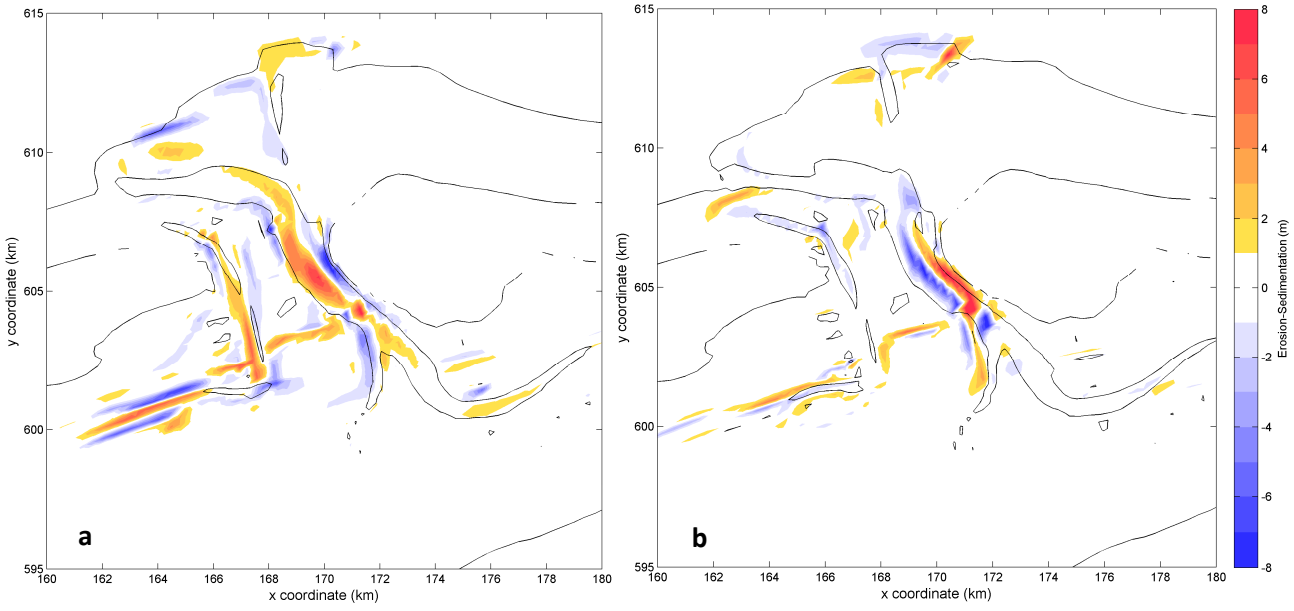

Figure 5.34. Bathymetric difference after 75 year (a) Ashld 0.35-0.7 and (b) Ashld 1.5-0.7. The 0 and -10 m depth contour lines are given.

6. Discussion

In this chapter the width depth ratios of the Ameland inlet are compared to those of the neighbouring Vlie inlet (chapter 6.1). In order to understand the effects of the different morphological boundary conditions, that were implemented, the model performance of the different scenarios is compared to each other and to literature for the short (chapter 6.2) and long-term runs (chapter 6.3).

6.1 Natural channel development

The model evaluation in this report is based on the assumption of stable natural inlet channels of the Ameland. Since natural systems are depicted by dynamic equilibriums (Van der Wegen, 2010) the variation of the Ameland inlet needs to be determined in order to have a valid frame of reference for the model evaluation. The historical development indicated that the overall morphological development of the inlet consisted of a laterally mobile inlet channel and migrating of shoals on the seaward part of the inlet (Israel and Dunsbergen, 1998).

In the basins detailed erosion/sedimentation plots and cross-sectional profiles (chapter 5.1) indicate that lateral movement and width depth variations were present in the past 85 years. The Ameland inlet channel remained relatively stable between 1971 and 1981. After 1981 the gorge increased in depth and the Dantziggat shifted eastward. The increased channel depth remained present up to 1993, which marked the start of a westward directed channel displacement and a reduction in depth by 2009. The same response is given in the cross-sectional profiles and w/h ratios.

The development of deeper and narrower channels coincides with the straightening of the inlet to a direct seaward orientation. After 1999 the channel started to curve again to the east and an overall reduction in the channel depth as well as a westward directed lateral shift was present in the erosion/sedimentation plots and the cross-sectional profiles. This similarity between the seaward channel orientation and basin response should be further investigated.

Based on the natural channel (85 year) development some basic boundaries can be distinguished for the natural channel development:

- -w/h ratios reduce in the basin direction
- -Maximum depths did not exceed the -27 m NAP mark in the gorge and -25 m in the basin.
- -Variation in depth was reduced to +/- 5 m per location
- -Lateral displacement did not exceed 0.5 channel width (0.5w) between 1971 and 2008

The degree of natural channel variability is similar to the neighbouring Vlie inlet. In both environments the reduction in depth, when moving into the basin, is larger than the reduction in width and thus w/h ratios increased and w/h ratios larger than 100 were found. The Terschelling Zeegat gorge depth displayed depth variation but did not exceed -35 m NAP. Finally cross-sectional profiles of the Vlie inlet displayed lateral displacement limited at approximately 0.5w (Terwisscha van Scheltinga, 2012). This means that, although the natural channels of the Ameland inlet were not fixed in space and their dimensions varied over time, the range and variability time was constant in the past 100 years. This supports the main assumption for evaluation of the model results, that the channel incision and lateral mobility should be limited when simulating long (100 year) intervals.

6.2 Short term model

6.2.1 Hydrodynamic validity

The order of magnitude of the depth averaged velocity (bedform roughness), on the seaward side of the ebb-delta and in the gorge (~1 m/s), is similar to the natural inlet (Cheung et al., 2007). Furthermore the discharge over a single tide, $30*10^3$ for flood and $-30*10^3$ m^3/s is in accordance with the measurements of Briek et al. (2003). Water levels (+/-1 m) in the model indicate a similar value in comparison with the natural inlet (Dissanayake, 2012). Since the aim was to evaluate the morphologic boundary conditions as opposed to accurately represent the Ameland inlet the model can be deemed sufficiently valid for the presented parameter evaluation in this report.

6.2.2 Short term parameter evaluation

The short model runs proved useful for rapidly evaluating potential extreme responses of the system. Such an extreme response was present in the response to a different sediment transport predictor (chapter 5.2.2). The model morphology already displayed a deeply incised channel after the 2 year period, whereas the Van Rijn (2007) resulted in more stable channels. The use of the short model runs in rooting out the unrealistic cases is also given by the *AlfaBn* bedslope tuning parameter. Larger values resulted in a significant change in the short model runs. This suggests that using this tuning parameter is a dominant controlling factor on the long term morphology.
However the need for incorporating long term simulations in the overall sensitivity analysis should not be overlooked. Some effects only manifest themselves over longer intervals. An example is the Koch-Flokstra (1980) tuning parameter *Ashld* (chapter 5.2.2). In the short evaluations identical morphologies were found, whereas the longer simulations displayed a significant difference in the final morphology. Therefore long term model runs are necessary to evaluate the morphologic boundary conditions.

6.3 Long term model

The long term model results illustrated the effects of different model approaches and parameter range sensitivities. First the optimal setting is discussed in terms of morphologic similarity with the natural inlet as a result of the sediment transport prediction and roughness definition. Later the model performance as a result of different parameter settings is given (chapter 6.4).

6.3.1 Sediment transport prediction

The Van Rijn (2007) sediment transport proved the greatest improvement of the morphologic development of the model regardless of the roughness definition. The prediction greatly reduced the incision of the main channel at both the basin gorge cross-sectional locations. The VR93 incised through the specified sediment bed (25 m), whereas the VR07 halted the erosion at the initial bed level in the gorge and at -40 m in the basin after 100 years. Furthermore it improved the morphologic similarity between the initial and final morphology by reducing the seaward directed outbuilding of the ebb-delta. The reason for the reduced incision and delta outbuilding is due to a reduced cumulative sediment transport through the inlet. This suggests that the recalibrated VR07 is better suited to model tidal inlet systems than the default VR93. Therefore it should be used as a basis in future research.

6.3.2 Roughness

In terms of hydrodynamics the bedform prediction (*RpC* 1, *MrC* 1) reduced the peak flow velocities in the main tidal channel with 0.08 m/s compared to the Chézy (65 $m^{0.5}/s$) and by 0.04 m/s in relation to the spatial Manning file roughness definitions. Although slight, this peak velocity reduction could be responsible for the more realistic morphological development with the bedform and spatial Manning and fixed 0.026 roughness definitions.

The bedform roughness (*RpC* 0.5, *MrC* 0.5) parameter setting velocity was equal to the spatial Manning file velocities. Both the bedform prediction and Manning roughness file had an absence of severe incision in the cross-sectional profiles and were stable over the first 40 years of the model run, whereas the Chézy roughness run displayed a strong outbuilding of the ebb-delta. Furthermore compared to a 0.021 and 0.026 Manning roughness the use of a space variable prediction closer resembles the initial morphology.

The reason for the less stable morphology with a single fixed roughness value, in this case the Chézy response, is due to the inability to accurately represent the correct roughness for all parts of the system. This is because the fixed Chézy value, for example underestimates the roughness of shallow channels when it approximates the correct roughness of the deeper tidal channels. With Manning the opposite is true and smaller channels are rougher with a correct roughness value for deep water. These inaccuracies are potentially solved by using a fixed local roughness value file that distinguishes between different parts of the system. However this method is less effective in long term simulations.

This is illustrated by comparing the spatial Manning and bedform roughness. In both runs the incised channel depths and volumetric responses are similar, but the morphology of the Manning file run is determined by the initial roughness. This resulted in the formation of an island in the eastern part of the gorge and affected the channel morphology on the ebb-delta. So the main benefit of using a space varying prediction is the ability of the model to cope and respond to morphologic developments whilst predicting appropriate roughness values.

The sensitivity of the roughness value in relation to water depth and thus the problem of using a fixed value can be explained by regarding figure 6.2. The k_s range on the horizontal axis was converted to a Chézy (equation 12) and Manning value for h= 5, 15 and 25 m. When comparing the predicted bedform roughness height ranges, k_s 0.05 - 0.22 m, it can be seen that the k_s interval overlaps a wide range of Chézy (76-45 $m^{0.5}/s$) and Manning (0.023-0.033) values. This suggests that a single homogenous roughness and non-temporal spatially variable roughness values are less suitable to predict the roughness characteristics of a natural system. This inability is increased by the variation in the Chézy and Manning values for the presented range of water levels. Therefore homogeneous roughness values should be used with care when modelling realistic system scenarios. This contradicts the suggestion by Van der Wegen (2010) that seasonal variability and local roughness become less important in longer term simulations.

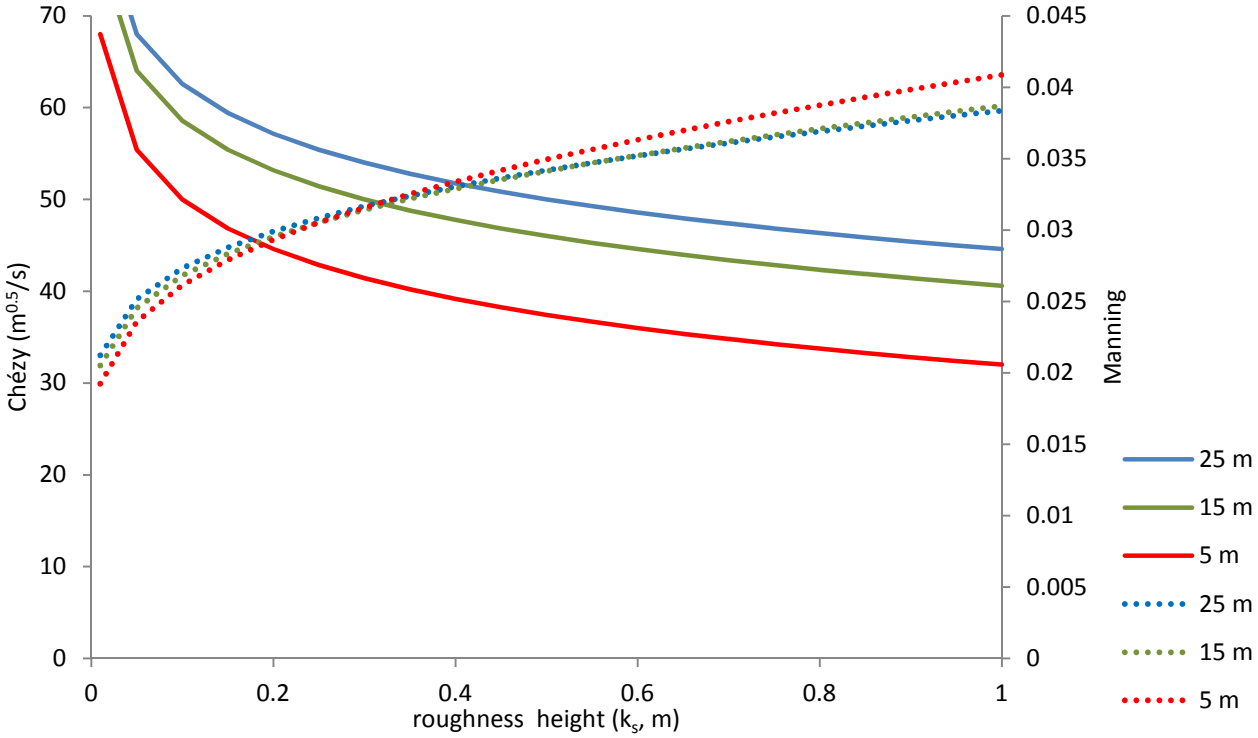

Figure 6.1. Chézy (continuous line) and Manning (dotted line) values plotted as a function of the roughness height for different water depths (5, 15 and 25 m).

6.3.3 Predicted roughness height validity

The validity of the predicted roughness height depends on the presence of bedforms and their varying dimensions in the natural system. Since the roughness height does not represent an actual height (Van Rijn, 2007) a direct comparison between the roughness height and natural form dimensions is not possible. However measurements in natural environments indicate an approximate relation between dune dimensions and the roughness height of $k_s = 0.5h_{form}$ (Van den Berg et al., 1995, Bartholdy et al., 2010). This means that based on the predicted maximum combined bedform roughness height, the dimensions of natural forms should not exceed 0.4 m in the Ameland inlet.

This predicted maximum form height (0.4 m) is small compared to similar natural environments where the smallest dunes were in the order of 0.5 m (Bartholdy et al., 2002, Elias, 2006). Similar Nikuradse roughness height values, of 0.2 m, were found in field measurements of Van den Berg et al. (1995).This means the used roughness height values are a safe estimation of the natural system roughness heights and do not present an overestimation. This safe estimation might suggest increasing the roughness height in order to match the dimensions of natural bedforms. This is supported by other local features such as shell banks and aquatic vegetation that have the potential to increase the roughness.

Although a further increase of the roughness height in Delft3D resulted in more stable channels it also caused a reduction of the flow velocities. The non-realistic flow invalidates the hydrodynamics of the model. So although increased bedform dimensions remain comparable with natural form dimensions the bedform roughness should not be exaggerated in order to produce more stable morphologies.

6.3.4 Stable channels

The incorporation of the VR07 sediment transport prediction reduced the morphologic development of the ebb-delta with and a homogenous 300 µm sediment bed, figure 6.2a and c, and limited the incision of the main channels (figure 6.3a and b) with a homogenous Chézy of 65. Further improvements were found for both sediment predictions by using a space and time variable bedform prediction (figure 6.2b and d) (Van Rijn, 2007). The most stable channels were found with the combined VR07 sediment transport and Van Rijn (2007) bedform prediction with ripples and mega-ripples. These settings produced stable tidal inlet channels over the initial 40 year period. The increase in channel incision after 40 years, which could be related to the shift of the system from a 1 to a 2 channel inlet, lies outside the validity range of the model and the scope of this report. The natural channel stability criteria (chapter 6.1) were fulfilled over the initial 40 year model period:

- The main channel in the gorge and basin did not deepen by more than 5 meters.
- The lateral displacement was lower than 0.5 channel width
- The maximum depth was not surpassed in the gorge and basin profile locations.

It is important to note that although the basic channel behaviour is modelled well the model should not be directly compared with the natural development, due to the use of approximate hydrodynamic boundary conditions (chapter 4.2).

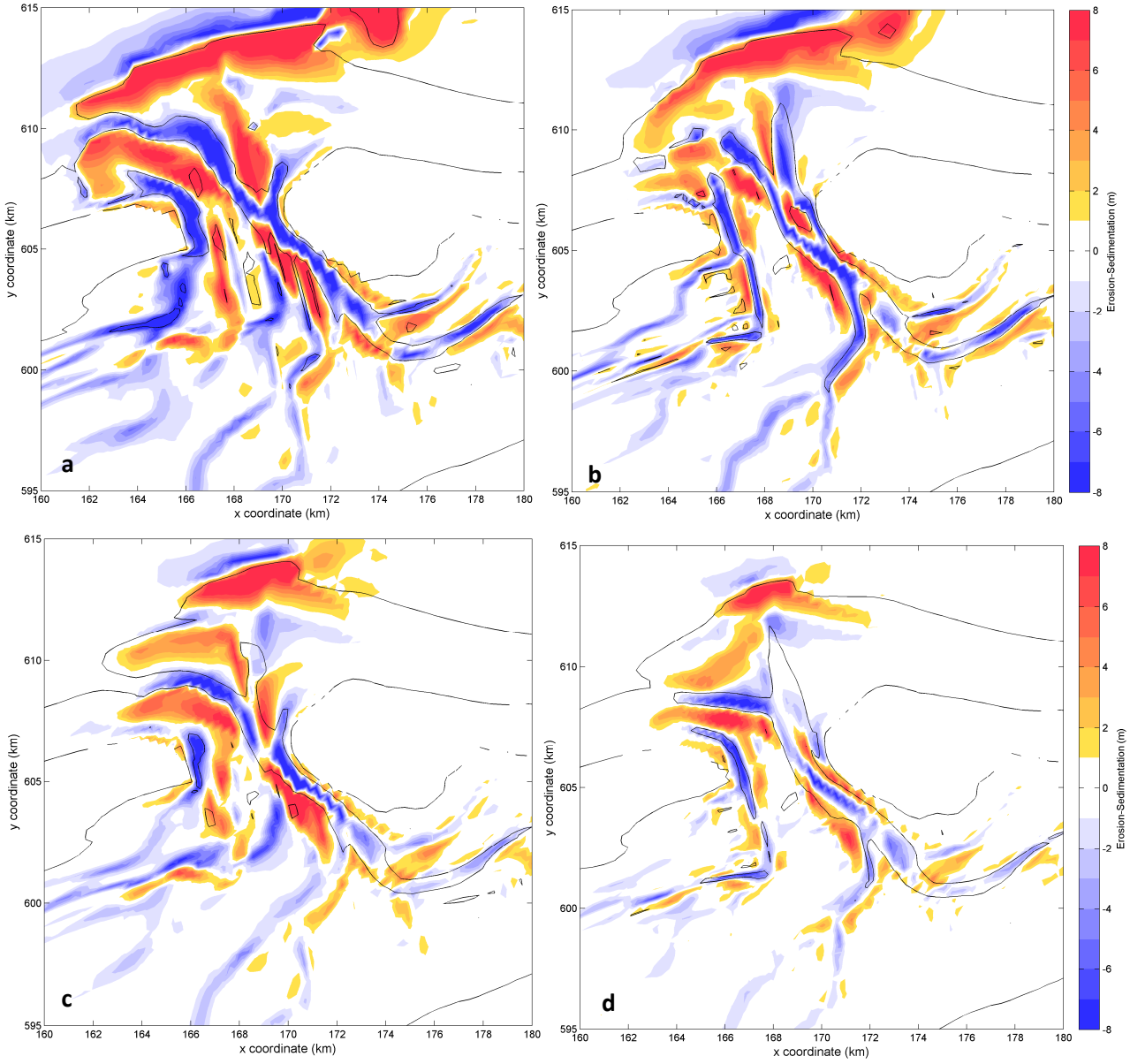

Figure 6.2 (a)VR93 C65 (b) VR93 bedform roughness (RpC 1) (c) VR07 C65 (d) VR07 bedform roughness (RpC 1).Sedimentation erosion patterns between the initial an d 50 years bathymetry.

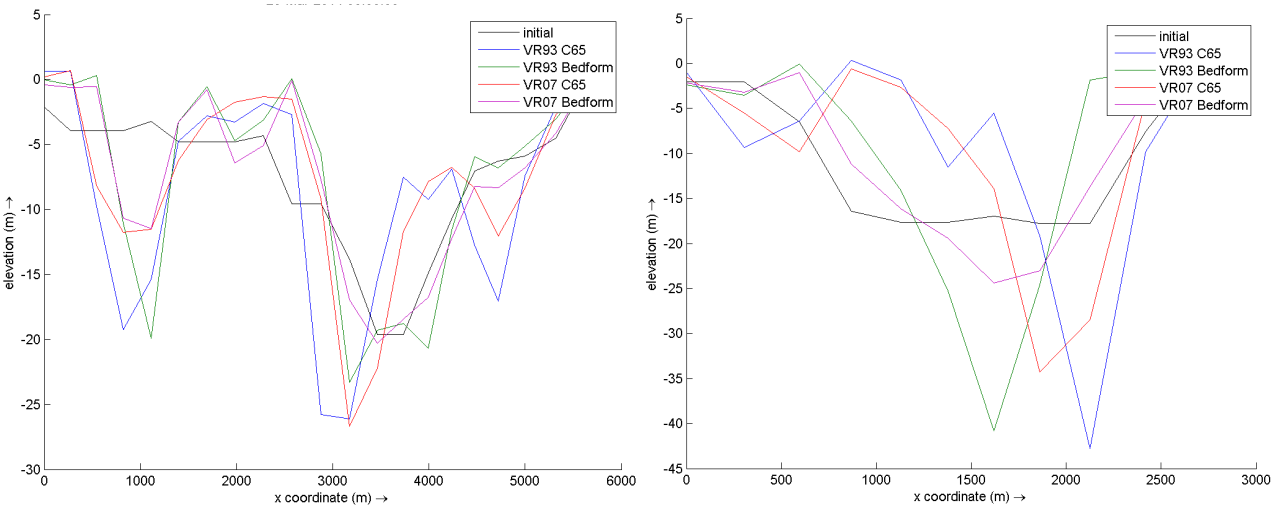

Figure 6.3. Cross-sectional development in the (a) gorge and (b) basin. After 50 years of morphologic development.

6.4 Additional morphologic boundary responses

6.4.1 Homogenous Sediment

The use of a homogenously distributed sediment bed was strongly depended on the specified fraction. The transition form 200 µm to 300 µm reduced the channel incision and resulted in an overall morphology that closer resembled the initial system (chapter 5.3.2). A comparison of the 300 µm value to the Sedimentatlas data indicates that this is an overestimation of the grain size on the intertidal areas and correct for the main channel and gorge sediments. The sensitivity of the overall model response to the homogenous sediment fraction has not been addressed in other modelling studies. Furthermore studies that suggested a space varying bed composition, with larger fractions in the channels (Schouten and Van Hout, 2009, Dastgheib, 2012), compared their model results against a fine homogeneous sediment bed that corresponded to the intertidal flat sediment sizes.

6.4.2 Graded bed

The model results with a graded sediment bed produced different final morphologies due to the specified active layer and initial sediment thicknesses.

Active layer

A thin active layer promoted the formation of a coarser system. This is because the small layer allowed more fine sediment to be transported from the bed. The transported active layer sediment was filled by the underlayer composition. The continued removal of the fine fractions leads to a relative increase in coarse sediment. The time span of this coarsening effect is increased with a thicker initial layer, similar to the description given by Sloff and Ottenvanger (2008). The larger fine sediment transport fluxes (figure 5.23) illustrate the increased availability of fine sediment, due to an absence of coarsening, with a thicker active layer.

Initial layer

The initial layer thickness controlled the mean D_{50} at the beginning of the model run. Less thick initial fine layers resulted in larger mean D_{50} values. Apart from the mean grain size the fine layers controlled the outbuilding of the ebb-delta. This is because the system is suspension dominated and fine sediment is more easily transported out of the basin. A reduction of fines means a reduction in the fine sediment transport and thus the outbuilding of the ebb-delta. In addition less fines reduced

the incision of the main channels. The reduction in channel incision as a result of less thick fine sediment layers was comparable to the incorporation of a larger coarse fraction (Increased I scenario).
The graded bed results of Dastgheib (2012) consisted of a reduction in the channel incision, due to an incorporation of multiple sediment fractions. The fractions used were based on the Texel inlet sediment characteristics, which are too coarse in relation to the Ameland environment (Sedimentatlas). This means the natural characteristics of Ameland were not represented. The implementation of a graded bed, with realistic fractions (chapter 5.3), did not improve the channel response compared to the homogeneous bed run. In contrast all of the graded bed scenarios, including the coarsest increased II scenario had deeper tidal channels.
It can be suggested, based on the presented graded bed model response, that the graded bed method predominantly reduces the incision as a result of the relative increase in the incorporation of coarse sediment.

6.4.3 Transverse bedslope

The range of used *AlfaBn* values differs significantly between studies. Dastgheib (2012) and Van der Wegen (2010) both used 10. In the modelling of this report a lower value of 5 reduced the channel incision, but the effect was limited and did not present a significant improvement compared to the default run value of 1.5 (chapter 5.3.8). Larger values (*AlfaBn* 25) were required to obtain a 100 year morphology in the basin comparable with the initial profile. However the model response with 25 did no longer represent realistic cross-sectional profile morphologies. The overall response was characterised by wide and shallow channels. So, although the channel depth reduces for larger *AlfaBn* values it should not be used as a simple tuning parameter to correct for channel incision. This is because the model results illustrate: a large variation in morphologic response (figures 5.32a and b), a sensitivity to the used grain size (chapter 5.2) and the less-realistic channel morphology in the model output. Furthermore stable channels were found with the default 1.5 *AlfaBn* value over a 40 year period.
The incorporation of Koch-Flokstra (1980) reduced the channel incision and led to an increased outbuilding of the ebb-delta compared to the default bedslope run with a homogenous 300 µm sediment bed. A larger reduction in channel incision was found for lower *Ashld* tuning parameters. Lower values represent an increased effect of gravity on the grain. The found reduction in depth is in accordance with the fluvial system sensitivity analysis of Van Breemen (2011). The increased outbuilding was due to an increased suspended and bedload transport (figure 6.4). Unfortunately, the lack of tidal inlet modelling with the Koch-Flokstra (1980) effect prevents a comparison with other results. It can only be suggested to further investigate the K-F implementation in tidal system modelling due to the effect on the channel depth and width.

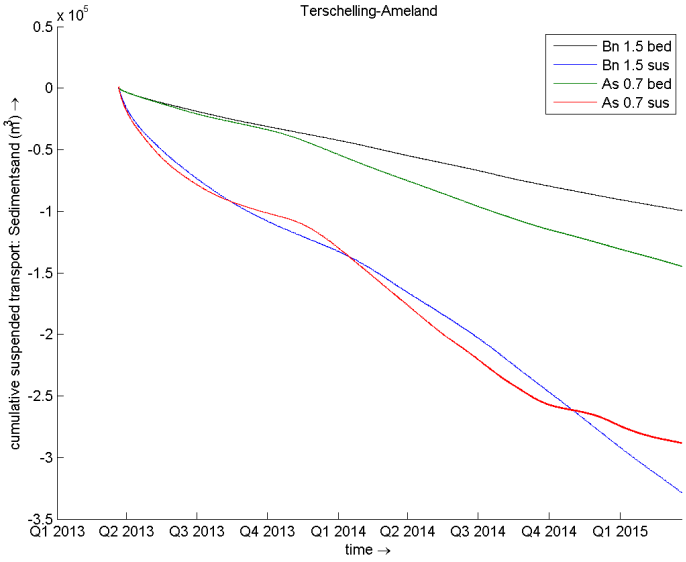

Figure 6.4 Cumulative suspended and bedload sediment transport through the inlet for the default AlfaBn 1.5 and K-F Ashld 0.7 runs.

6.5 Research recommendations

The sensitivity analysis indicates that the most stable channel results are found with the TRANSPOR 2004 sediment transport prediction and the Van Rijn (2007) bedform roughness height prediction. Therefore the use of these settings should be implemented in future morphologic modelling of tidal inlet environments.

Furthermore these settings are almost identical to the settings of De Fockert (2008). Based on the stability of theVR07 bedform roughness model run over the first 40 of the 100 years (chapter 5.3) it is likely that the settings of De Fockert (2008) are valid in long term simulations. A next step would be to introduce the presented sensitivity analysis knowledge into such a model. Alternatively a flat initial bed (Dissanayake, 2012) schematized model could be used to repeat the Koch-Flokstra (1980), bedform roughness, sediment transport VR07 work with in order to compare results and provide a broader frame of reference for the suggested morphologic boundary conditions.

Finally the Koch-Flokstra (1980) transverse bedslope has a significant effect on the main channel locations, depths and outbuilding of the ebb-delta. So although it is commonly used in fluvial research it is a potentially important factor to consider in tidal inlet modelling.

7. Conclusions

The presented model results illustrate the sensitivity of Delft3D to various morphological boundary conditions. The main aim was to determine what morphological boundary conditions are required to create stable tidal inlet channels in long term simulations. The Ameland based model results indicate the incorporation of VR07 and a variable bedform roughness height resulted in more stable channels. The presented results and discussion allow the sub -questions to be answered.

Question 1: What is the natural Ameland inlet channel development in the previous 85 years and what are the corresponding width depth ratios?

The natural Ameland inlet is characterised by lateral movement of the channels and depth variation. The degree of lateral variability was confined to approximately 0.5 channel widths and +/-5 m depth variation over the last 40 year period. In the basin direction the w/h ratios increase from around 60 in the gorge to 80-140 in the Dantziggat. The w/h ratios display variations over time due to variations in channel dimensions in a single location. This dynamic natural stability of the channels, over the past 85 years, validates the main equilibrium assumption of the modelling carried out in this report.

Question 2: On what timescale are morphological boundary conditions to be evaluated?

In short term runs only severe effects result in a different morphology. This allows a rapid evaluation of non-optimal boundary condition responses. Less sensitive parameters do not give a response in the short term morphology, but are essential for the long term development. Therefore Long term simulations are essential to accurately determine the effects of these less sensitive parameters.

Question 3: What is the difference between the default (Van Rijn, 1993) and the Van Rijn (2007) sediment transport prediction on the morphologic development?

The Van Rijn (2007) sediment transport predictor leads to a reduced incision of the central channel and confined the seaward outbuilding of the ebb-delta compared to the default Van Rijn (1993) equation.

Question 4: What are the effect of a homogenously distributed single sediment fraction and graded bed on the long term stability of the channels?

The use of coarse single fraction sediment stabilizes the system, but the homogeneously distributed required D_{50} values are unrealistic (1 mm) in the Van Rijn (1993) runs. The Van Rijn (2007) results show stable results with 300 µm sediment sizes, but remain unrealistic with fine 100 and 200 µm sediment beds. The use of realistic graded sediment is characterised by a strong dependency on the initial and active layer thicknesses. Small active layers promote a rapid coarsening of the system. Large initial volumes of fine (100 µm) sediment lead to an increased outbuilding of the ebb-delta and incision of the channel, whereas smaller fine layers reduce the outbuilding and channel incision comparable to the incorporation of significantly larger sediment fractions.

Question 5: What is the effect using a fixed homogenous roughness compared to a space depended bedform based roughness value on the long term morphologic development?

The use of a constant roughness value is characterised by the inability to distinguish between different morphological features. A fixed space varying roughness is able to define separate roughness values, but is unable to deal with morphological change. Therefore the use of a space and time varying roughness prediction is more suited to use in long term simulations. Furthermore the morphologic response consists of a stable morphologic development with a limited seaward ebb-delta extension and channel incision.

Question 6: What is the effect of increasing the transverse bedslope effect and incorporating the Koch-Flokstra (1980) transverse bedslope correction?

The conventional use of a large transverse bedslope effect leads to more shallow tidal channels in the basin, but results in an unrealistic representation of the gorge for the same transverse slope value. A more complex Koch-Flokstra (1980) bedslope parameter reduces the incision and narrowing throughout the tidal channels. Therefore it might prove a potentially powerful tuning parameter in inlet system representations.

8. List of symbols

a = reference level (m)
A = cross-sectional area (m^2)
A_{fe} = area above mean sea level
A_b = basin area
C = Chézy roughness value ($m^{0.5}/s$)
Cr = courant number
c = wave propagation velocity (m/s)
c_f = roughness coefficient
D_{50} = 50^{th} percentile grain size
f_c =current related friction coefficient
g = gravitational acceleration (m^2/s)
h = water depth (m)
h_{av} = average depth (m)
h_{form}= bedform height (m)
k_s = Nikuradse roughness height (m)
$k_{s,r}$ = ripple roughness coefficient
$k_{s,mr}$ = mega-ripple roughness coefficient
$k_{s,d}$ = dune roughness coefficient
M = mobility parameter wave and currents
M_e = excess sediment mobility
n = Manning roughness value (-)
P = tidal prism (m^3)
q_b = bed load
q_s = suspended load
q_t = total load
S = Slope (m/m)
S_b = bed load transport (kg/m/s)
T = tidal period (s)
u_e = effective velocity (m/s)
u_{cr} = critical velocity (m/s)
U = depth averaged velocity (m/s)
u_e = effective velocity due to currents and waves (m/s)
U_w = peak orbital wave velocity (m/s)
U_δ = representative peak orbital velocity
V = mean tidal velocity (m/s)
$V_{channel}$ = channel volume (m^3)
V_{delta} = ebb-delta volume (m^3)
w = channel width (m)
w_s = settling velocity
x = x-direction
y = y-direction
z = reference level

α = tuning parameter
α_s = transverse bedslope tuning parameter
γ = correction factor
Δ = relative density
ζ = water level (m)
θ = non-dimensional Shields umber
ρ_s = density of sediment (kg/m^3)
ρ_w = density of water (kg/m^3)
τ_b = bed shear stress (N/m)
ϕ_s = modified direction of sediment transport
ϕ_t = original direction of sediment transport
ψ = wave-current mobility parameter

9. References

Bagnold, R.A., 1966, An approach to the sediment transport problem from general physics
US government print office

Bartholdy, J., Bartholomae, A., Flemming, B.W, 2002, Grain-size control of large compound flow-transverse bedforms in a tidal inlet of the Danish Wadden Sea
Marine geology, Vol. 188, p. 391

Bartholdy, J., Flemming, B.W., Ernstsen, V.B., Winter, C., Bartholomä, A., 2010, Hydraulic roughness over simple subaqueous duns.
Geo-Mar let. Vol. 301, p.63-76

Briek, J., Huizinga, M.A., Hut, H.J., 2003, Stroommeting zeegat van ameland 2001
Rijkswaterstaat report

Cheung, K.F., Gerritsen, F., Cleveringa, J., 2007, Morphodynamics and sand bypassing at Ameland inlet, The Netherlands
Jounral of Coastal Research, No. 231, p.106-118

DastGheib, A., 2012, Long-term process-based morphological modelling of large tidal basins
Phd-dissertation

De Fockert, A., 2008, Impact of relative sea level rise on the Amelander inlet Morphology
Master thesis Deflt University

De Swart, H.E., Zimmerman, J.T.F., 2009, Morphodynamics of tidal inlet systems
Annual review of fluid mechanics, Vol. 41, p.203-229

Dissanayake, P.K., 2011, Modelling morphological response of large tidal inlet systems to sea level rise.
Phd-dissertation

Ehlers, J., 1988, The morphodynamics of the Wadden Sea
Balkema Rotterdam

Elias, E., 2006, Morphodynamics of Texel inlet
Phd-dissertation

Elias, E., Bruens, A., 2012, Morfologische analyse Boschplaat
Deltares report

Engelund, F., Hansen, E., 1967, A monograph on sediment transport in alluvial streams
Teknisk Forlag, Copenhagen

Hasselaar, R.W., 2012, Development of a generic automated instrument fort he calibration of morphodynamic Delft3D model applications.
MSc. Thesis TU Delft.

Kleinhans, M.G., Van der Vegt, M., Terwisscha van Scheltinga, R., Baar, A.W., Markies, H., 2012, Turning the tide: experimental creation of tidal channel networks and ebb deltas.
Netherlands Journal of Geosciences, Vol. 91, No.3, p.311-323

Koch, F.G., Flokstra, C., 1980, Bed level computations for curved alluvial channels
Proceedings of the XIXth congress of the international association for Hydraulic Research, New Delhi india, Vol. 2, p357-364

Louters , T., Gerritsen, F., 1994, Het mysterie van de Wadden: Hoe een getijdesytemeem inspeelt op zeespiegelstijging
Report Rijkswaterstaat

Lesser, G., 2009, An approach to medium-term coastal morphological modelling
Phd-dissertation

Lobo, F.J. Harnandez-Molina, F.J., Somoza, L., Rodero, J., Maldonado, A., Barnolas, A., 2000, Patterns of bottom current flow deduced from dune asymmetries over the Gulf of Cadiz shelf (southwest Spain)
Marine geology, Vol.164, p.91-117

Oost, A.P., 1995, Dynamics and sedimentary development of the Dutch Wadden Sea with emphasis on the Frisian inlet. A study of barrier islands, ebb-tidal deltas, inlets and drainage basins
Geologica Ultraiectina, Mededelingen van de Faculteit Aardwetenschappen, no. 126

Reynolds, O., 1887, Papers on mechanical and physical subjects.
University of California. Volume II, chapter 55, page 326-335.

Roelvink, J.A., 2006, Coastal morphodynamic evolution techniques
Coastal engineering, Vol. 53, p277-287

Schouten, J.J., Van der Hout, A., 2009, Study on sensitivity of applying spatially varying bed characteristics
Deltares report.

Sloff, C.J., Ottevanger, W., 2008, Multiple-layer graded-sediment approach: Improvement and implications
River flow, 2008

Stefanon, L., Carniello, L., D'Alpos, A.D., Lanzoni, S., 2009, Experimental analysis of tidal network growth and development
Continental Shelf research Vol.30, p.950-962

Swinkels, C.M., Bijlsma, A.C., 2011, Understanding the hydrodynamics of a North Sea tidal inlet by numerical simulation and radar current measurements
Deltares report

Terwisscha van Scheltinga, R., 2012, Analysis of recent morphological changes in the tidal inlet system Vlie, the Netherlands
Rijkswaterstaat internship report, Utrecht University
Van Breemen, D., 2011, conceptual flow models for the prediction of transverse slopes in river bends for uniform sand misxtures
Internship report Deltares/Utrecht University
Van der Spek, A.J.F., 1994, Reconstruction of tidal inlet and channel dimensions in the Frisian Middelzee, a former tidal basin in the Dutch Wadden Sea.
Spec. Publs int. Ass. Sediment Vol. 24, p.239-258
Van der Spek, A.J.F., 1996, Holocene depositional sequences in the Dutch Wadden Sea south of the island of Ameland.
Mededelingen Rijks Geologische Dienst, Nr.57, 1996
Van der Wegen, 2008, Modelling morphodynamic evolution in alluvial estuaries
Phd-dissertation
Van de Werf, J., 2012, Actualisatie Delft 3D van de Westerschelde
Deltares/Arcadis report
Van der Berg, J.H., Asselman, N.E.M., Ruessink, B.G., 1995, Hydraulic Roughness of a Tidal Channel, Westerschelde Estuary, The Netherlands
Spec. Publs int. Ass.Sediment, Vol. 24, p.19-32
Van der Vegt, M., Schuttelaars, H.M., de Swart, H.E., 2006, Modelling the equilibrium of tide-dominated ebb-tidal deltas
Journal of Geophysical Research, Vol. 111
Van Dijk, W.M., Van de Lageweg, W.I., Kleinhans, M.G., 2012, Experimental meandering river with chute cutt-offs
Journal of geophysical research
Van Rijn, L.C., 1993, Principles of sediment transport in rivers, estuaries and coastal seas
Aqua publications, The Netherlands
Van Rijn, L.C., 2004, Description of TRANSPOR2004 and implementation in Delft3D-ONLINE
WL-Delft Hydraulics
Van Rijn, L.C., 2007, Unified view of sediment transport by currents and waves I: Initiation of motion, bed roughness and bed-load transport.
Journal of Hydraulic engineering, Vol.133, No.6
Walton, T.L., Adams, W.D., 1976, Capacity of inlet outer bars to store sand
Proc. 15th Coastal Eng. Conf. Honolulu, ASCE, New York, Vol.2
Wang, Z.B., Jeuken, C., De Vriend, H.J., 1999, Tidal asymetry and residual sediment trasnport in estuaries
Deltares report
Wang, Z.B., Vroom, J., Van Prooijen, B.C., Labeur, R.J., Stive, M.J.F., Jansen, M.H.P, 2011, Development of tidal watersheds in the Wadden Sea
River, coastal and estuarine morphodynamics: RCEM 2011
Wang, Z.B., Hoekstra, P., Burchard, H., Ridderinkhof, H., De Swart, H.E., Stive, H.J.F, 2012, Morphodynamics of the Wadden Sea and its barrier island system
Ocean & Coastal Management, Vol. 68
Zarillo, G.A., 1982, Stability of Bedforms in a tidal environment
Marine Geology, Vol.48, p.337-351

Others
Delft3D manual, 2011, Simulation of multi-dimensional hydrodynamic flows and sediment transport phenomena, including sediments
Deltares, Delft

Appendix

In the appendices the model run specific input is given together with a more elaborate overview of the model results.

I. Fixed model parameters

FlOW-Module

Parameter	**Value**	**Description**
Vicouv	1.0	Horizontal eddy viscosity (m^2/s)
Dicouv	1.0	Horizontal eddy diffusivity (m^2/s)
Rhow	1025	Density of water (kg/m^3)
Tempw	15	Water temperature (°C)
Ag	9.81	Gravity
Dpsopt	Max	Depth at grid cell centres
Dpuoupt	Mor	Depth at grid cell faces
Dco	-999	Marginal depth
Tlfsmo	60	Smoothing
Momsol	Cyclic	Advection for momentum
Trasol	Cyclic	Advection for transport
CstBnd	#Y#	Neuman boundaries

Morphological

Parameter	**Value**	**Description**
MorStt	900	Spin up (min)
SedThr	0.1	Minimum depth sediment calc (m)
AksFac	1	Van Rijn reference height (-)
Thresh	0.05	Threshold sediment thickness (m)
ThetSd	0	Dry cell erosion factor
AlfaBs	1	Longitudinal bedslope
AlfaBn	1.5	Transversal bedslope
Sus	1.0	Transport calibration
Bed	1.0	Transport calibration

Sediment

Parameter	**Value**	**Description**
RhoSol	2650	Specific density (kg/m^3)
CDryB	1600	Dry bed density (kg/m^3)
IniSedThick	25	Initial sediment bed (m)

II. Trachytope bedform incorporation

The incorporation of a bedform based roughness prediction requires an additional .inp and .trt file.

.inp

1 1 103 94 1 1	The range of the M and N grid size

.trt

1 105	Content of .trt file for bedfrom roughness

In the mdf file additional keywords are required when using the VR07 sediment transport prediction and the VR bedfrom roughness prediction.

Trtrou = #Y#	Flag for trachytopes
Trtdef = #vrijn2004.trt#	Set the used roughness predciton (105)
Trtu = #trtuv.inp#	Define U and V direction boundaries
Trtv = #trtuv.inp#	Define U and V direction boundaries
TrtDt = 1.0	Updating of roughness needs to be a multiple of Dt e.g 0.5 means every two time steps
BdfRpC = 1.0	Ripple roughness calibration (0-limitless)

BdfRpR = 1.0	Ripple relaxation in Dt
BdfMrC = 1.0	Mega-ripple roughness calibration (0-1)
BdfMrR = 1.0	Mega-ripple relaxation in Dt
BdfDnC = 0.0	Dune roughness calibration
BdfDnR = 0.0	Dune relaxation in Dt
BdfD50 = 0.00030	Grain size of sediment bed
BdfOut = #Y#	Flag for roughness height output to trim file

III. Koch-Flokstra (1980)

In the .mor file

ISlope	= 3	[-]	Flag for bed slope effect
AShld	= 1.0	[-]	Bed slope parameter Koch&Flokstra
BShld	= 0.5	[-]	Bed slope parameter Koch&Flokstra